

OFFICE OF CIVILIAN RADIOACTIVE WASTE MANAGEMENT  
SPECIAL INSTRUCTION SHEET

Complete Only Applicable Items

MB 10/15/1999  
1. QA ~~N/A~~ ~~QA~~  
Page: 1 of: 1

This is a placeholder page for records that cannot be scanned or microfilmed

2. Record Date  
~~10/04/99~~ MB 10/15/1999  
09/30/1999

3. Accession Number  
MOL.19991014.0235

4. Author Name(s)  
Sedat Goluoglu

5. Author Organization  
M&O

6. Title  
Evaluation of Codisposal Viability for MOX (FFTF) DOE-Owned Fuel

7. Document Number(s)  
BBA000000-01717-5705-00023

8. Version  
00

9. Document Type  
Design Document

10. Medium  
Optic/Paper

11. Access Control Code  
PUB

12. Traceability Designator  
BBA000000-01717-5705-00023

13. Comments  
Approved document, COLORED ILLUSTRATIONS / This OAK

CAN BE LOCATED THROUGH  
THE RECORDS PROCESSING  
CENTER

**QA: L**

**Civilian Radioactive Waste Management System  
Management & Operating Contractor**

**Evaluation of Codisposal Viability for MOX (FFTF) DOE-Owned Fuel**

**BBA000000-01717-5705-00023 REV 00**

**September 1999**

Prepared for:

National Spent Nuclear Fuel Program  
1955 Fremont Ave, MS 3135  
Idaho Falls, ID 83415-1625

Prepared by:

Civilian Radioactive Waste Management System  
Management & Operating Contractor  
1261 Town Center Drive  
Las Vegas, NV 89144

Under Contract Number  
DE-AC08-91RW00134

#### **DISCLAIMER**

This report was prepared as an account of work sponsored by an agency of the United States Government. Neither the United States, nor any agency thereof, nor any of their employees, make any warranty, expressed or implied, or assume any legal liability or responsibility for the accuracy, completeness, or usefulness of any information, apparatus, product, or process disclosed, or represent that its use would not infringe privately owned rights. Reference herein to any specific commercial product, process, or service by trade name, trademark, manufacturer, or otherwise, does not necessarily constitute or imply its endorsement, recommendation, or favoring by the United States Government or any agency thereof. The views and opinions of authors expressed herein do not necessarily state or reflect those of the United States Government or any agency thereof.

**Civilian Radioactive Waste Management System  
Management & Operating Contractor**

**Evaluation of Codisposal Viability for MOX (FFTF) DOE-Owned Fuel**

**BBA000000-01717-5705-00023 REV 00**

**September 1999**

Prepared by:



Sedat Goluoglu  
Waste Package Operations

9/28/99

Date

Checked by:

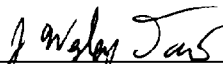


Donald Nitti  
Waste Package Operations

9/28/99

Date

Approved by:



J. Wesley Davis, Lead  
DOE Fuel Analysis

9/30/99

Date

INTENTIONALLY LEFT BLANK

## HISTORY OF CHANGE PAGE

**Revision Number**  
00

**Description of Change**  
Initial Issue

INTENTIONALLY LEFT BLANK

## EXECUTIVE SUMMARY

### INTRODUCTION

There are more than 250 forms of U.S. Department of Energy (DOE)-owned spent nuclear fuel (SNF). Due to the variety of the spent nuclear fuel, the National Spent Nuclear Fuel Program (NSNFP) has designated nine representative fuel groups for disposal criticality analyses based on fuel matrix, primary fissile isotope, and enrichment. Fast Flux Test Facility (FFTF) fuel has been designated as the representative fuel for the mixed-oxide (MOX) fuel group which is a mixture of uranium and plutonium oxides. Demonstration that other fuels in this group are bounded by the FFTF analysis remains for the future before acceptance of these fuel forms. The results of the analyses performed will be used to develop waste acceptance criteria. The items that are important to safety are identified based on the information provided by NSNFP. Prior to acceptance of fuel from the MOX fuel group for disposal, the items important to safety for the fuel types that are being considered for disposal under the MOX fuel group must be demonstrated to satisfy the conditions determined in this report.

The analyses have been performed by following the disposal criticality analysis methodology, which was documented in the topical report submitted to U.S. Nuclear Regulatory Commission (YMP/TR-004Q, *Disposal Criticality Analysis Methodology Topical Report*). The methodology includes analyzing the geochemical and physical processes that can breach the waste package and degrade the waste forms and other internal components, as well as the structural, thermal, and shielding analyses, and intact and degraded criticality. Addenda to the topical report will be required to establish the critical limit for DOE SNF once sufficient critical benchmarks are identified and performed.

The waste package that holds the DOE SNF canister with FFTF MOX fuel also contains five high-level waste (HLW) glass pour canisters and a carbon steel basket. The FFTF DOE SNF canister is placed in a carbon-steel support tube that becomes the center of the waste package (see Figure ES-1). The five HLW canisters are evenly spaced around the FFTF DOE SNF canister. The FFTF DOE SNF canister is designed for five intact FFTF fuel assemblies spaced around a center position. The center position will contain either another assembly or a pin container, referred to as Ident-69, which holds up to 217 individual FFTF fuel pins. The Ident-69 pin container can only fit in the center position. The DOE SNF canister basket structure is composed of a cylindrical stainless-steel tube, which occupies the center position and is supported by five equally spaced external divider plates that separate the intact FFTF assemblies from one another in the outer ring.

The 5-HLW/DOE SNF Long waste package is based on the Viability Assessment design of waste packages. The outer barrier is made of a corrosion-allowance material, 100 mm thick carbon steel. The corrosion-resistant inner barrier is fabricated from a 20 mm thick high-nickel alloy. Both the top and bottom lids are also based on the two-barrier principle and use the same materials.



This report presents the results of analyzing the 5-HLW/DOE SNF Long waste package against various design criteria. Section 2.2 provides the criteria, and Section 2.3 provides the key assumptions for the various analyses.

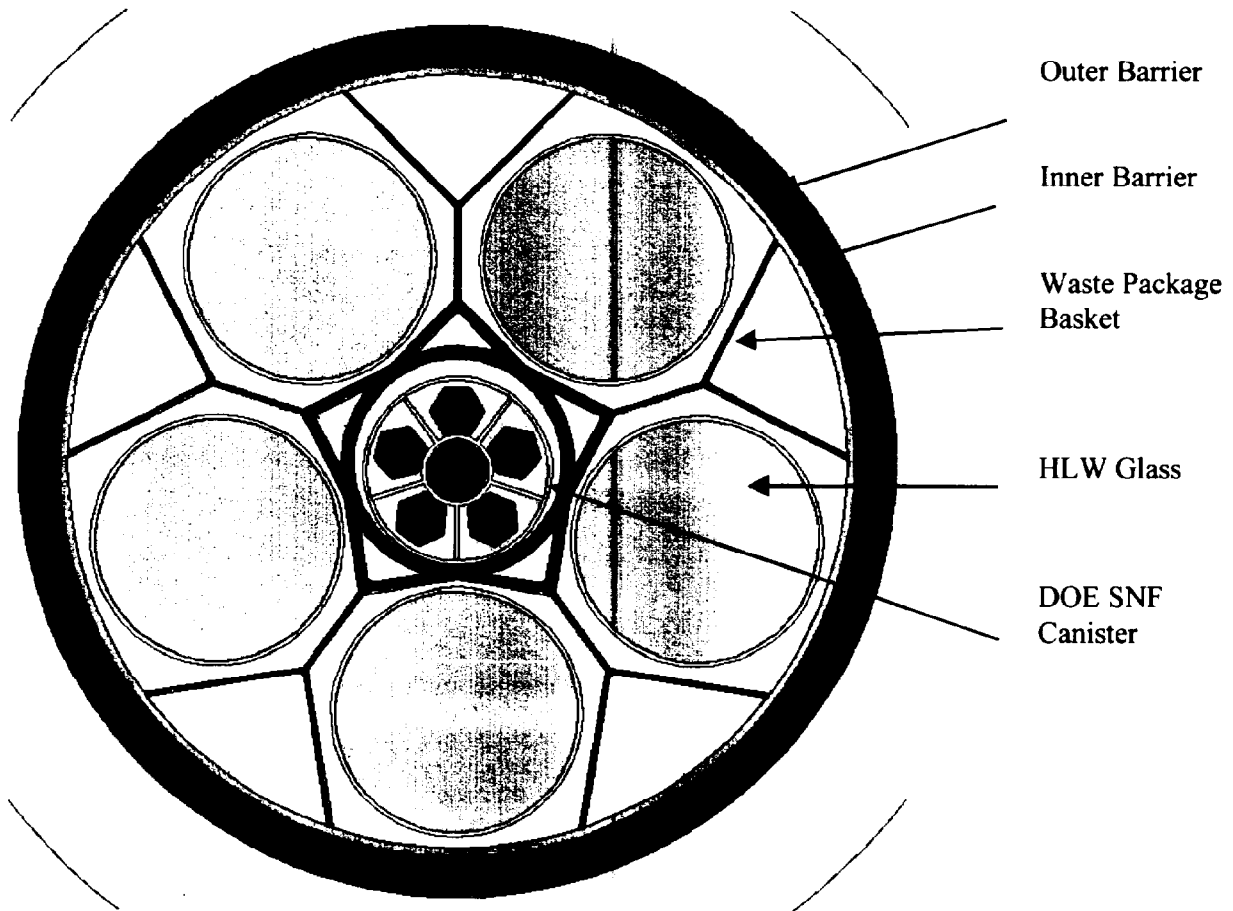


Figure ES-1. 5-HLW/DOE SNF Long Waste Package

## STRUCTURAL ANALYSES

ANSYS Version 5.4 – a finite-element analysis (FEA) computer code – is used for the structural analysis of the 5-HLW/DOE SNF Long waste package with the FFTF DOE SNF canister in the center. A two-dimensional (2-D) finite-element representation of this waste package was developed to determine the effects of loads on the container's structural components due to a waste package tipover design-basis event (DBE). Calculations of maximum potential energy for each handling accident scenario (2.4 m horizontal drop, 2.0 m vertical drop, and tipover DBEs) show that the bounding dynamic load results from a tipover case in which the rotating top end of the waste package experiences the highest g-load. Therefore, tipover structural evaluations are bounding for all handling accident scenarios considered in the DBEs document.

The maximum deformation of the DOE SNF canister basket is determined for the case of 5-HLW/DOE SNF Long waste package representation that includes the structural components of

the waste package and the DOE SNF (FFTF) canister. The results of the waste package tipover structural analysis show that the maximum deformation of the DOE SNF canister basket is 7.3 mm. The available gap between the FFTF driver fuel assembly (DFA) and the basket is 11.6 mm. Therefore, the DFA will not be crushed within the basket structure. Similarly, there will be no interference between the Ident-69 pin container and the DOE SNF basket support tube.

## **THERMAL ANALYSES**

The FEA computer code used for the thermal analysis of the 5-HLW/DOE SNF Long waste package with the FFTF DOE SNF canister in the center is ANSYS Version 5.4. The maximum heat generation from a Hanford 15-foot HLW canister is projected to be 2,540 watts. The thermal conductivity of the HLW glass is approximated as that of pure borosilicate glass, while the properties of density and specific heat are approximated as those of Pyrex glass. The FFTF DOE SNF canister is analyzed with both helium and argon as fill gases, while the waste package is filled with helium.

Using conservative input values, the analyses show that the FFTF waste package satisfies all relevant governing criteria. The highest peak fuel temperature occurs with argon fill gas in the DOE SNF canister, and is 280.3 °C.

## **SHIELDING ANALYSES**

The Monte Carlo particle transport code, MCNP, Version 4B2, is used to calculate average dose rates on the surfaces of the waste package. Dose-rate calculations were performed for four cases: a waste package containing Savannah River Site (SRS) HLW and FFTF fuel, a waste package containing Hanford HLW and FFTF fuel, a waste package containing only SRS HLW, and a waste package containing only Hanford HLW. The dose rates at the surface of the waste package containing Hanford HLW glass are approximately 20% higher than surface-dose rates of the waste package containing SRS glass, thus only the results from Hanford cases are summarized in this document.

The highest dose rate of 15.9 rem/h is calculated on a radial outer surface segment of the waste package that contains the FFTF DOE SNF canister. The maximum dose rate on the outer surfaces of the waste package is below the criteria limiting value of 355 rem/h for the cases investigated by over a factor of 20. The dose rate from primary gamma rays dominates the neutron dose rate by approximately three orders of magnitude.

## **DEGRADATION AND GEOCHEMISTRY ANALYSES**

The degradation analyses follow the general methodology developed for application to all waste forms containing fissile material. This methodology evaluates potential critical configurations from the intact (but breached) waste package through the completely degraded waste package. The waste package design developed for the intact configuration is used as the starting point. Sequences of events and/or processes of component degradation are developed. Standard scenarios from the master scenario list in the topical report are refined using unique fuel characteristics. Potentially critical configurations are identified for further analysis.

The EQ3/6 geochemistry code was used to determine the chemical composition of the solid degradation products with particular emphasis on the chemical conditions that could lead to a loss of neutron absorbers (particularly Gd) from the waste package and that would allow the fissile materials to remain. Gadolinium is assumed to be present as gadolinium phosphate ( $\text{GdPO}_4$ ), which is selected due to its insolubility, distributed on or in the DOE SNF canister basket.

EQ6 cases were constructed to span the range of possible Gd and fuel corrosion, and to test effects of varying glass composition. Some cases test the alkaline regime, achieving a high pH by exposing the fuel to degrading glass. While these cases produce the highest Gd loss, the total loss is  $\leq 0.7\%$  in  $\geq 100,000$  years; furthermore, when the glass is allowed to degrade rapidly, the alkaline conditions produce high U and Pu loss (up to 100%), reducing the chances of internal criticality.

Some cases test the effect of exposing the Gd, Pu, and U to long-lived acidic conditions (pH  $\sim 5$  to 6). No loss of Gd is observed and the highest fissile loss is less than 3% of the Pu or U content.

#### **INTACT AND DEGRADED CRITICALITY ANALYSIS**

The intact criticality analyses consider two general cases, one where an Ident-69 pin container is in the center position of the basket inside the DOE SNF canister and the other where a DFA is in the center position. In all cases the other five positions of the basket contain DFAs.

The results from the intact criticality analyses show that  $k_{\text{eff}} + 2\sigma$  (at 95% confidence) are less than or equal to 0.93 for six DFAs in the DOE SNF canister. This configuration does not need any neutron absorber in the canister basket or elsewhere in the waste package. For the cases that include an Ident-69 container and five DFAs, the basket must contain at least 0.5% (1.93 kg) Gd by weight uniformly distributed over the entire canister basket.

The calculations for degradation within the DOE SNF canister can be divided into three general categories depending upon the level of degradation of the fuel components: (1) partially degraded DFAs and intact Ident-69 pin container, (2) completely degraded DFAs and intact Ident-69 container, and (3) DFAs and Ident-69 container are both completely degraded. In the first two of these three categories, the basket may or may not be intact, while in the last the entire contents of the (intact) DOE SNF canister are degraded, including the basket. In addition, the calculation was performed with the center position of the basket of the DOE SNF canister containing a DFA rather than an Ident-69 container.

The second part of degraded criticality analysis considers configurations with full degradation of the DOE SNF canister along with degradation of HLW glass and waste package internals. These configurations include the following: (1) the DOE SNF canister degradation products on top of the degraded HLW and (2) degraded HLW on top of degraded DOE SNF canister. Additionally, two parametric studies are performed to investigate the sensitivity of the analyses described above to other factors.

The results from the criticality analysis for the intact DOE SNF canister show that a  $k_{\text{eff}} + 2\sigma$  less than or equal to 0.93 is achievable. For the cases that include an Ident-69 container, all degradation configurations result in  $k_{\text{eff}} + 2\sigma$  of less than or equal to 0.93 with 2.75% Gd on or in the DOE SNF canister basket as long as only four DFAs are included in the package. All degradation configurations for six DFAs (no Ident-69) in the DOE SNF canister result in  $k_{\text{eff}} + 2\sigma$  of less than or equal to 0.93 if the Gd content is 2%.

Analyses also show that the configurations involving degraded FFTF fuel in, above, or below the HLW clay material are below the threshold of concern for exceeding the interim critical limit, even without credit for the Gd or iron oxide ( $\text{Fe}_2\text{O}_3$ ) content.

The decay of the plutonium isotopes affects the  $k_{\text{eff}}$  of the system. For a homogenous layer of fuel and clay containing Gd, the  $k_{\text{eff}}$  is maximum at time zero and decreases in time. Pu-239 decays to U-235, which has lower thermal fission cross section; Pu-240 decays to U-236 whose absorption cross section is several orders of magnitude lower. When there is a sufficient amount of Gd, almost all of the absorption is by Gd. Therefore, the decay of Pu-240 to U-236 has very little effect on criticality. However, if the Gd is not present, the decay of Pu-240 reduces the overall absorption (Pu-240 is a much stronger absorber than U-236). As a consequence, the  $k_{\text{eff}}$  peaks after approximately 24,100 years. At this time, approximately 92% of the Pu-240 has decayed to U-236 and only 50% of the Pu-239 has decayed to U-235. As more Pu-239 decays to U-235,  $k_{\text{eff}}$  decreases.

## CONCLUSIONS

In summary, the structural, thermal, and shielding criteria are met for a fully loaded DOE SNF canister containing FFTF SNF. The waste package can contain six DFAs, which corresponds to utilizing the maximum number of basket locations, and falls below the interim critical limit of 0.93 with at least 7.62 kg of Gd distributed on (e.g., flame deposit), or in the DOE SNF canister basket. However, the waste packages with an Ident-69 pin container must have one of the circumferential basket locations blocked so that only four DFAs can be disposed of with the Ident-69 container with at least 9.29 kg of Gd on, or in the DOE SNF canister basket. With this design, there will be approximately 64 DOE SNF canisters with FFTF SNF, which corresponds to 64 waste packages. Alternatively, the Ident-69 pin container can be filled with iron shot, thereby allowing all five circumferential basket locations to be filled with DFAs with an Ident-69 container filling the center basket location. With this design, there will be approximately 58 DOE SNF canisters with FFTF SNF, which corresponds to 58 waste packages.

INTENTIONALLY LEFT BLANK

## CONTENTS

	Page
EXECUTIVE SUMMARY .....	vii
1. INTRODUCTION AND BACKGROUND .....	1
1.1 OBJECTIVE .....	2
1.2 SCOPE .....	3
1.3 QUALITY ASSURANCE .....	3
2. DESIGN INPUTS .....	4
2.1 DESIGN PARAMETERS .....	4
2.1.1 Codisposal Waste Package .....	4
2.1.2 HLW Glass Pour Canisters .....	5
2.1.3 DOE SNF Canister .....	6
2.1.4 FFTF DOE SNF .....	10
2.1.5 Thermal .....	13
2.1.6 Shielding Source Term .....	14
2.1.7 Material Compositions .....	16
2.1.8 Degradation and Geochemistry .....	19
2.1.8.1 Physical and Chemical Characteristics of the FFTF Waste Package .....	19
2.1.8.2 Chemical Composition of J-13 Well Water .....	21
2.1.8.3 Drip Rate of J-13 Water into a Waste Package .....	22
2.2 DESIGN CRITERIA .....	22
2.2.1 Structural .....	22
2.2.2 Thermal .....	23
2.2.3 Shielding .....	23
2.2.4 Degradation and Geochemistry .....	23
2.2.5 Intact and Degraded Criticality .....	24
2.3 ASSUMPTIONS .....	24
2.3.1 Structural .....	24
2.3.2 Thermal .....	24
2.3.3 Shielding .....	25
2.3.4 Degradation and Geochemistry .....	25
2.3.5 Intact and Degraded Criticality .....	26
2.4 BIAS AND UNCERTAINTY IN CRITICALITY CALCULATIONS .....	27
2.4.1 Benchmarks Related to Intact Waste Package Configurations .....	27
2.4.1.1 FFTF Fuel Pin Array Experiments .....	27
2.4.1.2 Saxton Plutonium Experiments .....	28
2.4.1.3 Water-Moderated Hexagonally Pitched Lattices of Highly Enriched Fuel Rods of Cross-Shaped Cross Section .....	28
2.4.2 Benchmarks Related to Degraded Waste Package Configurations .....	29
2.4.2.1 Critical Experiments with Mixed Plutonium and Uranium	

## CONTENTS (Continued)

	Page
Nitrate Solution .....	29
2.4.2.2 Critical Experiments with Highly Enriched Uranium Nitrate Solution.....	29
2.4.3 Critical Limit .....	29
3. STRUCTURAL ANALYSIS.....	30
3.1 USE OF COMPUTER SOFTWARE.....	30
3.2 STRUCTURAL DESIGN ANALYSIS .....	30
3.3 CALCULATIONS AND RESULTS .....	30
3.3.1 Description of the Finite-Element Representation.....	30
3.3.2 Results with No Credit for the Structural Components of the DOE SNF Canister.....	32
3.3.3 Results with Structural Credit for the DOE SNF Canister Components .....	32
3.4 SUMMARY .....	33
4. THERMAL ANALYSIS .....	34
4.1 USE OF COMPUTER SOFTWARE.....	34
4.2 THERMAL DESIGN ANALYSIS.....	34
4.3 CALCULATIONS AND RESULTS .....	36
4.4 SUMMARY .....	37
5. SHIELDING ANALYSIS .....	38
5.1 USE OF COMPUTER SOFTWARE.....	38
5.2 DESIGN ANALYSIS .....	38
5.3 CALCULATIONS AND RESULTS .....	38
5.3.1 Waste Package Containing Hanford HLW and FFTF Fuel.....	41
5.3.2 Waste Package Containing Only Hanford HLW .....	41
5.4 SUMMARY .....	42
6. DEGRADATION AND GEOCHEMISTRY ANALYSIS .....	44
6.1 USE OF COMPUTER SOFTWARE.....	44
6.2 DESIGN ANALYSIS .....	44
6.2.1 Systematic Investigation of Degradation Scenarios and Configurations.....	44
6.2.1.1 Degraded Assembly (Intact Basket).....	51
6.2.1.2 Degraded Basket and Intact SNF .....	51
6.2.1.3 Degraded DOE SNF canister Contents and Degraded HLW and other Waste Package Components .....	52
6.2.1.4 Completely Degraded DOE SNF canister above Clay from HLW and Waste Package Internals .....	52
6.2.1.5 Clay from HLW and Waste Package Internals above Completely Degraded DOE SNF canister .....	52
6.2.2 Basic Design Approach for Geochemical Analysis.....	52
6.3 CALCULATIONS AND RESULTS .....	53

## CONTENTS (Continued)

	Page
6.3.1 Gadolinium Solubility Scoping Calculations .....	53
6.3.2 Results of EQ6 Runs .....	56
6.4 SUMMARY .....	57
7. INTACT AND DEGRADED CRITICALITY ANALYSES .....	59
7.1 USE OF COMPUTER SOFTWARE .....	59
7.2 DESIGN ANALYSIS .....	59
7.3 CALCULATIONS AND RESULTS – PART I: INTACT CRITICALITY ANALYSIS .....	59
7.3.1 Determination of Most Reactive Assemblies .....	60
7.3.2 Optimal Spacing and Optimum Number of Fuel Pins in an Ident-69 Pin Container .....	61
7.3.3 Optimum Moderation in the Waste Package and DOE SNF canister .....	62
7.3.4 DOE SNF Canister in the Waste Package .....	63
7.3.5 Summary .....	63
7.4 CALCULATIONS AND RESULTS – PART II: SCENARIOS WITH FISSILE MATERIAL RETAINED IN DOE SNF CANISTER .....	64
7.4.1 Degradation Inside the DFAs .....	65
7.4.2 Degraded DFA Ducts .....	68
7.4.3 Degraded Basket and Intact SNF .....	69
7.4.4 Intact Fuel Pins in DOE SNF Canister with Degraded Basket and Assembly Ducts .....	69
7.4.5 DOE SNF Canister Containing an Intact Ident-69 Container and Five Degraded DFAs .....	70
7.4.6 DOE SNF Canister Containing a Degraded Ident-69 Container and Five Degraded DFAs in the Waste Package .....	71
7.4.7 DOE SNF Canister Containing Degraded Fuel or Fuel Components with the Waste Package Contents Degraded .....	72
7.4.8 DOE SNF Canister with Degraded FFTF Fuel and Surrounded by Degraded HLW .....	73
7.4.8.1 Degraded FFTF Mixture in a Flooded DOE SNF Canister .....	74
7.4.8.2 Minimum Mass of Gd Required .....	74
7.5 CALCULATIONS AND RESULTS – PART III: SCENARIOS WITH FISSILE MATERIAL DISTRIBUTED IN WASTE PACKAGE .....	75
7.5.1 Degraded DOE SNF Canister above Settled HLW Clay .....	75
7.5.2 Degraded DOE SNF Canister Settled at the Bottom .....	77
7.6 SUMMARY .....	78
8. CONCLUSIONS .....	79
8.1 STRUCTURAL ANALYSIS .....	79
8.2 THERMAL ANALYSIS .....	79
8.3 SHIELDING ANALYSIS .....	79



## CONTENTS (Continued)

	<b>Page</b>
8.4 GEOCHEMISTRY ANALYSIS .....	80
8.5 INTACT AND DEGRADED CRITICALITY ANALYSES .....	80
8.6 ITEMS IMPORTANT TO SAFETY .....	81
9. REFERENCES .....	83
9.1 DOCUMENTS CITED.....	83
9.2 CODES, STANDARDS, REGULATIONS, AND PROCEDURES .....	87

## FIGURES

	Page
2-1. Cross Section of 5-HLW/DOE SNF Long Waste Package.....	5
2-2. HLW Glass Canister.....	6
2-3. The Standardized 18-in. DOE SNF Canister.....	8
2-4. Cross-sectional View of the FFTF DOE SNF Canister .....	9
2-5. Isometric View of the FFTF DOE SNF Canister.....	9
2-6. FFTF Test Fuel Assembly.....	11
2-7. FFTF DFA Cross Section.....	11
2-8. Standard DFA Fuel Pin .....	12
2-9. Cross-sectional View of Partially Loaded Ident-69 Fuel Pin Container.....	12
3-1. Stresses in 5-HLW/DOE SNF Long Waste Package .....	33
4-1. Node Locations and Numbers on Part 1 of the Finite-element Representation (WP Basket and Hanford 15 ft HLW Canister) .....	35
4-2. Node Locations and Numbers on Part 2 of the Finite-element Representation (Ident-69 Fuel Pin Container).....	36
4-3. Temperature History for FFTF Codisposal WP.....	37
5-1. Vertical and Horizontal Cross Sections of MCNP Geometry Representation.....	39
5-2. Radial Segments Used for Dose-Rate Calculations.....	40
5-3. MCNP Estimates for Dose Rates in rem/h over Axial Surfaces and Segments .....	43
6-1. Internal Criticality Master Scenarios, Part 1 .....	47
6-2. Internal Criticality Master Scenarios, Part 2.....	48
6-3. Examples of Degraded Configurations from Class 1.....	49
6-4. Examples of Degraded Configurations from Class 2.....	49
6-5. Example of Degraded Configurations from Class 3 .....	49
6-6. Example of Degraded Configurations from Class 4 .....	50
6-7. Examples of Degraded Configurations from Class 5.....	50
6-8. Example of Degraded Configurations from Class 6 .....	50
6-9. Gd Species Concentration as a Function of pH .....	54
6-10. Concentrations of Phosphate Species in Equilibrium with $GdPO_4 \cdot 2H_2O$ , for Total Phosphate Concentrations of $10^{-5}$ , $10^{-3}$ , and $10^{-2}$ molal .....	55
7-1. Cross Section of 5-HLW/DOE SNF Long Waste Package with Six DFAs .....	61
7-2. Fuel Pin Configuration for Ident-69 Pin container Representations.....	62
7-3. Degradation Inside the DFAs .....	66
7-4. Axially Separated Fuel Pellets Inside the DFAs with Reflected Array Ident-69 Pin Container.....	67
7-5. Plutonium Decay Effects for Six DFAs and Five DFAs and a Uniform Array Ident-69 Pin Container .....	67
7-6. Degraded Assembly Ducts Inside Intact DOE SNF Canister Basket .....	68
7-7. Intact Fuel Pins in DOE SNF Canister with Degraded Basket and Assembly Ducts.....	70
7-8. Intact Ident-69 Container and Five Fully Degraded DFAs .....	71
7-9. DOE SNF Canister Containing a Degraded Ident-69 Container and Five Fully Degraded DFAs .....	72

## FIGURES (Continued)

	<b>Page</b>
7-10. Plutonium Decay Effects for Four DFAs and a Uniform Array Ident-69 Pin Container.....	73
7-11. Cross-sectional View of the DOE SNF Canister Settled in the Middle and on the Bottom of the WP .....	74
7-12. Degraded DOE SNF on Top of the Degraded HLW Glass Clay .....	76
7-13. WP Filled with HLW Clay Material Layer and FFTF SNF Layer .....	77
7-14. Layer of Fuel Mixed with the Layer of HLW Clay .....	77
7-15. Degraded DOE SNF Mixed with HLW Glass Clay at the Bottom of the WP .....	78

## TABLES

	Page
1-1. List of Supporting Documents.....	2
2-1. Codisposal Waste Package Dimensions and Material Specifications.....	5
2-2. Geometry and Material Specifications for HLW Glass Canisters .....	6
2-3. Geometry and Material Specifications for the DOE SNF Canister .....	7
2-4. Uranium and Plutonium Content of a Fresh DFA.....	13
2-5. Dimensions and Material Specifications for FFTF Types 4.1 and 4.2 Fuel Pins .....	13
2-6. Assembly Thermal Power .....	14
2-7. Gamma and Neutron Sources for a Type 4.1 (Outer) Assembly at 150 MWd/kg Burnup (decay of 5 years) .....	14
2-8. Gamma Sources for HLW Glass Canisters at One Day Decay Time .....	15
2-9. Neutron Sources for HLW Glass Canisters at One Day Decay Time .....	16
2-10. Chemical Composition of ASTM B 575 (Alloy 22) .....	16
2-11. Chemical Composition of ASTM A 516 Grade 70 Carbon Steel .....	16
2-12. Chemical Composition of Inconel Alloy 600 .....	17
2-13. Chemical Composition of Stainless Steel Type 304L .....	17
2-14. Chemical Composition of Stainless Steel Type 316L .....	17
2-15. Chemical Composition of Stainless Steel Type 302.....	18
2-16. Chemical Composition of SRS HLW Glass.....	18
2-17. Steel Degradation Rates .....	19
2-18. Glass Degradation Rates .....	19
2-19. MOX Characteristics and Degradation Rates .....	20
2-20. Composition of J-13 Well Water .....	21
3-1. Containment Structure Allowable Stress-Limit Criteria .....	30
3-2. 5-HLW/DOE SNF Long Waste Package FEA Stress Results .....	32
4-1. Physical Locations of Nodes of Interest.....	36
4-2. Peak Temperatures and Time of Occurrence for Each Case .....	37
5-1. Total Radial Dose Rates Averaged over a Height of 60 cm .....	41
5-2. Dose Rates in rem/h Averaged over Segment d .....	41
5-3. Radial Gamma Dose Rates in rem/hr Averaged over a Height of 60 cm.....	41
5-4. Dose Rates in rem/h Averaged over Segment d .....	41
6-1. Summary of Geochemistry Results.....	56
8-1. FFTF Codisposal WP Thermal Results and Governing Criteria .....	79

INTENTIONALLY LEFT BLANK

## ACRONYMS AND ABBREVIATIONS

ASME	American Society of Mechanical Engineers
BOL	beginning of life
BPVC	Boiler and Pressure Vessel Code
CRM	corrosion resistant material
CRWMS	Civilian Radioactive Waste Management System
CSCI	Computer Software Configuration Item
DBE	design basis event
DFA	driver fuel assembly
DOE	Department of Energy
EBOR	Experimental Beryllium Oxide Reactor
FEA	finite element analysis
FFTF	Fast Flux Test Facility
HLW	high-level waste
ID	inner diameter
IP	internal to the package
$k_{eff}$	effective multiplication factor
LCE	laboratory critical experiment
LLNL	Lawrence Livermore National Laboratory
M&O	Management and Operating Contractor
MGR	Monitored Geologic Repository
MOX	mixed-oxide
NSNFP	National Spent Nuclear Fuel Program
OCRWM	Office of Civilian Radioactive Waste Management
OD	outer diameter
PC	personal computer
PPF	power peaking factor
PWR	pressurized water reactor
QARD	Quality Assurance Requirements and Description
QAP	Quality Assurance Procedure
SCM	Software Configuration Management
SDD	System Description Document
SNF	spent nuclear fuel
SQR	Software Qualification Report
SRS	Savannah River Site
SS	stainless steel
TBV	to-be-verified
2-D	two-dimensional
3-D	three-dimensional

INTENTIONALLY LEFT BLANK

## **1. INTRODUCTION AND BACKGROUND**

There are more than 250 forms of U.S. Department of Energy (DOE)-owned spent nuclear fuel (SNF). Due to the variety of the spent nuclear fuel, the National Spent Nuclear Fuel Program (NSNFP) has designated nine representative fuel groups for disposal criticality analyses based on fuel matrix, primary fissile isotope, and enrichment. The Fast Flux Test Facility (FFTF) fuel has been designated as the representative fuel (INEEL 1998) for the mixed-oxide (MOX) fuel group, which is a mixture of uranium and plutonium oxides. Demonstration that other fuels in this group are bounded by the FFTF analysis remains for the future before acceptance of these fuel forms. As part of the criticality licensing strategy, NSNFP has provided a reviewed data report (INEEL 1998) with traceable data for the representative fuel type. The results of the analyses performed by using the information from this reviewed data report will be used to develop waste acceptance criteria which must be met by all fuel forms within the MOX fuel group including FFTF. The items that are important to safety are identified based on the information provided in the reviewed data report. Prior to acceptance of the fuel from MOX fuel group for disposal, the safety items of the fuel types that are being considered for disposal under the MOX fuel group must be demonstrated to satisfy the conditions set in Section 8.6, Items Important to Safety.

FFTF is DOE's 400-megawatt (thermal) sodium-cooled nuclear test reactor. The facility, which is located about 15 miles north of Richland, Washington, was built in 1978 to test plant equipment and fuel for the liquid-metal reactor development program. Although the FFTF is not a breeder reactor, this program demonstrated the technology for commercial breeder reactors. The FFTF was operated to verify the safety and optimal performance of the important reactor systems and components. FFTF also demonstrated the design and performance of MOX.

The analyses have been performed by following the disposal criticality analysis methodology that was documented in the topical report submitted to U.S. Nuclear Regulatory Commission (CRWMS M&O 1998a). The methodology includes analyzing the geochemical and physical processes that can breach the waste package and degrade the waste forms as well as the structural, thermal, shielding, and intact and degraded criticality. Addenda to the topical report will be required to establish the critical limit for the DOE SNF once sufficient critical benchmarks are identified and run. In this report, a conservative and simplified bounding approach is employed to designate an interim critical limit.

In this technical report there are numerous references to "codisposal container" and "waste package". Since the use of these two terms may be confusing, a definition of the terms is included here:

"(Co)disposal container" means the container barriers or shells, spacing structures and baskets, shielding integral to the container, packing contained within the container, and other absorbent materials designed to be placed internal to the container or immediately surrounding the disposal container (i.e., attached to the outer surface of the disposal container). The disposal container is designed to contain SNF and high-level waste (HLW), but exists only until the outer weld is complete and accepted. The disposal container does not include the waste form or the encasing containers or canisters (e.g., HLW pour canisters, DOE SNF codisposal canisters, multi-purpose canisters of SNF, etc.).



“Waste package” means the waste form and any containers (i.e., disposal container barriers and other canisters), spacing structures or baskets, shielding integral to the container, packing contained within the container, and other absorbent materials immediately surrounding and individual waste container placed internally to the container or attached to the outer surface of the disposal container. The waste package begins its existence when the outer lid weld of the disposal container is complete and accepted.

## 1.1 OBJECTIVE

The objective of this report is to provide sufficient detail to establish the technical viability for disposing of MOX (FFTF) SNF in the potential Monitored Geologic Repository (MGR). This report sets limits and establishes values that if and when these limits are met by a specific fuel type under the MOX fuel group, the results will be bounded by the results reported in this technical report.

Section 2, Design Inputs, describes the design basis, and identifies requirements and assumptions. Analytical results to demonstrate the adequacy of the design and evaluate the feasibility of codisposing the MOX (FFTF) SNF in the MGR are presented in Section 3 for Structural Analysis, Section 4 for Thermal Analysis, Section 5 for Shielding Analysis, Section 6 for Degradation and Geochemistry Analysis, and Section 7 for Intact and Degraded Criticality Analyses. Section 8, Conclusions, provides the connections between the design criteria and analytical results to establish technical viability. In addition, Section 8 gives recommendations regarding any additional needs for analysis or documentation. References are given in Section 9.

This technical document summarizes and analyzes the results of the detailed calculations that were performed in support of determining the evaluation of codisposal viability of MOX (FFTF) fuel. These calculation documents and the corresponding section in which they are summarized are shown in Table 1-1.

Table 1-1. List of Supporting Documents

Discipline	Document Title	Section Summarized	Reference
Structural	<i>5-High Level Waste DOE Spent Fuel Waste Package Structural Calculations</i>	Section 3	CRWMS M&O (1998b)
Thermal	<i>Thermal Evaluation of the FFTF Codisposal Waste Package</i>	Section 4	CRWMS M&O (1999b)
Shielding	<i>Dose Calculations for the Codisposal WP of HLW Canisters and the Fast Flux Test Facility (FFTF) Fuel</i>	Section 5	CRWMS M&O (1998c)
Degradation and Geochemistry	<i>EQ6 Calculations for Chemical Degradation of Fast Flux Test Facility (FFTF) Waste Packages</i>	Section 6	CRWMS M&O (1998e)
Intact Criticality	<i>Fast Flux Test Facility (FFTF) Reactor Fuel Criticality Calculations</i>	Section 7	CRWMS M&O (1999e)
Degraded Criticality	<i>Fast Flux Test Facility (FFTF) Reactor Fuel Degraded Criticality Calculation: Intact SNF Canister</i>	Section 7	CRWMS M&O (1999f)
	<i>Fast Flux Test Facility (FFTF) Reactor Fuel Degraded Criticality Calculation: Degraded SNF Canister</i>	Section 7	CRWMS M&O (1999g)

## 1.2 SCOPE

This technical report *Evaluation of Codisposal Viability for MOX (FFTF) DOE-Owned Fuel* evaluates and reports the performance of MOX (FFTF) SNF in a waste package. This technical document summarizes the evaluation of viability of the 5-HLW/DOE SNF Long (codisposal) waste package design with MOX (FFTF) SNF, which is the representative fuel for MOX fuel group. The remaining fuels in the same group must be demonstrated to be bounded by the values obtained from the reviewed data report, which is based on the FFTF DOE SNF.

## 1.3 QUALITY ASSURANCE

This technical document is based in part on existing data. However, the existing data is only used to determine the bounding values and items that are important to safety for the fuel group by establishing the limits based on the representative fuel type (FFTF) for this group (MOX fuel). Hence, the input values used for evaluation of codisposal viability of MOX (FFTF) SNF do not constitute data that have to be qualified prior to use of any results from this technical document for input into document supporting procurement, fabrication, or construction. They merely establish the bounds for acceptance. Since the input values are not relied upon directly to address safety and waste isolation issues, nor do the design inputs affect a system characteristic that is critical for satisfactory performance, according to the governing procedure (NLP-3-15, Rev. 5), data do not need to be controlled as TBV (to be verified). However, prior to acceptance of the fuel for disposal, the items that are identified as important to safety in Section 8.6 must be qualified by any means (e.g., experiment, non-destructive test, chemical assay, qualification under a program subject to DOE/RW-0333P, *Quality Assurance Requirements and Description* [QARD], requirements, etc.).

This technical document was prepared in accordance with the CRWMS M&O Quality Administrative Procedures (QAPs). The responsible manager for DOE Fuel Analysis has evaluated this report development activity in accordance with QAP-2-0, *Conduct of Activities*. The evaluation (CRWMS M&O 1999a) concluded that the development of this report is subject to the DOE Office of Civilian Radioactive Waste Management (OCRWM) *Quality Assurance Requirements and Description* controls. The Quality Assurance program applies to the development of this report. The information provided in this report is to be indirectly used in the evaluation of the codisposal viability of MOX fuel. The primary quality assurance requirement for the development and review of these documents will be provided by QAP-3-5, *Development of Technical Documents*.

There is no determination of importance evaluation developed in accordance with Nevada Line Procedure, NLP-2-0, *Determination of Importance Evaluations*, Rev. 5, since the report does not involve any field activity.

## **2. DESIGN INPUTS**

The data that were obtained from ASTM B 575-94, ASTM A 516/A 516M-90, ASTM G 1-90, Inco Alloys International, Inc. (1988), ASTM A 240/A 240M-97a, ASM (1990), ASTM A 276-91a, Inco Alloys International, Inc. (1985), ASME (1995), and Parrington et al. (1996) are considered accepted data. These references are standard handbooks, and due to the nature of these sources, the data in it are established fact and are therefore considered accepted. The data from Taylor (1997), Harrar et al. (1990), PNL (1987), OECD-NEA (1997), Bierman et al. (1979), and Taylor (1965) are considered qualified. The data from all other references are considered existing.

The number of digits in the values cited herein may be the result of a calculation or may reflect the input from another source; consequently, the number of digits should not be interpreted as an indication of accuracy.

### **2.1 DESIGN PARAMETERS**

Each of the following sections either describes the design of the waste package or identifies the basis of major parameters.

#### **2.1.1 Codisposal Waste Package**

The codisposal waste package contains five high-level waste (HLW) canisters surrounding a DOE standardized 18-in. SNF canister. The 5-HLW/DOE SNF Long waste package is based on the Viability Assessment (DOE 1998a) design of waste packages. The barrier materials of the waste package are typical of those used for commercial SNF waste packages. The inner barrier is composed of 20 mm of high-nickel alloy ASTM B 575 (Alloy 22) and serves as a corrosion-resistant material. The outer barrier comprises 100 mm of carbon steel (ASTM A 516 Grade 70) and serves as a corrosion-allowance material (CRWMS M&O 1997a, pp. 56 and 72). The outside diameter of the waste package is 2,120 mm and the length of the inside cavity is 4,617 mm (CRWMS M&O 1998b), which is designed to accommodate Hanford 15-foot HLW canister. The lids of the inner barrier are 25 mm thick; those of the outer barrier, 110 mm thick. There is a 30 mm gap between the inner and outer barrier upper lids. Each end of the waste package has a 225 mm long skirt. Table 2-1 summarizes the dimensions and materials of the waste package.

The DOE SNF canister is placed in a 31.75 mm thick carbon steel (ASTM A 516 Grade 70) support tube with a nominal outer diameter of 565 mm. The support tube is connected to the inside wall of the waste package by a web-like structure of carbon-steel (ASTM A 516 Grade 70) basket plates to support five long HLW canisters, as shown in Figure 2-1. The support tube and the plates are 4,607 mm long.

Table 2-1. Codisposal Waste Package Dimensions and Material Specifications

Component	Material	Parameter	Dimension (mm)
Outer barrier shell	ASTM A 516 Grade 70	Thickness	100
		Outer diameter	2,120
Inner barrier shell	ASTM B 575	Thickness	20
		Inner length	4,617
Top and bottom outer barrier lids	ASTM A 516 Grade 70	Thickness	110
Top and bottom inner barrier lids	ASTM B 575	Thickness	25
Gap between the upper inner and outer closure lids	Air	Thickness	30
Support tube	ASTM A 516 Grade 70	Outer diameter	565
		Inner diameter	501.5
		Length	4,607

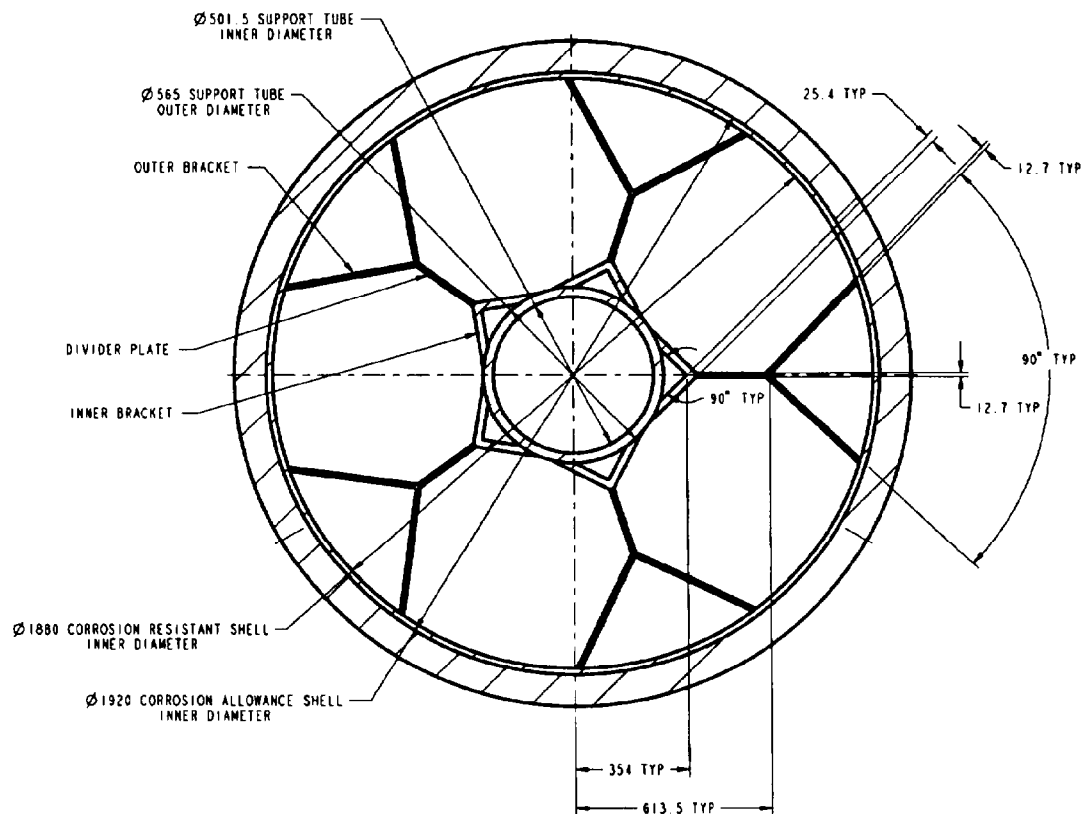


Figure 2-1. Cross Section of 5-HLW/DOE SNF Long Waste Package

### 2.1.2 HLW Glass Pour Canisters

There is no long Savannah River Site (SRS) HLW canister. Therefore, the Hanford 15-foot HLW canister is used in the FFTF waste package (Figure 2-2). Since the specific composition of

the Hanford HLW glass is not known at this time, the SRS glass composition is used in all analyses (Table 2-16) (TBV-3022). The Hanford 15-foot HLW canister is 4,572 mm long stainless steel Type 304L canister with an outer diameter of 610 mm (24.00 in.) (Taylor). The wall thickness is 10.5 mm. The maximum loaded canister weight is 4,200 kg and the fill volume is 87%. The heat generation from a single canister is 2,540 W. The geometry and material specifications for HLW glass canisters are given in Table 2-2.

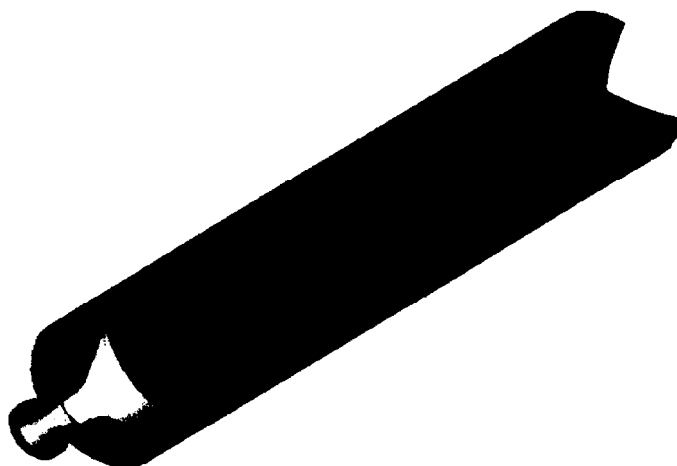


Figure 2-2. HLW Glass Canister

Table 2-2. Geometry and Material Specifications for HLW Glass Canisters

Component	Material	Parameter	Value
Hanford 15-ft Canister	SS 304L	Outer diameter	610 mm
		Wall thickness	10.5 mm
		Length	4,572 mm
		Total weight of canister and glass	4,200 kg
		Fill volume of glass in canister	87%

### 2.1.3 DOE SNF Canister

The information on the 18-in. DOE SNF canister conceptual design information is taken from INEEL (1998, pp. 5 and 6) and DOE (1998b). It is recognized that DOE (1998b) has been revised (DOE 1998c); however, only Revision 0 was available at the time the calculations reported in this technical document were performed. A review of the changes to the canister dimensions indicated that the impact on current results would be negligible (less than 0.7% decrease in internal cavity length; no material changes). The canister is a right circular cylinder of stainless steel (Type 316L) that contains a stainless steel (Type 316L) basket. The basket is not a standard part of the DOE SNF canister. The basket design is modified for each specific fuel type. The basket provides material for controlling criticality, provides structural support, and acts as a guide for assemblies during loading. The dimensions for the DOE SNF canister are a 457.2 mm (18.00 in.) outer diameter with a 9.525 mm (0.375 in.) wall thickness (Table 2-3).

The nominal internal length of the canister is 4,145 mm (163.2 in.); the nominal overall length, 4,569 mm (179.87 in.). A curved bottom carbon-steel impact disk that varies in thickness from 15.24 mm to 50.8 mm is located at both the top and bottom of the canister (see Figure 2-3). In addition, there is a 12.7 mm thick curved plate and a 12.7 mm thick flat plate in each end of the canister.

The DOE SNF canister for FFTF fuels contains six basket locations; one center position surrounded by five outer positions. Either an Ident-69 fuel pin container or a driver fuel assembly (DFA) can be placed in the center position. All outer positions are filled with DFAs only. Maximum loaded weight of the canister is 2,721 kg. A cross-sectional and an isometric view of the DOE SNF canister containing five FFTF assemblies and an Ident-69 fuel pin container are shown in Figures 2-4 and 2-5, respectively.

The basket consists of a cylindrical center tube and five divider plates extending radially from the center tube to the DOE SNF canister wall as shown in Figure 2-4. The center tube is stainless steel (Type 316L) with a 153 mm inside diameter and 10 mm wall thickness. The divider plates are also stainless steel (Type 316L) with a 10 mm thickness. The basket height is 4,125 mm.

Table 2-3. Geometry and Material Specifications for the DOE SNF Canister

Component	Material	Parameter	Dimension (mm)
Circular cylinder	SS 316L	Outer diameter	457.2
		Wall thickness	9.525
		Internal length	4,145
Impact plate	ASTM A 516 Grade 70	Thickness	from 15.24 to 50.8 at the top and bottom
Top and bottom curved plates	SS 316L	Thickness	12.7
Top and bottom flat plates	SS 316L	Thickness	12.7

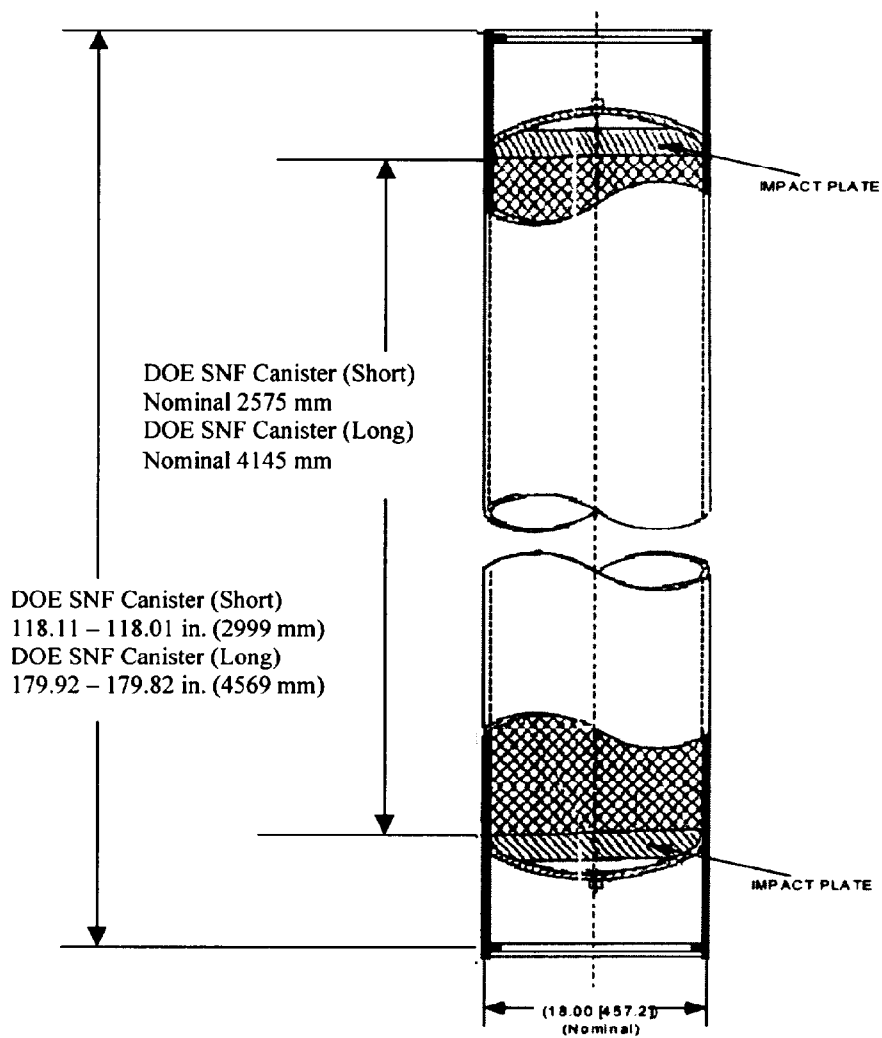


Figure 2-3. The Standardized 18-in. DOE SNF Canister

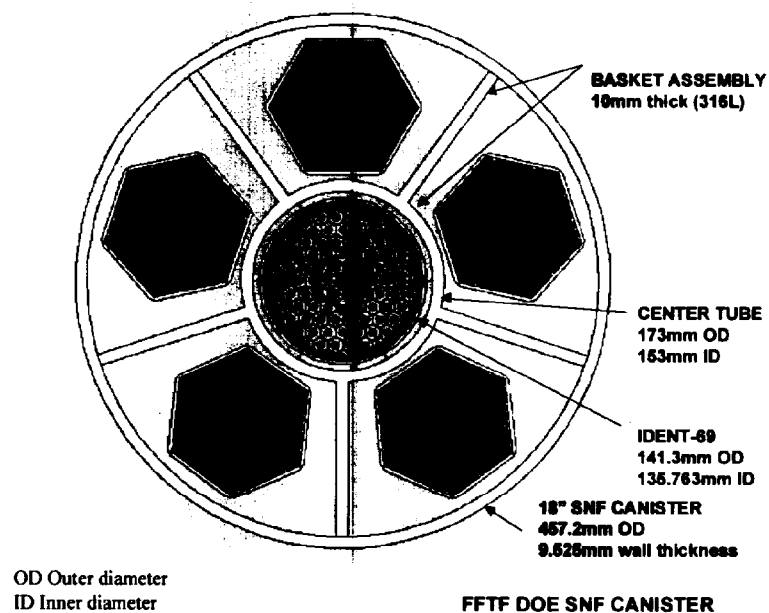


Figure 2-4. Cross-sectional View of the FFTF DOE SNF Canister

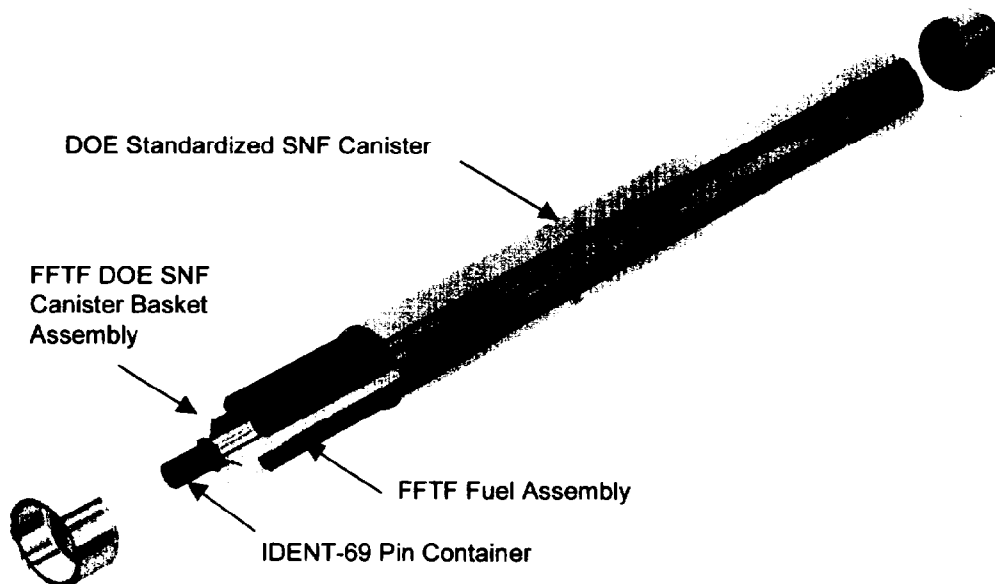


Figure 2-5. Isometric View of the FFTF DOE SNF Canister



#### 2.1.4 FFTF DOE SNF

The following dimensions and information in this section are from INEEL (1998, pp. 1-5). The FFTF standard DFA contains 217 cylindrical fuel pins and is hexagonally shaped. An axial view of a typical test fuel (169 fuel pins) assembly is shown in Figure 2-6 and a cross-sectional view of a typical DFA (217 fuel pins) appears in Figure 2-7 – the hexagonal cells seen in the figure are an artifact of the analysis modeling. The assembly is 3,657.6 mm long. The overall height of a fuel pin is 2,372.36 mm for Types 3.1 and 4.1 fuel pins, and 2,377.44 mm for Types 3.2 and 4.2 fuel pins. The stainless steel (Type 316) cladding is 0.381 mm (0.015 in.) thick. The inner and outer diameters of the cladding are 5.08 mm (0.200 in.) and 5.842 mm (0.230 in.), respectively. Each fuel pin has a 914.4 mm (36 in.) long fuel region containing fuel pellets with an outer diameter of 4.9403 mm (0.1945 in.). The fuel region is centered 1,663.7 mm (65.5 in.) from the bottom of the assembly. Each fuel pin is helically wrapped with a 1.4224 mm (0.056 in.) diameter stainless steel Type 316 wire to provide lateral spacing along its length. The wire pitch is 304.8 mm (12 in.). The fuel pins are arranged with a triangular pitch within the hexagonal duct. The fuel density is reported as 90.4% of the theoretical density, which corresponds to a fuel pellet density of 10.02 g/cm<sup>3</sup>. The mixed oxide (MOX – UO<sub>1.96</sub> and PuO<sub>1.96</sub>) fuel region is followed by 20.32 mm (0.8 in.) of natural UO<sub>2</sub> insulator pellets and 144.78 mm (5.7 in.) of Inconel 600 reflector on each end. The density of natural uranium insulator pellets is 10.42 ± 0.22 g/cm<sup>3</sup>. The reflector outer diameter is 4.8133 mm (0.1895 in.). Above the top reflector are a stainless steel Type 302 spring (125.5 mm long by 0.8052 mm in diameter) and a stainless steel Type 316 plenum (862.1 mm long with a 4.9022 mm outer diameter and 0.1397 mm wall thickness). The maximum stainless steel spring volume is 2.7264 cm<sup>3</sup>. The fuel pin is closed with top and bottom caps having a 5.842 mm diameter. The length of the top cap is 104.6 mm. The bottom cap length for Type 3.1 and 4.1 fuels is 35.6 mm. The bottom cap length for Type 3.2 and 4.2 fuels is 40.6 mm. Each fuel pin weighs 455 g (~1 lb). A simplified axial view of a fuel pin is shown in Figure 2-8. The fuel enrichments and isotopic fractions for all four types of fresh FFTF fuel are given in Table 2-4. Table 2-5 summarizes dimensions and material specifications for fuel pins. Note that Types 3.1 and 4.1 fuel pins and Types 3.2 and 4.2 fuel pins have the same dimensions.

The DFA comprises a hexagonal duct that surrounds the fuel pins, discriminator, inlet nozzle, neutron shield and flow orifice region, load pads, and handling socket. The duct is stainless steel Type 316 with a wall thickness of 3.048 mm (0.12 in.). The duct-tube outer dimension is 116.205 mm (4.575 in.) across the hexagonal flats and 131.064 mm (5.16 in.) across the opposite hexagonal points. The fuel pin pitch is 7.2644 mm (0.286 in.). The maximum assembly width is determined by the load pads, which are 138.1125 mm (5.4375 in.) wide across the opposite hexagonal points. The assembly is 3657.6 mm (144 in.) high. Total weight of a DFA is 172.819 kg (~381 lb).

Some of the assemblies have been disassembled and the fuel pins placed in fuel pin containers named Ident-69 pin containers. Although there are several types of pin containers, the most reactive pin container is the compartmented model, which can hold up to 217 fuel pins. The total container length is 3,657.6 mm (144 in.). The Ident-69 containers are made with 5 in. stainless steel Type 304L pipe (actual outer diameter is 5.563 in. or 141.30 mm) with a transition to 2.5 in.

pipe (actual outer diameter is 2.875 in., or 73.02 mm) at 431.8 mm (17 in.) from the bottom. The inside diameter of the container is 135.763 mm (5.345 in.). The fuel pins are supported on a grid plate with 1.5875 mm (0.0625 in.) diameter holes. The central compartment has inside and outside radii of 20.701 mm (0.815 in.) and 22.225 mm (0.875 in.), respectively. The empty weight of an Ident-69 container is 59.09 kg (130 lb). A cross-sectional view of a partially loaded Ident-69 fuel pin container is shown in Figure 2-9.

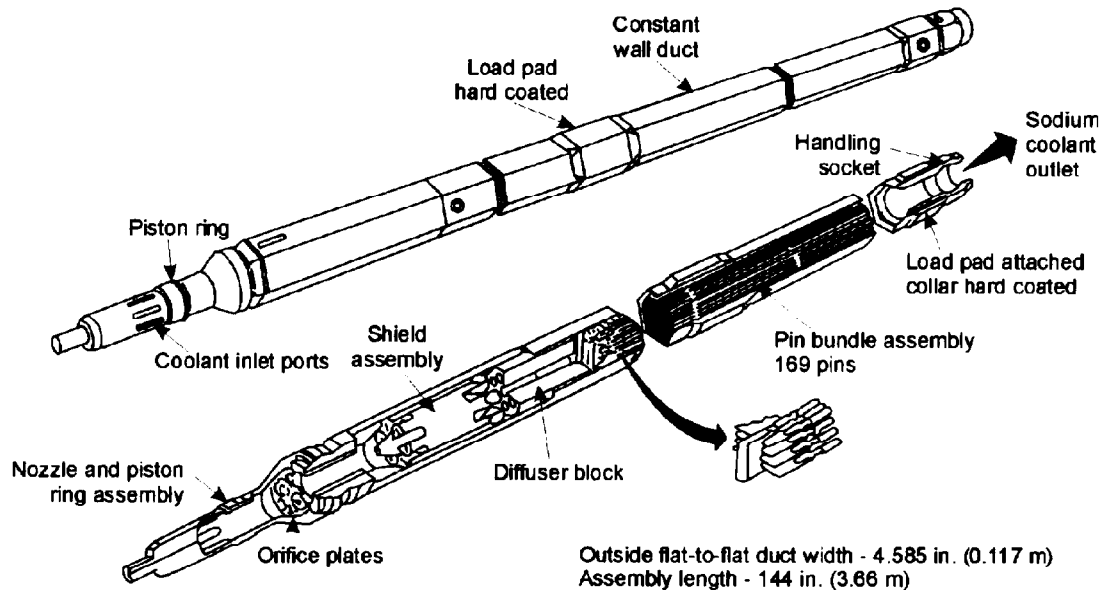


Figure 2-6. FFTF Test Fuel Assembly

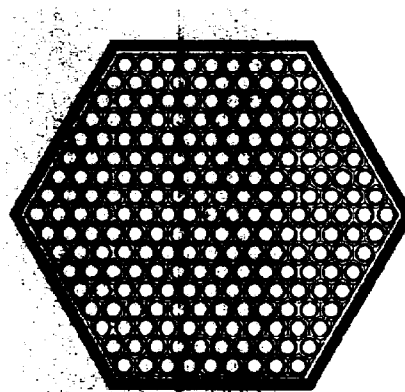
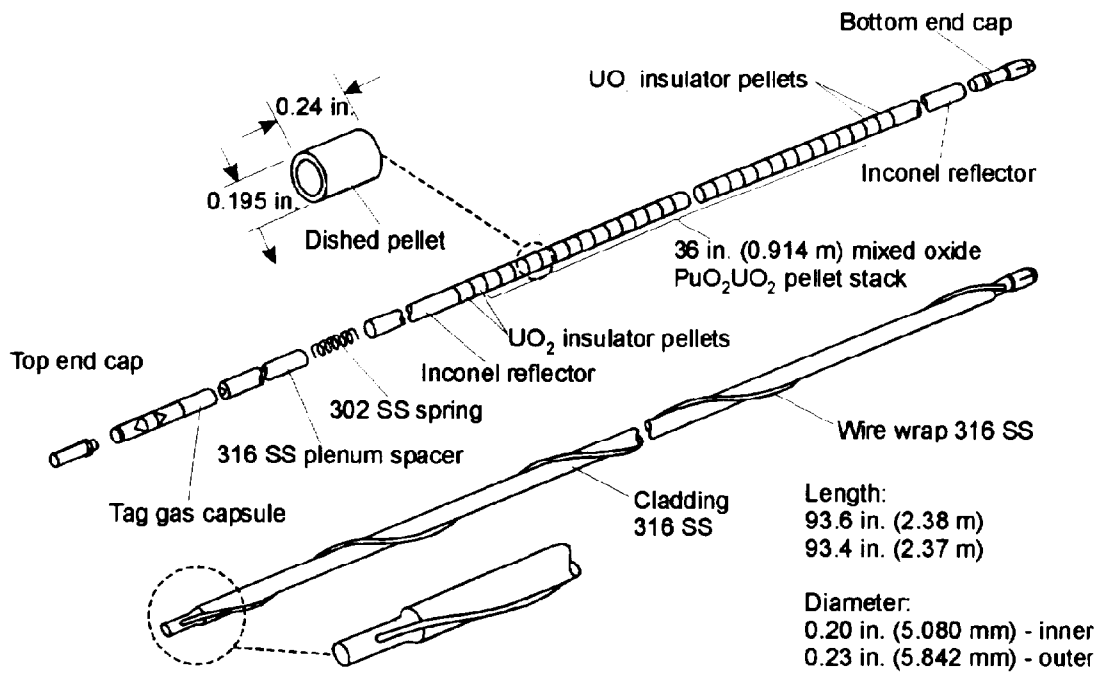


Figure 2-7. FFTF DFA Cross Section



C98 0602 2

Figure 2-8. Standard DFA Fuel Pin

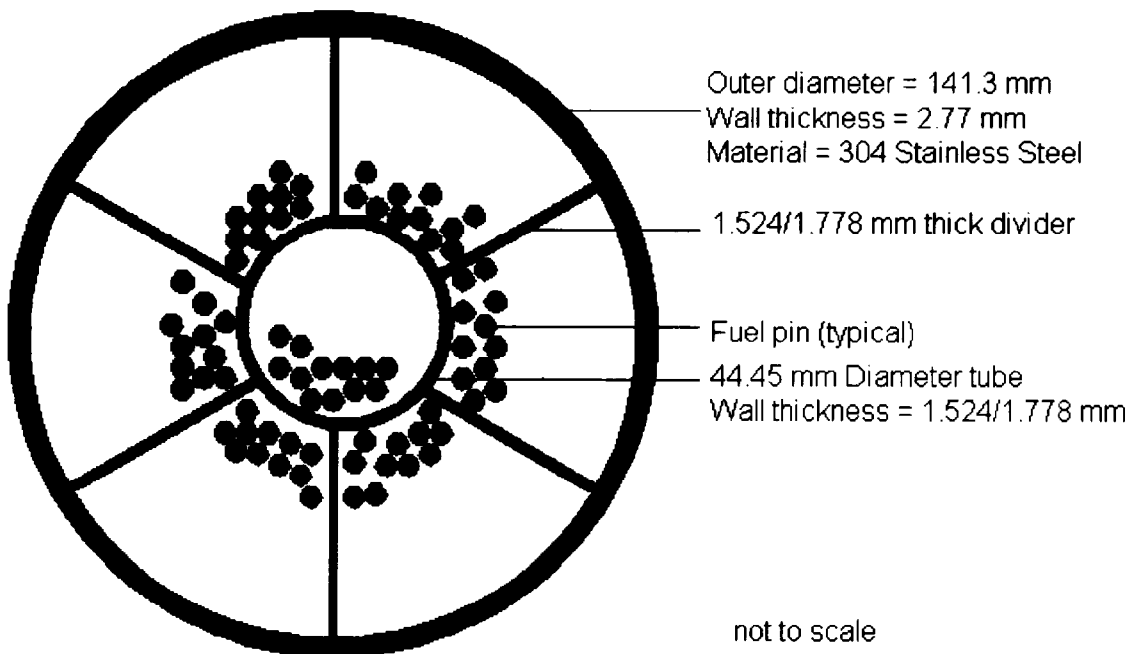


Figure 2-9. Cross-sectional View of Partially Loaded Ident-69 Fuel Pin Container

Table 2-4. Uranium and Plutonium Content of a Fresh DFA

		Driver Fuel Type			
		3.1	3.2	4.1	4.2
<b>Plutonium</b>					
	Enrichment (%Pu/[Pu+U])	27.37	22.43	29.28	25.14
	Assembly content (kg)	9.071	7.421	9.722	8.333
	Fuel pin content (g)	41.8	34.2	44.8	38.4
	Isotopic fraction				
	Pu-239	0.8696	0.8696	0.8711	0.8711
	Pu-240	0.1173	0.1173	0.1163	0.1163
	Pu-241	0.0104	0.0104	0.0102	0.0102
<b>Uranium</b>					
	Enrichment (%U/[Pu+U])	72.63	77.57	70.72	74.86
	Assembly content (kg)	24.070	25.666	23.481	24.813
	Fuel pin content (g)	110.9	118.3	108.2	114.3
	Isotopic fraction				
	U-235	0.007	0.007	0.002	0.002
	U-238	0.993	0.993	0.998	0.998

Note: Each assembly nominally holds 1.5 kg of uranium in insulator pellets.

Table 2-5. Dimensions and Material Specifications for FFTF Types 4.1 and 4.2 Fuel Pins

Component	Material	Parameter	Value
Mixed oxide	UO <sub>1.96</sub> -PuO <sub>1.96</sub>	Outer diameter	4.9403 mm
		Length	914.4 mm
		Density	10.02 g/cm <sup>3</sup>
Insulator	Natural UO <sub>2</sub>	Parts/fuel rod	2
		Length	20.32 mm
		Outer diameter	5.08 mm
		Density	10.42 ± 0.22 g/cm <sup>3</sup>
		U weight/assembly	15 kg
Reflector	Inconel 600	Parts/fuel rod	2
		Length	144.78 mm
		Outside diameter	4.8133 mm
Spring	SS 302	Volume	2.7264 cm <sup>3</sup>
Plenum	SS 316	Length	862.1 mm
		Outer diameter	4.9022 mm
		Wall thickness	0.1397 mm
Top cap	SS 316	Length	104.6 mm
		Outer diameter	5.842 mm
Bottom cap	SS 316	Length	40.6 mm, Type 4.2 35.6 mm, Type 4.1
		Outer diameter	5.842 mm
Cladding	SS 316	Inner diameter	5.08 mm
		Outer diameter	5.842 mm
		Length	2,232.24 mm

### 2.1.5 Thermal

The heat generation rate from a Hanford 15-foot HLW glass canister is 2,540 W (Taylor 1997). The total heat released from the fuel irradiated to 150 MWd/kgHM (megawatt day per kilogram of heavy metal) burnup is given in Table 2-6 (INEEL 1998, Table B-3). The thermal properties of the FFTF fuel are determined as described in CRWMS M&O (1999b).

Table 2-6. Assembly Thermal Power

Time	Type 4.1 Fuel (W/assembly)	Type 4.2 Fuel (W/assembly)
Discharge	2.367E+05	3.153E+05
1 year	1.521E+03	1.783E+03
5 years	2.307E+02	2.447E+02
10 years	1.388E+02	1.379E+02
20 years	1.135E+02	1.103E+02
30 years	9.992E+01	9.617E+01
40 years	8.928E+01	8.522E+01
50 years	8.064E+01	7.639E+01
60 years	7.356E+01	6.921E+01
100 years	5.588E+01	5.137E+01

The thermal conductivity of the HLW glass is approximated as that of pure borosilicate glass, while the properties of density and specific heat are approximated as those of Pyrex glass. As with the other waste package components, only the axial cross section at the center of the canister is represented in the calculations. The values of thermal conductivity, specific heat, and density for borosilicate glass are 1.1 W/m/K, 835.0 J/kg/K, and 2,225.0 kg/m<sup>3</sup> respectively. The thermal conductivity is the mid-range value for a temperature range of 100 °C to 500 °C (CRWMS M&O 1995a, p. 13). The density and specific heat are taken to be the same as that of Pyrex glass at 27 °C (300 K) (CRWMS M&O 1995a, p. 13).

#### 2.1.6 Shielding Source Term

The maximum irradiation exposure of any standard DFA or test DFA is less than 150 MWd/kgHM. The photon spectrum for outer Type 4.1 and inner Type 4.2 DFAs with a burnup rate of 150 MWd/kgHM and 5 years' decay are given in Table 2-7 (INEEL 1998, pp. B-2, B-3). The total neutron source for outer Type 4.1 and inner Type 4.2 DFAs with a burnup rate of 150 MWd/kgHM and 5 years' decay are 5.532E+06 and 5.304E+06, respectively.

The Hanford 15-ft HLW canister (CRWMS M&O 1997b, Attachment IV, pp. 17-18) gamma and neutron source spectra per canister are given in Tables 2-8 and 2-9, respectively.

Table 2-7. Gamma and Neutron Sources for a Type 4.1 (Outer) Assembly at 150 MWd/kg Burnup (decay of 5 years)

Upper Energy Boundary (MeV)	Average Energy (MeV)	Type 4.1 (Outer) Assembly Gamma Intensity (photons/sec)	Type 4.2 (Inner) Assembly Gamma Intensity (photons/sec)
0.02	0.0150	3.948E+14	4.324E+14
0.03	0.0250	1.084E+14	1.192E+14
0.05	0.0375	1.088E+14	1.170E+14
0.07	0.0575	8.088E+13	8.850E+13
0.10	0.0850	5.942E+13	6.503E+13
0.15	0.1250	5.091E+13	5.659E+13
0.30	0.2250	4.498E+13	5.026E+13

Upper Energy Boundary (MeV)	Average Energy (MeV)	Type 4.1 (Outer) Assembly Gamma Intensity (photons/sec)	Type 4.2 (Inner) Assembly Gamma Intensity (photons/sec)
0.45	0.3750	3.533E+13	3.936E+13
0.70	0.5750	6.744E+14	7.092E+14
1.00	0.8500	9.899E+13	1.168E+14
1.50	1.2500	3.812E+13	4.495E+13
2.00	1.7500	1.210E+12	1.394E+12
2.50	2.2500	6.720E+11	8.051E+11
3.00	2.7500	3.660E+10	4.274E+10
4.00	3.5000	4.726E+09	5.515E+09
6.00	5.0000	2.234E+05	2.147E+05
8.00	7.0000	2.564E+04	2.465E+04
14.00	11.0000	2.941E+03	2.827E+03
	Total	1.697E+15	1.842E+15

Table 2-8. Gamma Sources for HLW Glass Canisters at One Day Decay Time

Upper Energy Boundary (MeV)	Average Energy (MeV)	Hanford Total (photons/sec)
0.05	0.0300	1.8146E+15
0.10	0.0750	5.4889E+14
0.20	0.1500	4.7466E+14
0.30	0.2500	1.2071E+14
0.40	0.3500	9.1562E+13
0.60	0.5000	1.7230E+14
0.80	0.7000	1.6393E+15
1.00	0.9000	3.7161E+13
1.33	1.1650	2.0984E+13
1.66	1.4950	7.9660E+12
2.00	1.8300	1.1438E+12
2.50	2.2500	8.7440E+12
3.00	2.7500	4.7252E+10
4.00	3.5000	5.0532E+09
5.00	4.5000	6.0452E+04
6.50	5.7500	2.4156E+04
8.00	7.2500	4.7201E+03
10.00	9.0000	9.9949E+02
	Total	4.9381E+15

Table 2-9. Neutron Sources for HLW Glass Canisters at One Day Decay Time

Upper Energy Boundary (MeV)	Average Energy (MeV)	Hanford Total (n/sec)
20.000	13.2150	4.000E+04
6.430	4.7150	1.145E+07
3.000	2.4250	8.683E+06
1.850	1.6250	1.733E+06
1.400	1.1500	1.834E+06
0.900	0.6500	1.563E+06
0.400	0.2500	5.418E+05
0.100	0.0585	7.144E+04
0.017		
	Total	2.591E+07

### 2.1.7 Material Compositions

The chemical compositions of the materials used in the analyses are given in Tables 2-10 through 2-16. The composition of the HLW glass shown in Table 2-16 is based on the assumption that both 3-m and 15-ft canisters have the same glass composition.

Table 2-10. Chemical Composition of ASTM B 575 (Alloy 22)

Element	Composition (wt%)	Value Used (wt%)
Carbon (C)	0.015 (max)	0.15
Manganese (Mn)	0.50 (max)	0.50
Silicon (Si)	0.08 (max)	0.08
Chromium (Cr)	20.0 - 22.5	21.25
Molybdenum (Mo)	12.5 - 14.5	13.5
Cobalt (Co)	2.50 (max)	2.50
Tungsten (W)	2.5 - 3.5	3.0
Vanadium (V)	0.35 (max)	0.35
Iron (Fe)	2.0 - 6.0	4.0
Phosphorus (P)	0.02 (max)	0.02
Sulfur (S)	0.02 (max)	0.02
Nickel (Ni)	Remainder	54.63
Density = 8.69 g/cm <sup>3</sup>		

Source: ASTM B 575-94, page 2.

Table 2-11. Chemical Composition of ASTM A 516 Grade 70 Carbon Steel

Element	Composition (wt%)	Value Used (wt%)
Carbon (C)	0.30 (max)	0.30
Manganese (Mn)	0.85-1.20	1.025
Phosphorus (P)	0.035 (max)	0.035
Sulfur (S)	0.035 (max)	0.035
Silicon (Si)	0.15-0.40	0.275
Iron (Fe)	Balance	98.33
Density* = 7.832 g/cm <sup>3</sup>		

Source: ASTM A 516/A 516M-90, page 2.

\*Density of this material is given as 7.850 g/cm<sup>3</sup> in ASTM G 1-90, page 7.

Table 2-12. Chemical Composition of Inconel Alloy 600

Element	Composition (wt%)	Value Used (wt%)
Nickel (Ni)	72.00 (min)	74.335
Chromium (Cr)	14.0 - 17.0	15.5
Iron (Fe)	6.0 - 10.0	8.0
Carbon (C)	0.15 (max)	0.15
Manganese (Mn)	1.0 (max)	1.0
Sulfur (S)	0.015 (max)	0.015
Silicon (Si)	0.5 (max)	0.5
Copper (Cu)	0.5 (max)	0.5
Density = 8.47 g/cm <sup>3</sup>		

Source: Inco Alloys International, Inc. (1988, p. 9).

Table 2-13. Chemical Composition of Stainless Steel Type 304L

Element	Composition (wt%)	Value Used (wt%)
Carbon (C)	0.03 (max)	0.03
Manganese (Mn)	2.00 (max)	2.00
Phosphorus (P)	0.045 (max)	0.045
Sulfur (S)	0.03 (max)	0.03
Silicon (Si)	0.75 (max)	0.75
Chromium (Cr)	18.00 - 20.00	19.00
Nickel (Ni)	8.00 - 12.00	10.00
Nitrogen (N)	0.10	0.10
Iron (Fe)	Balance	68.045
Density* = 7.94 g/cm <sup>3</sup>		

Source: ASTM A 240/A 240M-97a, page 2.

\*Density of this material is given as 7.94 g/cm<sup>3</sup> in ASTM G 1-90, page 7 and as 8.0 g/cm<sup>3</sup> in ASM (1990, p. 871).

Table 2-14. Chemical Composition of Stainless Steel Type 316L

Element	Composition (wt%)	Value Used (wt%)
Carbon (C)	0.03 (max)	0.03
Manganese (Mn)	2.00 (max)	2.00
Phosphorus (P)	0.045 (max)	0.045
Sulfur (S)	0.03 (max)	0.03
Silicon (Si)	1.00 (max)	0.75
Chromium (Cr)	16.00 - 18.00	17.00
Nickel (Ni)	10.00 - 14.00	12.00
Molybdenum (Mo)	2.00 - 3.00	2.50
Nitrogen (N)	0.10 (max)	0.10
Iron (Fe)	Balance	65.545
Density* = 7.98 g/cm <sup>3</sup>		

Source: ASTM A 276-91a, page 2.

\*Density of this material is given as 7.98 g/cm<sup>3</sup> in ASTM G 1-90, page 7 and as 8.0 g/cm<sup>3</sup> in ASM (1990, p. 871).



Table 2-15. Chemical Composition of Stainless Steel Type 302

Element	Composition (wt%)	Value Used (wt%)
Carbon (C)	0.15	0.15
Manganese (Mn)	2.0	2.0
Phosphorus (P)	0.045	0.045
Sulfur (S)	0.03	0.03
Silicon (Si)	0.75	0.75
Chromium (Cr)	17.0 - 19.0	18.0
Nickel (Ni)	8.0 - 10.0	9.0
Nitrogen (N)	0.10 (max)	0.10
Iron (Fe)	Balance	69.925
Density* = 8.00 g/cm <sup>3</sup>		

Source: ASM (1990, p. 843).

\*Density of this material is from ASM (1990, p. 871).

Table 2-16. Chemical Composition of SRS HLW Glass

Component	Water Free Weight Percent	Radioisotope	g/Canister
Ag	0.05	Rh-103m	0.5028E-15
Al <sub>2</sub> O <sub>3</sub>	3.96	Sm-149	0.742E+1
B <sub>2</sub> O <sub>3</sub>	10.28	U-233	0.1636E-3
BaSO <sub>4</sub>	0.14	U-234	0.5485E+1
Ca <sub>3</sub> (PO <sub>4</sub> ) <sub>2</sub>	0.07	U-235	0.7278E+2
CaO	0.85	U-236	0.1742E+2
CaSO <sub>4</sub>	0.08	U-238	0.3122E+5
Cr <sub>2</sub> O <sub>3</sub>	0.12	Np-237	0.1263E+2
Cs <sub>2</sub> O	0.08	Pu-238	0.8667E+2
CuO	0.19	Pu-239	0.2076E+3
Fe <sub>2</sub> O <sub>3</sub>	7.04	Pu-240	0.3809E+2
FeO	3.12	Pu-241	0.1620E+2
K <sub>2</sub> O	3.58	Pu-242	0.3206E+1
Li <sub>2</sub> O	3.16	Am-241	0.3210E+1
MgO	1.36	Am-242m	0.1488E-2
MnO	2.00	Am-243	0.2902E-1
Na <sub>2</sub> O	11.00	Cm-245	0.3910E-4
Na <sub>2</sub> SO <sub>4</sub>	0.36		
NaCl	0.19		
NaF	0.07		
NiO	0.93		
PbS	0.07		
SiO <sub>2</sub>	45.57		
ThO <sub>2</sub>	0.21		
TiO <sub>2</sub>	0.99		
U <sub>3</sub> O <sub>8</sub>	2.20		
Zeolite	1.67		
ZnO	0.08		
Others	0.58		
Total	100.00		
Density at 25°C = 2.85 g/cm <sup>3</sup> (CRWMS M&O 1998c, Attachment V)			

Source: Stout, R.B. and Leider, H.R. (1991), pages 2.2.1.4-3 through 2.2.1.4-5, and page 2.2.1.4-11.

### 2.1.8 Degradation and Geochemistry

This section identifies the degradation rate of the principal alloys, the chemical composition of J-13 well water, and the drip rate of J-13 well water into a waste package. These rates are used in Section 6, Degradation and Geochemistry Analysis.

#### 2.1.8.1 Physical and Chemical Characteristics of the FFTF Waste Package

Table 2-17 summarizes the degradation rates of the principal alloys used in the calculations. The upper rate for A 516 is 60 °C, 100-year rate from Figure 5.4-3 of CRWMS M&O (1995b), and the lower rate for A 516 is the 0-year rate from the same figure and reference. The 304L and 316L rates are estimated from CRWMS M&O (1997c, pp. 11-13). For a comparable specific surface area, the carbon steel is expected to degrade much more rapidly than the stainless steels (Type 316L and Type 304L). In addition, the stainless steels contain significant amounts of chromium (Cr) and molybdenum (Mo), and under the assumption of complete oxidation, would produce more acid, per unit volume, than the carbon steel.

Table 2-17. Steel Degradation Rates

	A 516 Carbon Steel	SS 304L	SS 316L	SS 316L with 3 wt% GdPO <sub>4</sub>
Average rate (μm/year)	35	0.1	0.1	0.1
Average rate (moles/cm <sup>2</sup> /sec)	1.58E-11	4.58E-14	4.55E-14	4.55E-14
High rate (μm/year)	100.0	1.0	1.0	1.0
High rate (moles/cm <sup>2</sup> /sec)	4.51E-11	4.58E-13	4.55E-13	4.55E-13

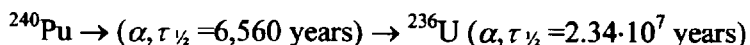
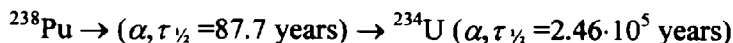
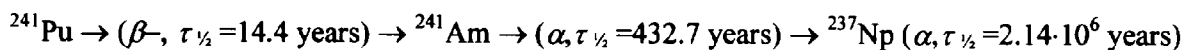
Table 2-18 rates for glass degradation are taken from CRWMS M&O (1995b), Figure 6.2-5. The high rate corresponds approximately to a pH 9 at 70 °C; the low rate, to a pH 8 at 25 °C.

Table 2-18. Glass Degradation Rates

Low rate (g/m <sup>2</sup> /day)	1E-04
Low rate (moles/cm <sup>2</sup> /sec)	1.1574E-15
High rate (g/m <sup>2</sup> /day)	3E-02
High rate (moles/cm <sup>2</sup> /sec)	3.4722E-13

Table 2-19 summarizes the characteristics and degradation rates of the MOX fuel. The calculations used the composition of fresh fuel. Using values for fresh fuel is conservative, since most fission products have significant neutron-absorption cross sections, and the unirradiated fuel has a higher fissile content than that of partially spent fuel. However, since it is expected that very few waste packages will be breached before 3,000 years post-emplacement (CRWMS M&O 1998d, p. 3-65), and that most of the calculation will involve post-emplacement periods greater than 10,000 years, the "fresh fuel" composition used in EQ6 geochemistry calculations is altered to pre-decay some of the shorter-lived isotopes. Since EQ3/6 does not have the capability

to decay isotopes, this must be done manually. The isotopes Pu-241, Pu-238, and Pu-240 are decayed per the following decay chains prior to being input to the EQ3/6 calculations:



where  $\tau_{1/2}$  is the decay half-life for the specified decay mode (Parrington et al. 1996).

In a waste package breach scenario, the carbon steel waste package basket will be exposed to water before the rest of the waste package, and is expected to degrade within a few hundred to a few thousand years after breach. The transformation of the basket into hematite ( $\text{Fe}_2\text{O}_3$ ) can decrease the remaining void space in the package by approximately 13%, and the transformation to goethite ( $\text{FeOOH}$ ) can decrease the void space by approximately 22% (CRWMS M&O 1998e, p. 20).

Table 2-19. MOX Characteristics and Degradation Rates

Average molecular weight (U, Pu, Np) $\text{O}_2$	270.37
Density fuel pellets ( $\text{g}/\text{cm}^3$ )	10.02
Average fuel degradation rate ( $\text{mg}/\text{m}^2/\text{day}$ )	2.8234
Average fuel degradation rate ( $\text{moles}/\text{cm}^2/\text{sec}$ )	1.2087E-14
Fast fuel degradation rate ( $\text{mg}/\text{m}^2/\text{day}$ )	13.837
Fast fuel degradation rate ( $\text{moles}/\text{cm}^2/\text{sec}$ )	5.9235E-14

Source: CRWMS M&O (1995b, p. 6-2), CRWMS M&O (1998e, p. 19).

$\text{GdPO}_4$  is used in the waste package to decrease the potential for internal criticality.  $\text{GdPO}_4$  is in or on the basket structure inside the DOE canister, but the method of inclusion is not yet determined. For this study,  $\text{GdPO}_4$  is added as solid inclusions to hypothetical stainless steel Type 316L. The rate of exposure of the  $\text{GdPO}_4$ -steel mix is then taken to be the corrosion rate of stainless steel Type 316L (Table 2-17).

Each fuel pin contains two Inconel reflectors. Based on corrosion rates listed in Inco Alloys International, Inc. (1985), this Inconel alloy has general corrosion properties similar to Alloy 22 and is considered inert per Assumption 2.3.4.2.

While the composition of unirradiated MOX is as shown in Table 2-4, the characteristics of irradiated fuel must be considered in estimating reaction rates. In particular, irradiated FFTF fuels can have numerous cracks and central voids. The degradation rates in Table 2-19 are the degradation rates for irradiated commercial fuel (CRWMS M&O 1995b, p. 6-2, equation 6.2-1) and a multiplication factor (CRWMS M&O 1995b, p. 6-5) is used to account for the increased surface areas due to fractures and porosity resulting from irradiation.

### 2.1.8.2 Chemical Composition of J-13 Well Water

The geochemistry calculations reported in this document have used the well-known J-13 composition, which is reproduced in Table 2-20 (Harrar, et al. 1990), for water dripping into the waste package. Since this water composition was determined from a well drilled into the saturated zone beneath the planned repository location, there is some question of the compositional deviations to be expected for water dripping into the repository drift, which is in the unsaturated zone. Several alternative versions of the J-13 composition have been proposed and used in other geochemistry calculations. The following two paragraphs summarize current thinking on the sensitivity of geochemistry results to potential variations in the composition of the indripping water.

Table 2-20. Composition of J-13 Well Water

Component	(mg/l)
Na <sup>+</sup>	45.8
K <sup>+</sup>	5.04
Ca <sup>2+</sup>	13.0
Mg <sup>2+</sup>	2.01
NO <sub>3</sub> <sup>-</sup>	8.78
Cl <sup>-</sup>	7.14
F <sup>-</sup>	2.18
SO <sub>4</sub> <sup>2-</sup>	18.4
Si <sup>2+</sup>	28.5
PO <sub>4</sub> <sup>3-</sup>	0.12
Alkalinity (assumed to be HCO <sub>3</sub> <sup>-</sup> )	128.9
pH = 7.41	

Source: Harrar et al., Tables 4.1 and 4.2.

Two major factors control how the J-13 chemistry might affect EQ6 calculations. The first factor is the presumed CO<sub>2</sub> pressure of equilibration, which is closely coupled to the pH of the J-13; and the second is the content of dissolved species, which may react with package materials and fuel, and thus affect solubilities. An example of the second factor is the amount of available dissolved silica, which can precipitate uranium as insoluble minerals like soddyite and uranophane.

In other analyses of codisposal packages, order of magnitude variations in CO<sub>2</sub> pressure have not had significant effects on the calculated (CRWMS M&O 1998f, Table 5.3-1) Gd loss. In codisposal packages, the chemistry of the package water is influenced, overwhelmingly, by the degradation of glass and other package materials. The alkali and alkaline earth content of the glass completely swamped the native J-13 composition in the bulk of the EQ6 scenarios run for the EQ6 geochemical calculations (CRWMS M&O 1998e). The combination of steel and glass degradation drove the pH from ~3 to ~10, far greater than the range that exists in native J-13 water (CRWMS M&O 1998e, Figures 5-2 through 5-20). The silica content built into the glass is enormously greater than the amount of silica that can be contributed from J-13, even with long periods of flushing at high rates. The calculations in CRWMS M&O (1998e) showed that in

cases of significant U and Pu solubility, the dominant aqueous species were carbonate and phosphate complexes. The phosphate was supplied overwhelmingly from the  $\text{GdPO}_4$  criticality control material and the glass, and the high aqueous carbonate was controlled by the pH (which resulted from glass dissolution and the assumption of fixed  $\text{CO}_2$  pressure).

### 2.1.8.3 Drip Rate of J-13 Water into a Waste Package

The rates at which water drips onto a waste package and flows through it are represented as being equal. The drip rate is taken from a correlation between the percolation rate and the drip rate (CRWMS M&O 1998g, pp. 2.3-105 through 2.3-107, and Figure 2.3-110). Specifically, percolation rates of 40 mm/yr and 8 mm/yr correlate with drip rates onto the waste package of  $0.15 \text{ m}^3/\text{yr}$  and  $0.015 \text{ m}^3/\text{yr}$ , respectively.

For the present study, the range of allowed drip rates is extended to include an upper value of  $0.5 \text{ m}^3/\text{year}$  and a lower value of  $0.0015 \text{ m}^3/\text{yr}$ . The upper value corresponds to the 95 percentile upper limit for a percolation rate of 40 mm/yr (as determined in CRWMS M&O 1998g, pp. 2.3-105 through 2.3-107 and CRWMS M&O 1998d, pp. 10-19 through 10-24), and the lower value is simply 0.1 times the mean value for the present 8 mm/yr percolation rate. These extreme values are used, because prior studies (CRWMS M&O 1998f, pp. 18-19) suggested that when ceramic waste forms are codisposed with glass, the greatest chance of Gd removal occurs when: (1) initial high drip rates cause glass leaching and removal of alkali, and (2) subsequent low drip rates allow acid to build up from the degradation of the steel.

## 2.2 DESIGN CRITERIA

The design criteria are based on *DOE Spent Nuclear Fuel Disposal Container System Description Document* (CRWMS M&O 1998h), which is referred to as the SDD. The SDD numbers that follow are paragraph numbers from that document. In this section, the key waste package design criteria from the SDD are identified for the following areas: structural, thermal, shielding, intact criticality, degradation and geochemistry, and degraded criticality.

### 2.2.1 Structural

- 2.2.1.1 "The disposal container shall retain the capability to be unloaded after the occurrence of the events listed in Section 1.2.2.1."

[SDD 1.2.1.17]

- 2.2.1.2 "The disposal container shall be designed to withstand transfer, emplacement, and retrieval operations without breaching."

[SDD 1.2.1.22]

- 2.2.1.3 "During the preclosure period, the disposal container, while in a vertical orientation, shall be designed to withstand a drop from a height of 2 m (6.6 ft) (TBV-245) without breaching. During the preclosure period, the disposal container, while in a horizontal orientation, shall be designed to withstand a drop from a height of 2.4 m (7.9 ft) (TBV-245) without breaching. During the preclosure period, the disposal container shall be

designed to withstand a tip over from a vertical position with slap down onto a flat, unyielding surface without breaching.”

[SDD 1.2.2.1.3] [TBV-245] [SDD 1.2.2.1.4] [TBV-245] [SDD 1.2.2.1.6] [TBV-245]

Calculations of maximum potential energy for each handling accident scenario (horizontal drop, vertical drop, and tipover design-basis events [DBEs]) showed that the bounding dynamic load is obtained from a tipover case in which the rotating top end of the waste package experiences the highest g-load with maximum velocity of 8.93 m/sec (CRWMS M&O 1998b, p. 10). The maximum velocities of the waste package for 2.4 m horizontal and 2.0 m vertical drops are approximately 6.86 m/sec and 6.26 m/sec, respectively. Therefore, tipover structural evaluations are bounding for all handling accident scenarios considered in the SDD. Section 3.3 addresses these requirements. All other accident scenarios are considered non-credible.

The tipover DBE may only take place during a waste package transfer operation from vertical to horizontal (just after waste package closure) or horizontal to vertical (upon retrieval). Section 3, Structural Analysis, demonstrates that the waste package will not breach under such a handling-accident scenario.

## **2.2.2 Thermal**

2.2.2.1 “The disposal container shall limit the zircaloy and stainless steel cladding temperature to less than 350 °C (TBV-241). Temperature of other types of DOE fuel cladding shall be limited to (TBD-179) °C. Exceptions to these temperature limits are given in Section 1.2.2.1.”

[SDD 1.2.1.8] [TBV-241]

2.2.2.2 “The disposal container shall be designed to have a maximum thermal output of 18 kW (1025 BTU/min.) (TBV-251) or less. This criteria identifies the primary disposal container interface with the Ex-Container System.”

[SDD 1.2.4.9]

The criterion is met as described in Sections 4 and 8.2.

## **2.2.3 Shielding**

“Disposal container design shall reduce the dose rate at all external surfaces of a loaded and sealed disposal container to 355 rem/hr (TBV-248) or less. This criteria identifies the primary disposal container interface with the Waste Emplacement System and the Disposal Container Handling System.”

[SDD 1.2.4.7] [TBV-248]

The criterion is met as described in Sections 5 and 8.3.

## **2.2.4 Degradation and Geochemistry**

There are no degradation and geochemistry criteria in the SDD to address.

## **2.2.5 Intact and Degraded Criticality**

2.2.5.1 “The disposal container provides sufficient criticality control during loading and after it is loaded with waste.”

[SDD 1.1.3]

The criterion is met as described in Sections 7.3, 7.4, 7.5 and 8.5.

2.2.5.2 “During the preclosure period, the disposal container shall be designed such that nuclear criticality shall not be possible unless at least two unlikely, independent, and concurrent or sequential changes have occurred in the conditions essential to nuclear criticality safety. The system must be designed for criticality safety assuming occurrence of design basis events, including those with the potential for flooding the disposal container prior to disposal container sealing (TBD-235) or misloading canisters (TBD-235). The calculated effective multiplication factor ( $k_{eff}$ ) must be sufficiently below unity to show at least a 5 percent margin, after allowance for the bias in the method of calculation and the uncertainty in the experiments used to validate the method of calculation.”

[SDD 1.2.1.5]

As stated in Section 8.5, the results from the intact criticality analysis show that the requirement of  $k_{eff}$  plus bias and uncertainty less than or equal to 0.95 is satisfied.

## **2.3 ASSUMPTIONS**

In the course of developing this document, assumptions are made regarding the waste package structural, thermal, shielding, intact criticality, degradation and geochemistry, and degraded criticality analyses. The list of the major assumptions that are essential to this technical document are provided below.

### **2.3.1 Structural**

2.3.1.1 The two containment barriers are assumed to have solid connections, that is the inner and outer barriers will be either shrunk fit or the inner barrier will be weld clad onto the outer barrier inner surface (CRWMS M&O 1997a). This assumption is used in Section 3.

2.3.1.2 The target surface is conservatively assumed to be essentially unyielding by using a large elastic modulus for the target surface compared to the waste package. This assumption is used in Section 3.

### **2.3.2 Thermal**

2.3.2.1 An axial power peaking factor (PPF) of 1.25 was assumed for the FFTF fuel assemblies. The value of 1.25 is a conservative value for pressurized water reactor (PWR) fuel (CRWMS M&O 1997d, p. 29). The HLW canisters are assumed to have an axial PPF = 1.00 (CRWMS M&O 1997d, p. 53). This assumption is used in Section 4.

2.3.2.2 Representing only conduction and radiation heat transfer inside the waste package is assumed to provide conservative temperature results. The basis for this assumption is that natural convective heat transfer due to the circulation of helium fill gas within the small basket cavities is not significant. Also, neglecting convective heat transfer is conservative because any convection will improve heat transfer from hot regions of the waste package, and thus reduce the peak temperatures. This assumption is used in Section 4.

### **2.3.3 Shielding**

2.3.3.1 The FFTF assemblies, the basket, and the Ident-69 container with fuel pins are homogenized inside the volume of the DOE SNF canister. This model is conservative, because the homogenization process essentially moves the radiation source closer to the outer surfaces of the waste package. Therefore more particles are allowed to reach the outer surface and the self-shielding of the fuel is decreased (Parks et al. 1988, p. 85). This assumption is used to obtain the results provided in Section 5.3.

2.3.3.2 An assumed axial PPF of 1.25 is used for the FFTF source for bounding the axial source distribution. This value is based on the axial peaking factor shown in PNL (1987, p. 3-29, Fig. 3-18). This assumption is used to obtain the results provided in Section 5.3.

2.3.3.3 The Watt fission neutron spectrum (LANL 1997, p. 3-50) is used for the FFTF neutron fuel-source distribution. This spectrum has a most likely neutron energy of about 1 MeV for which the neutron quality factor has the highest value (LANL 1997, App. H, p. 5). Since the waste package surface dose rates are dominated by the gamma dose rates, the neutron spectrum used has negligible effect on the surface dose rates. This assumption is used to obtain the results provided in Section 5.3.

2.3.3.4 There are four types of FFTF fuel. Although their gamma source spectra are similar, Type 4.2 fuel has the highest intensity. Therefore, Type 4.2 fuel is for the shielding calculations. This assumption is used to obtain the results provided in Section 5.3.

2.3.3.5 The neutron source intensity is nine and eight orders of magnitude smaller than the gamma source intensity for the FFTF fuel and HLW, respectively. Therefore, the dose rate due to secondary gamma rays is negligible and no coupled neutron-photon calculation is performed. This assumption is used to obtain the results provided in Section 5.3.

### **2.3.4 Degradation and Geochemistry**

The assumptions in this section are used throughout Section 6.

2.3.4.1 It is assumed that water may circulate freely enough in the partially degraded waste package that all degraded solid products may react with one another in the aqueous solution. By facilitating contact of any acid that may result from the corrosion of steel with neutron absorbers in the spent fuel canister, the code conservatively enhances potential preferential loss of neutron absorbers from the waste package.



- 2.3.4.2 It is assumed that the inner corrosion resistant material (CRM) of the waste package will react so slowly with the infiltrating water (and water ponded in the waste package) that it will have a negligible effect on the chemistry. The bases consist of the facts that the CRM is fabricated from Alloy 22, which corrodes very slowly compared (1) to other reactions in the waste package and (2) to the rate at which soluble corrosion products will likely be flushed from the package.
- 2.3.4.3 It is assumed that precipitated solids that are deposited remain in place and are not mechanically eroded or entrained as colloids in the advected water. This assumption is made because it conservatively maximizes the size of potential deposits of fissile material inside the waste package.
- 2.3.4.4 It is assumed that over times of interest sufficient decay heat is retained within the waste package to cause convective circulation and mixing of the water inside the waste package (CRWMS M&O 1996a, Attachment VI).

### **2.3.5 Intact and Degraded Criticality**

The assumptions in this section are used throughout Section 7.

- 2.3.5.1 Beginning of life (BOL) pre-irradiation fuel compositions of FFTF SNF were used for all calculations. For FFTF SNF, it is conservative to assume fresh fuel as it is more neutronically reactive than spent fuel. The dished face of the fuel pellets is neglected and the fuel number density is determined by using the fuel mass and the footprint volume of the fuel.
- 2.3.5.2 Ident-69 pin containers are assumed to contain a most reactive configuration of FFTF fuel pins for the intact fuel cases.
- 2.3.5.3 The flanged head and neck of the HLW canister is neglected and the canister is modeled as a right circular cylinder with the same top-to-bottom height as the canister. The canister is assumed to be completely filled with HLW glass. The basis for this assumption is that it is conservative since the additional waste will make the system more reactive by increasing the total amount of fissile elements (by less than 1%) in the waste package.
- 2.3.5.4 For cases where the fuel pin cladding has become completely degraded the remaining fuel pellets are assumed to maintain their axial alignment (as in the fuel pin), and the radial spacing which can be affected by the expansion of corrosion products never becomes greater than the original spacing (pitch) of the DFA. This assumption is based on engineering judgement in that there is no physical mechanisms to push the fuel pins apart.

## 2.4 BIAS AND UNCERTAINTY IN CRITICALITY CALCULATIONS

The purpose of this section is to document the MCNP (CRWMS M&O 1998i), which is identified as Computer Software Configuration Item (CSCI) 30033 V4B2LV, evaluations of Laboratory Critical Experiments (LCEs) performed as part of the Disposal Criticality Analysis Methodology program. Only LCEs relevant to FFTF are studied. LCE's results listed in this section are given in CRWMS M&O (1999c) for the thermal compound mixed plutonium-uranium systems and for the thermal compound highly-enriched uranium systems and in CRWMS M&O (1999d) for the thermal solution mixed plutonium and uranium systems. The objective of this analysis is to quantify the MCNP Version 4B2 code system's ability to accurately calculate the effective neutron multiplication factor ( $k_{\text{eff}}$ ) for various configurations. MCNP is set to use continuous-energy cross sections processed from the evaluated nuclear data files ENDF/B-V (LANL 1997, App. G). These cross section libraries are part of the MCNP code system that has been obtained from the Software Configuration Management (SCM) in accordance with appropriate procedures. Each of the critical core configurations is simulated, and the results reported from the MCNP calculations are the combined average values of  $k_{\text{eff}}$  from the three estimates (collision, absorption, and track length) and the standard deviation of these results ( $\sigma$ ) listed in the final generation summary in the MCNP output. When MCNP underpredicts the experimental  $k_{\text{eff}}$ , the experimental uncertainty is added to the uncertainty at 95% confidence from the MCNP calculation to obtain the bias. This bias along with the 5% margin (see Section 2.2.5.2) is used to determine the interim critical limit for all MCNP calculations of the waste package with FFTF DOE SNF canister.

### 2.4.1 Benchmarks Related to Intact Waste Package Configurations

Four experiments are relevant for the FFTF fuel with respect to intact criticality analyses: the FFTF fuel pin array experiment (MIX-COMP-THERM-001, OECD-NEA1997), the Saxton plutonium experiment (MIX-COMP-THERM-003, OECD-NEA1997), a series of critical experiments with water moderated hexagonally pitched lattices with highly enriched fuel rods (HEU-COMP-THERM-003, HEU-COMP-THERM-004, HEU-COMP-THERM-005, HEU-COMP-THERM-006, HEU-COMP-THERM-007, HEU-COMP-THERM-008, and HEU-COMP-THERM-010, OECD-NEA1997). The experiments of EBOR (Experimental Beryllium Oxide Reactor) fuel pin in water were considered but were eliminated because of the presence of Be.

#### 2.4.1.1 FFTF Fuel Pin Array Experiments

A description of the experiment is given in OECD-NEA(1997) (MIX-COMP-THERM-001) and in CRWMS M&O (1999c, pp. 36, 87). The fuel used for the experiments was a mixture of  $\text{PuO}_2$  and  $\text{UO}_2$ , with the pins comprised of either 19.84 or 24.39 wt% plutonium (Bierman et al. 1979, p. 141). The plutonium contained 86.2% Pu-239 and 11.5 wt% Pu-240, and the uranium in the  $\text{PuO}_2$ - $\text{UO}_2$  mixture was natural uranium. Six different core configurations were studied. Various lattice pitches were used in the array, resulting in different numbers of fuel rods being required to obtain criticality. The results indicate that the maximum bias is 0.02 (CRWMS M&O 1999c, pp. 36, 87).

#### **2.4.1.2 Saxton Plutonium Experiments**

A detailed description of the experimental configuration for the MOX single-region experiments is provided in OECD-NEA(1997), pages 4, 7, and 24, MIX-COMP-THERM-003 (MCT-003), and a description of the multi-region and UO<sub>2</sub> single-region experiments is provided in Taylor (1965, Attachment B). Single and multi-region uranium and plutonium oxide fueled cores, water moderated, clean, and borated, have been used in this set of critical experiments. Criticality was achieved entirely by varying the water level inside the core tank. The fuel used in the experiments were UO<sub>2</sub> fuel with 5.74 wt% U-235 enrichment, and MOX fuel containing 6.6 wt% PuO<sub>2</sub> and natural enriched UO<sub>2</sub> (Radulescu, G. and Abdurrahman, N.M. 1997). The pitch, number of fuel rods, and boron concentration were the parameters that were varied. The results show that the maximum bias is 0.015 (CRWMS M&O 1999c, pp. 41, 88).

#### **2.4.1.3 Water-Moderated Hexagonally Pitched Lattices of Highly Enriched Fuel Rods of Cross-Shaped Cross Section**

A series of critical experiments with water moderated hexagonally pitched lattices of highly enriched fuel rods of cross-shaped cross section was performed over several years in the Russian Research Center "Kurchatov Institute". The 28 experiments analyzed under this category in this report consist of the following:

- 1) Fifteen critical two-zone lattice experiments corresponding to different combinations of inner and peripheral zones of cross-shaped fuel rods at two pitches. For detailed descriptions of these experimental configurations see pages 2, and 7 through 14 of OECD-NEA1997, HEU-COMP-THERM-003 (HCT-003).
- 2) Four critical configurations of hexagonal lattices of fuel rods with Gd or Sm rods. These experiments consisted of double lattices of fuel rods and absorber rods containing Gd or Sm. Detailed experimental configuration descriptions are available on pages 2, 7, and 8 of OECD-NEA1997, HEU-COMP-THERM-004 (HCT-004).
- 3) One critical configuration of hexagonal pitched clusters of lattices of fuel rods with copper (Cu) rods. Detailed experimental configuration descriptions are available on pages 2 through 8 of OECD-NEA1997, HEU-COMP-THERM-005 (HCT-005).
- 4) Three critical configurations with uniform hexagonal lattices with pitch values of 5.6, 10.0, and 21.13 mm. Detailed experimental configuration descriptions are available on pages 2, 5, and 6 of OECD-NEA1997, HEU-COMP-THERM-006 (HCT-006).
- 5) Three critical configurations with double hexagonal lattices of fuel rods and zirconium hydride rods. Detailed experimental configuration descriptions are available on pages 2 through 8 of OECD-NEA1997, HEU-COMP-THERM-007 (HCT-007).
- 6) Two critical configurations with double hexagonal lattices of fuel rods and boron carbide rods. Detailed experimental configuration descriptions are available on pages 2, 7, and 8 of OECD-NEA1997, HEU-COMP-THERM-008 (HCT-008).

The pitch, number of rods, number of fuel rods, and number of absorber rods (Gd or Sm) were the parameters that were varied. The maximum bias for this set of calculations is 0.019 (CRWMS M&O 1999c, pp. 18, 19, 76).

## **2.4.2 Benchmarks Related to Degraded Waste Package Configurations**

### **2.4.2.1 Critical Experiments with Mixed Plutonium and Uranium Nitrate Solution**

The objective of these experiments was to obtain data on the minimum fissile concentration for criticality in an effectively infinite cylindrical geometry. A detailed description of these experiments is given in OECD-NEA(1997) (MIX-SOL-THERM-001, MIX-SOL-THERM-002, MIX-SOL-THERM-003, MIX-SOL-THERM-004) and in CRWMS M&O (1997e, pp. 13 through 17). The concentration of fissile elements (Pu and U) in the solution, enrichment, amount of absorber (B<sub>4</sub>C concrete and polyethylene with Cd cover), tank diameter, and solution height were among the parameters that were varied. The maximum bias for this set of experiments is 0.011 (CRWMS M&O 1997e, pp. 14, 15, 16, 17; CRWMS M&O 1999d, pp. 11, 12).

### **2.4.2.2 Critical Experiments with Highly Enriched Uranium Nitrate Solution**

These experiments involving highly-enriched uranium (approximately 90 wt%) are described in detail in OECD-NEA (1997) (HEU-SOL-THERM-001, HEU-SOL-THERM-008, HEU-SOL-THERM-013, HEU-SOL-THERM-014, HEU-SOL-THERM-015, HEU-SOL-THERM-016, HEU-SOL-THERM-017, HEU-SOL-THERM-018, HEU-SOL-THERM-019). The concentration of fissile element in the solution, enrichment, amount and type of absorber (Gd and B), reflector type and thickness, tank diameter, and solution height were among the parameters that were varied. The maximum bias for this set of experiments is 0.018 (CRWMS M&O 1997e, pp. 26, 35-44; CRWMS M&O 1999d, pp. 14-18). It must be noted that MCNP generally overestimated the  $k_{\text{eff}}$  of these experiments with absorbers.

### **2.4.3 Critical Limit**

The worst-case bias, calculated from the MCNP simulations of the experiments described in Sections 2.4.1 and 2.4.2, is 0.02. This bias includes the bias in the method of calculation and the uncertainty in the experiments. Based on this bias, the interim critical limit is determined to be 0.93 after a 5 percent margin; allowance for the bias in the method of calculation, and the uncertainty in the experiments used to validate the method of calculation. This interim critical limit will be used until the addenda to the topical report is prepared to establish the final critical limit.

### 3. STRUCTURAL ANALYSIS

#### 3.1 USE OF COMPUTER SOFTWARE

The finite-element analysis (FEA) computer code used to analyze the 5-HLW/DOE SNF Long waste package with the FFTF DOE SNF canister in the center is ANSYS version V5.4. ANSYS V5.4 is identified with the CSCI 30040 V5.4 and is obtained from SCM in accordance with appropriate procedures. ANSYS V5.4 is a commercially available FEA code. ANSYS V5.4 software is qualified as documented in the Software Qualification Report (SQR) for ANSYS V5.4 (CRWMS M&O 1998j). ANSYS V5.4 is also referred to as ANSYS.

#### 3.2 STRUCTURAL DESIGN ANALYSIS

Finite-element solutions resulted from structural analyses for the components of the 5-HLW/DOE SNF Long waste package. A detailed description of the finite-element representations, the method of solution, and the results are provided in CRWMS M&O (1998b). The results of these analyses are compared to the design criteria obtained from the 1995 American Society of Mechanical Engineers (ASME) Boiler and Pressure Vessel Code (BPVC), Section III, Subsection NB (ASME 1995), so that conclusions can be drawn regarding the structural performance of the 5-HLW/DOE SNF Long waste package design.

The design approach for determining the adequacy of a structural component is based on the stress limits given in the 1995 ASME BPVC.  $S_u$  is defined as the ultimate tensile strength of the materials, and  $S_m$  is defined as the design stress intensity of the materials. Table 3-1 summarizes design criteria as obtained from appropriate sections of the 1995 ASME BPVC.

Table 3-1. Containment Structure Allowable Stress-Limit Criteria

Category	Containment Structure Allowable Stresses	
	Normal Conditions (ASME 1995, Division 1, Subsection NB, Articles NB-3221.1 and NB-3221.3)	Accident Conditions (Plastic Analysis, ASME 1995, Division 1, Appendix F, Article F-1341.2)
Primary Membrane Stress Intensity	$S_m$	$0.7S_u$
Primary Membrane and Bending Stress Intensity	$1.5S_m$	$0.9S_u$

This analysis is within the bounds of the structural criteria from the SDD (CRWMS M&O 1998h) and does not consider other DBEs (e.g., crane two-block events), which are considered non-credible.

#### 3.3 CALCULATIONS AND RESULTS

##### 3.3.1 Description of the Finite-Element Representation

A two-dimensional (2-D) finite-element representation of the 5-HLW/DOE SNF Long waste package is developed to determine the effects of loads from the tipover DBE on the structural

components. The representation of the waste package includes the outer and inner barriers, the basket, the support tube, the DOE SNF canister and its basket and support tube, and the HLW pour canisters. This representation corresponds to a 2-D (x-y) slice from the middle of the waste package. After a tipover DBE onto an unyielding surface, the waste package lies horizontally as shown in Figure 3-1. A half-symmetry finite-element representation of the waste package was used. The barriers are assumed to have solid connections at the adjacent surfaces (Assumption 2.3.1.1) and are constrained in a direction perpendicular to the symmetry plane. For the first of the finite-element representations, the DOE SNF canister is included as a point mass at the bottom of the waste package support tube (the waste package lies horizontally), and no credit is taken for its structure. Therefore, the resulting closure of gap between the support tube and the DOE SNF canister is realistically calculated. If it is determined that the gap is not closed, there will be no structural load transferred from the support tube to the DOE SNF canister. Since all calculations are 2-D, masses per unit length are calculated based on the maximum allowable weight limits. Although the weight limit for the DOE SNF canister is 2,721 kg (DOE 1998b), the maximum weight limit from the SDD (CRWMS M&O 1998h), which is 3,400 kg, is used to calculate the stresses. Therefore, actual deformations will be smaller than the ones reported in this technical report.

For the second part of the calculations, the finite-element representation is modified to take structural credit for the DOE SNF canister and basket components. This representation is used to determine the maximum closure of the clearance gaps inside the FFTF DFA and the Ident-69 fuel pin container. The deformation values can then be compared to the fuel-assembly and the Ident-69 pin container dimensions to determine if there is contact between these components and the basket-structure.

First, the impact velocity of the inner lid's outer surface is calculated for a waste package tipover DBE. Then, this velocity is conservatively used in the 2-D finite-element analysis. Since the 2-D representation does not model a lid, the calculations will indicate that the waste package components undergo more deflection and stress than would actually occur. The target surface is conservatively assumed to be essentially unyielding by using a large elastic modulus for the target surface compared to the waste package (Assumption 2.3.1.2). The target surface is constrained at the bottom to prevent horizontal and vertical motion. Contact elements are defined between the top HLW pour canister and the inner brackets, and between the outer barrier and the target surface. Initial configuration of the finite-element representation includes a negligibly small gap for each contact element defined in the representation. This configuration allows enough time and displacement for the waste package and its internals to ramp up to the specified initial velocity before the impact. With this initial velocity, the simulation is then continued through the impact until the waste package begins to rebound. At that time, the stress peaks and the maximum displacements have been obtained.

The vitrified HLW glass material properties are represented by ambient material properties of general borosilicate glass. This document does not specifically report any results for the HLW glass canisters.

### 3.3.2 Results with No Credit for the Structural Components of the DOE SNF Canister

The first finite-element representation does not take structural credit for the DOE SNF canister; the mass is included by using a point mass element at the lowest point inside the support tube. The structural response of the waste package to tipover accident loads is reported using maximum stress values and displacements obtained from the finite-element solution to the problem. The results indicate that the maximum deformation inside the waste package support tube is 32.3 mm (CRWMS M&O 1998b, p. 13). Available space between the support tube and the DOE SNF canister is 44.3 mm (CRWMS M&O 1998b, p. 13). Hence, there will be no interference between the two components because of tipover DBE. The stresses on the waste package components and the DOE SNF canister are shown in Figure 3-1. Table 3-2 presents the stresses in each component of the waste package, and shows that the inner barrier of the waste package will not breach since the peak stresses are below the  $0.9S_u$  which is the ASME code allowance stress limit shown in Table 3-1.

Table 3-2. 5-HLW/DOE SNF Long Waste Package FEA Stress Results

Component	Ultimate Tensile Strength (MPa)	$0.7S_u$ (MPa)	$0.9S_u$ (MPa)	Maximum Stress Intensity (MPa)	Maximum Membrane Stress (MPa)	Maximum Membrane Plus Bending Stress (MPa)
Outer barrier	483	338	435	372	25	486
Inner barrier	690	483	621	418	412	418
Basket plates and support tube	483	338	435	474	27	555

### 3.3.3 Results with Structural Credit for the DOE SNF Canister Components

The maximum deformation causing cavity closure around the fuel assembly is determined for the case of 5-HLW waste package representation that includes the structural components of the DOE SNF canister. The displacement results of the waste package tipover structural analysis showed that the maximum FFTF DFA cavity closure is 7.3 mm due to the deformation of the DOE SNF canister basket (CRWMS M&O 1998b, p. 13). The available gap between the FFTF DFA and the basket is 11.6 mm (CRWMS M&O 1998b, p. 13). Therefore, the DFA will not be crushed by the basket structure.

Similarly, the maximum deformation inside the Ident-69 container shell is determined to be 12.8 mm (CRWMS M&O 1998b, p. 13). On the other hand, available space between the FFTF DOE SNF canister center tube and the Ident-69 pin container is 11.7 mm (see CRWMS M&O 1998b, p. 13). This seems to result in an interference (1.1 mm) between these two parts due to impact. This is an artifact of the computational representation. The case was setup with the DOE SNF canister in contact with the waste package basket (support tube), which simplifies the calculations and reduces computing time. Since the 44.3 mm gap between the DOE SNF canister and the waste package support tube was not utilized, a significant part of the load that deformed the support tube in the waste package basket was transmitted directly to the DOE SNF canister and its basket structure in this representation. This causes excessive deformation of the DOE SNF canister basket and appears to trap the Ident-69 pin container in the center tube. As shown in Section 3.3.2, since the gap between the DOE SNF canister and the waste package

support tube does not fully close, there is no load transferred to the DOE SNF canister and its basket. Thus the deformation will be much less and there will be no interference between any of the fuel-assemblies or the Ident-69 container and the basket structure.

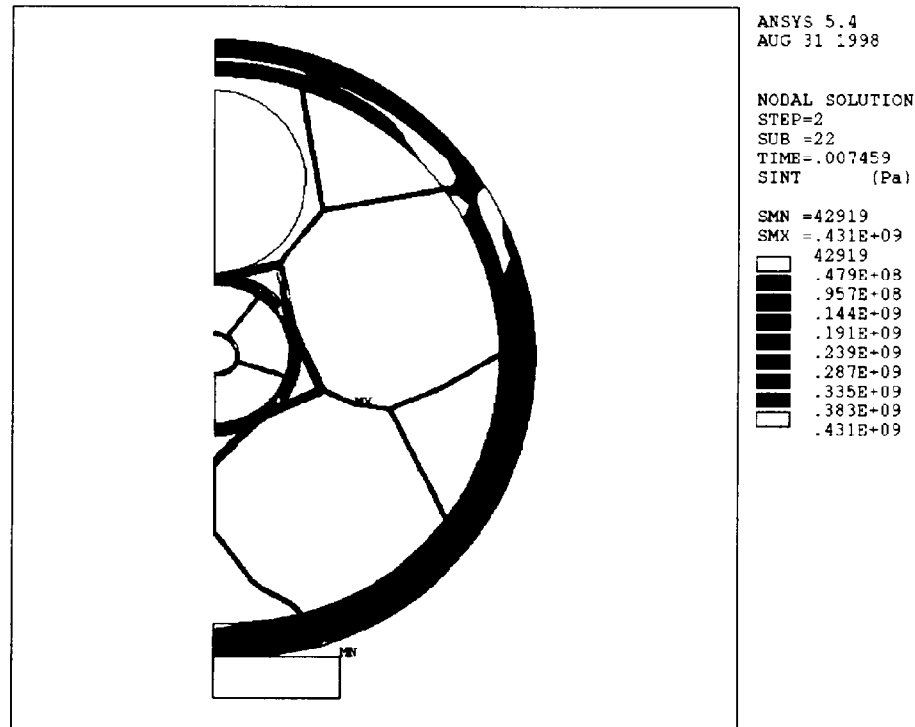


Figure 3-1. Stresses in 5-HLW/DOE SNF Long Waste Package

### 3.4 SUMMARY

The results given in Section 3.3 show that there is sufficient clearance between the inner diameter of the support tube and the outer diameter of the DOE SNF canister in the case of a tipover DBE. Hence, there will be no interference between the two components, and the DOE SNF canister can be removed from the support tube if needed to be set inside another waste package.



## **4. THERMAL ANALYSIS**

### **4.1 USE OF COMPUTER SOFTWARE**

The FEA computer code used to analyze the 5-HLW/DOE SNF Long waste package containing an FFTF DOE SNF canister is ANSYS Version V5.4. ANSYS V5.4 is identified as CSCI 30040 V5.4 and is obtained from SCM in accordance with appropriate procedures. ANSYS is a commercially available finite-element thermal- and mechanical-analysis code. ANSYS V5.4 software is qualified as documented in the SQR for ANSYS V5.4 (CRWMS M&O 1998j). ANSYS V5.4 is also referred to as ANSYS.

### **4.2 THERMAL DESIGN ANALYSIS**

A detailed description of the finite-element representations, the method of solution, and the results are provided in CRWMS M&O (1999b). Each DFA and the Ident-69 fuel pin container holds 217 fuel pins in this representation. The FFTF standard DFA representation in this calculation is a 2-D section of the hexagonal duct containing 217 pins, as shown in Figures 2-6 and 2-7. The wire spacers around each fuel pin are conservatively neglected in this calculation (wire spacers provide contact and thus increase the transfer of thermal energy by conduction to the outside), so that the pins are represented as floating within the driver duct. In this analysis, the axial cross section at the center of the fuel pin is represented.

The cross section of the Ident-69 fuel pin container is shown in Figure 2-9. For this calculation, which represents a loading of 217 pins, the pins are consolidated loosely into the container, and therefore, are allowed to settle. The pins are considered packed together near the center of the container. In reality, the settled configuration of the pins would vary a great deal between each of the six partitioned sections. However, in this analysis, the settled configuration of fuel pins is represented as a constant since this approach simplifies the calculation and is considered conservative.

As shown in Figure 2-1, the waste package outside of the support tube for the DOE SNF canister is divided into five sections by the plates of the waste package basket. The plates of the FFTF DOE SNF canister also divide the space around the central support tube for the Ident-69 container into five sections. Due to this symmetry, thermal conditions within each of the five sections (representing 72° of the entire 360° of the waste package) will be approximately the same. In addition, within each of the 72° sections, the waste package components possess a further radial line of symmetry. Therefore, transient conditions in the waste package can be represented by one-tenth of the total radial geometry (a 36° slice of the full 360°) as shown in Figure 4-1.

The waste package outside of the Ident-69 fuel pin container is divided evenly into 72° slices, but the interior of the Ident-69 container is symmetrically divided by 60° slices. For this reason, the interior of the Ident-69 fuel pin container cannot be accurately included in the same 36°-slice finite-element representation as the waste package outside of the Ident-69. The calculation is therefore divided into two parts, corresponding to the two parts of the finite-element representation.

Figures 4-1 and 4-2 give the designated node locations and numbers on each component of the finite-element representations. Note that the outer shell of the Ident-69 fuel pin container is included, in Part 1 of the finite-element representation.

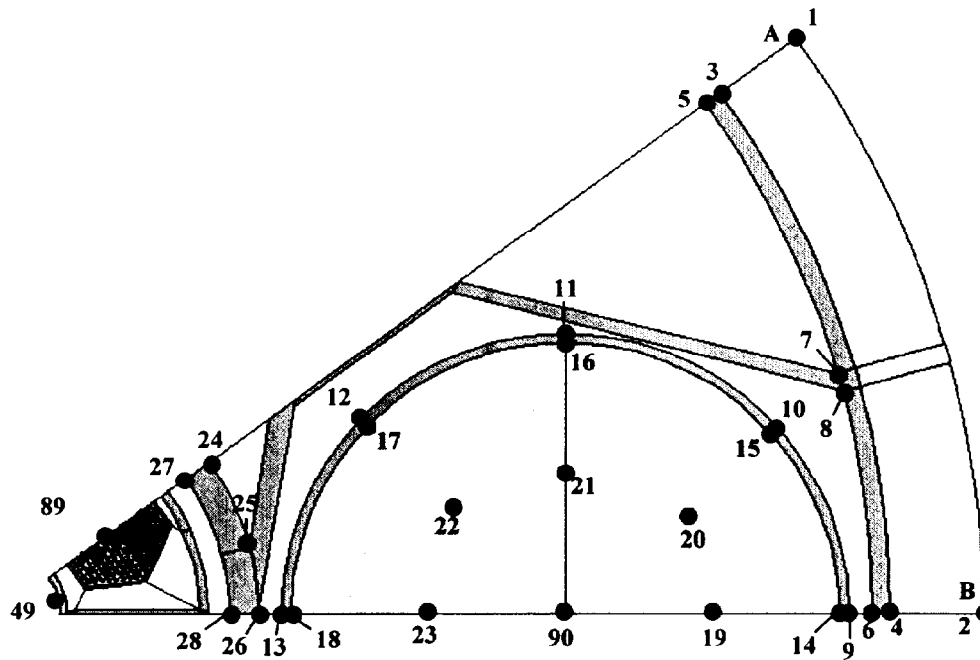


Figure 4-1. Node Locations and Numbers on Part 1 of the Finite-element Representation (WP Basket and Hanford 15 ft HLW Canister)

Two cases are considered, one with helium as the fill gas for the FFTF DOE SNF canister and the other with argon as the fill gas. The final fuel irradiations in FFTF were completed in March 1992 (INEEL 1998). Therefore, in all cases, the FFTF fuel is represented after ten years from discharge. The waste package total heat output is 13,533 W, and is based on five HLW glass canisters, five DFAs, and one Ident-69 pin container (Ident-69 pin container heat output is the same as one DFA).

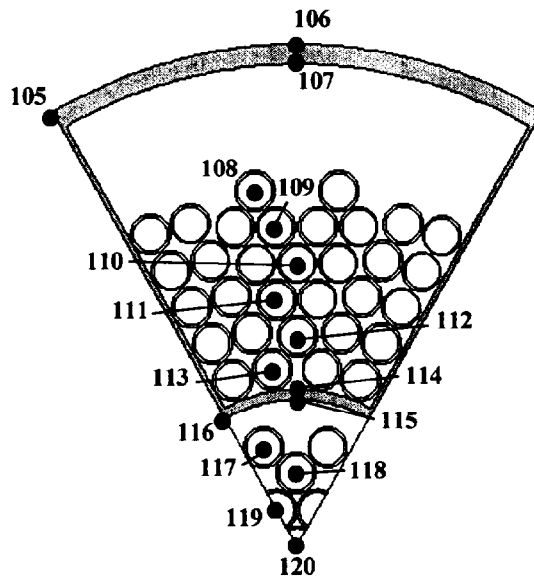


Figure 4-2. Node Locations and Numbers on Part 2 of the Finite-element Representation (Ident-69 Fuel Pin Container)

### 4.3 CALCULATIONS AND RESULTS

Table 4-1 lists the physical location of the most important nodes shown in Figures 4-1 and 4-2. Figure 4-3 shows the surface and peak fuel temperatures calculated in each case. The temperature distribution in the waste package at the time of peak fuel temperature can be found in CRWMS M&O (1999b), Attachments XIV through XVII. Table 4-2 summarizes the peak temperatures and time of occurrence for each case. The results indicate that argon fill gas in the FFTF DOE SNF canister causes the peak fuel temperature, which occurs after nine years, to be approximately 1.5% higher than helium fill gas. The peak HLW glass and waste package surface temperatures are not affected by the choice of the fill gas in the FFTF DOE SNF canister.

Table 4-1. Physical Locations of Nodes of Interest

Node Number	Physical Location
2	WP outer surface
90	HLW center
89	Standard DFA center fuel pin
49	Ident-69 outer surface, given as output of FEA, Part 1
106	Ident-69 outer surface, given as input to FEA, Part 2
120	Ident-69 center fuel pin

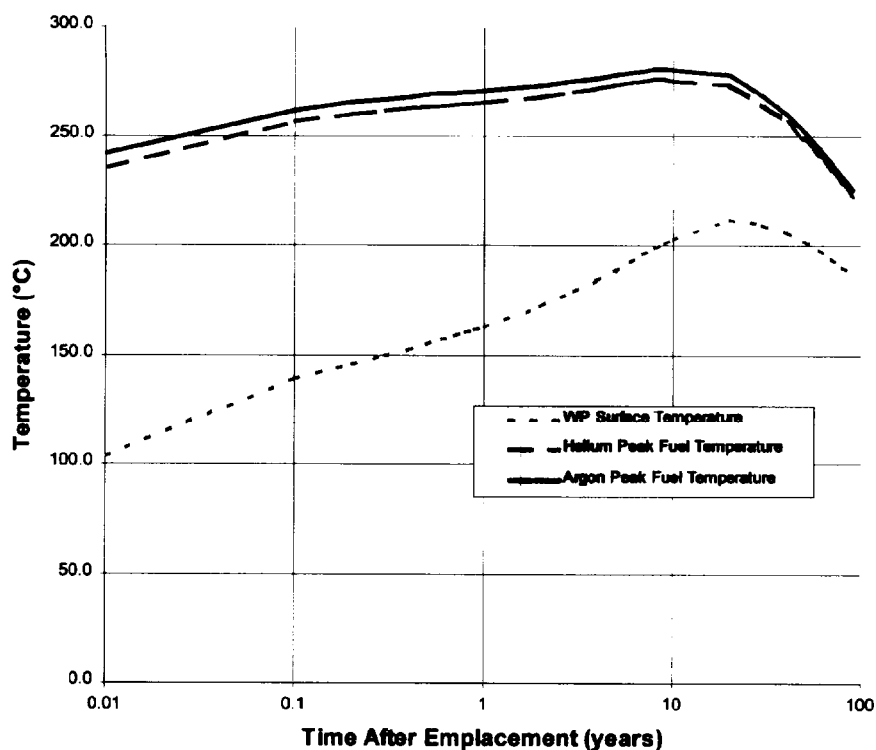


Figure 4-3. Temperature History for FFTF Codisposal WP

Table 4-2. Peak Temperatures and Time of Occurrence for Each Case

Case; FFTF DOE SNF Canister Fill Gas	Peak Fuel Temperature (°C)	Time of Peak Fuel Temperature (yr)	Peak Surface Temperature (°C)	Time of Peak Surface Temperature (yr)	Peak HLW Glass Temperature (°C)	Time of Peak HLW Glass Temperature (yr)
1; Helium	276.0	9	211.7	20	247.6	20
2; Argon	280.3	9	211.7	20	247.6	20

#### 4.4 SUMMARY

The results indicate that the maximum fuel and HLW glass temperatures occur with argon fill gas in the DOE SNF canister and are 280.3 °C and 247.6 °C, respectively.

## **5. SHIELDING ANALYSIS**

### **5.1 USE OF COMPUTER SOFTWARE**

The Monte Carlo radiation transport code, MCNP, Version 4B2, is used to calculate average dose rates on the surfaces of waste package. This code identified as CSCI 30033 V4B2LV was previously obtained from the SCM in accordance with appropriate procedures. MCNP software is qualified as documented in the SQR for the MCNP, Version 4B2 (CRWMS M&O 1998i).

### **5.2 DESIGN ANALYSIS**

The Monte Carlo method for solving the integral transport equation, which is implemented in the MCNP computer program, is used to calculate radiation dose rates for the waste packages. MCNP is set to use continuous-energy cross sections processed from the evaluated nuclear data files ENDF/B-V (LANL 1997, App. G). These cross section libraries are part of the qualified MCNP code system (CSCI 30033 V4B2LV). The flux averaged over a surface is tallied and the neutron and gamma flux to dose rate conversion factors (LANL 1997, App. H) are applied to obtain surface dose rates.

### **5.3 CALCULATIONS AND RESULTS**

Dose rate calculations are performed for four cases: a waste package containing SRS HLW glass and FFTF fuel, a waste package containing only SRS HLW glass, a waste package containing Hanford HLW glass and FFTF fuel, and a waste package containing only Hanford HLW glass. All calculations use the glass composition given in Section 2.1.7. These calculations evaluated dose rates on all barrier boundaries of the waste package. Details of the calculations and the results for all cases considered are given in CRWMS M&O (1998c). The geometric representation, which ignores the waste package basket, for the MCNP calculations is shown in Figure 5-1. The surface-dose rates of the waste package containing Hanford HLW glass are approximately 20% higher than those of the waste package containing SRS glass. In addition, only the dose rates on the outer surfaces of the waste package are of most interest. Therefore, only the results from Hanford cases on these surfaces of interest are summarized and analyzed in detail.

Figure 5-2 shows the segments and surfaces of interest. Segment c is a 600 mm long radial surface segment axially centered at the middle of glass canisters. Segment a<sub>1</sub> is a 30-degree wide angular segment of the 600 mm long radial surface (segment c) near glass canisters. Segment b<sub>1</sub> is a 30-degree wide angular segment of the 600 mm long radial surface (segment c) near the gap between glass canisters. Segment d is an axial surface segment centered at the center of the waste package (Figure 5-3).

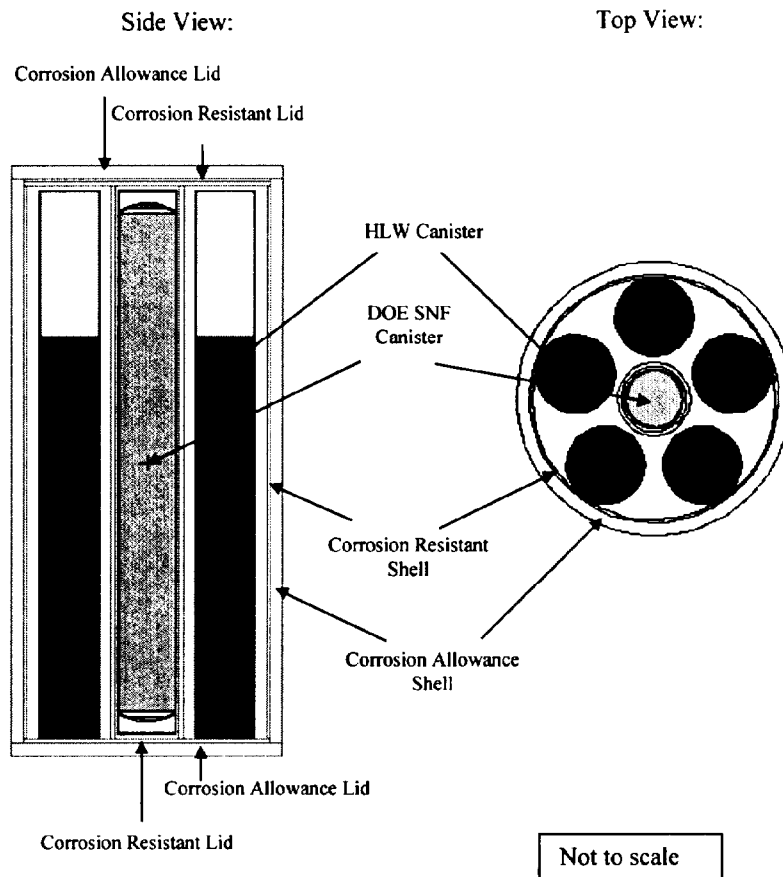


Figure 5-1. Vertical and Horizontal Cross Sections of MCNP Geometry Representation

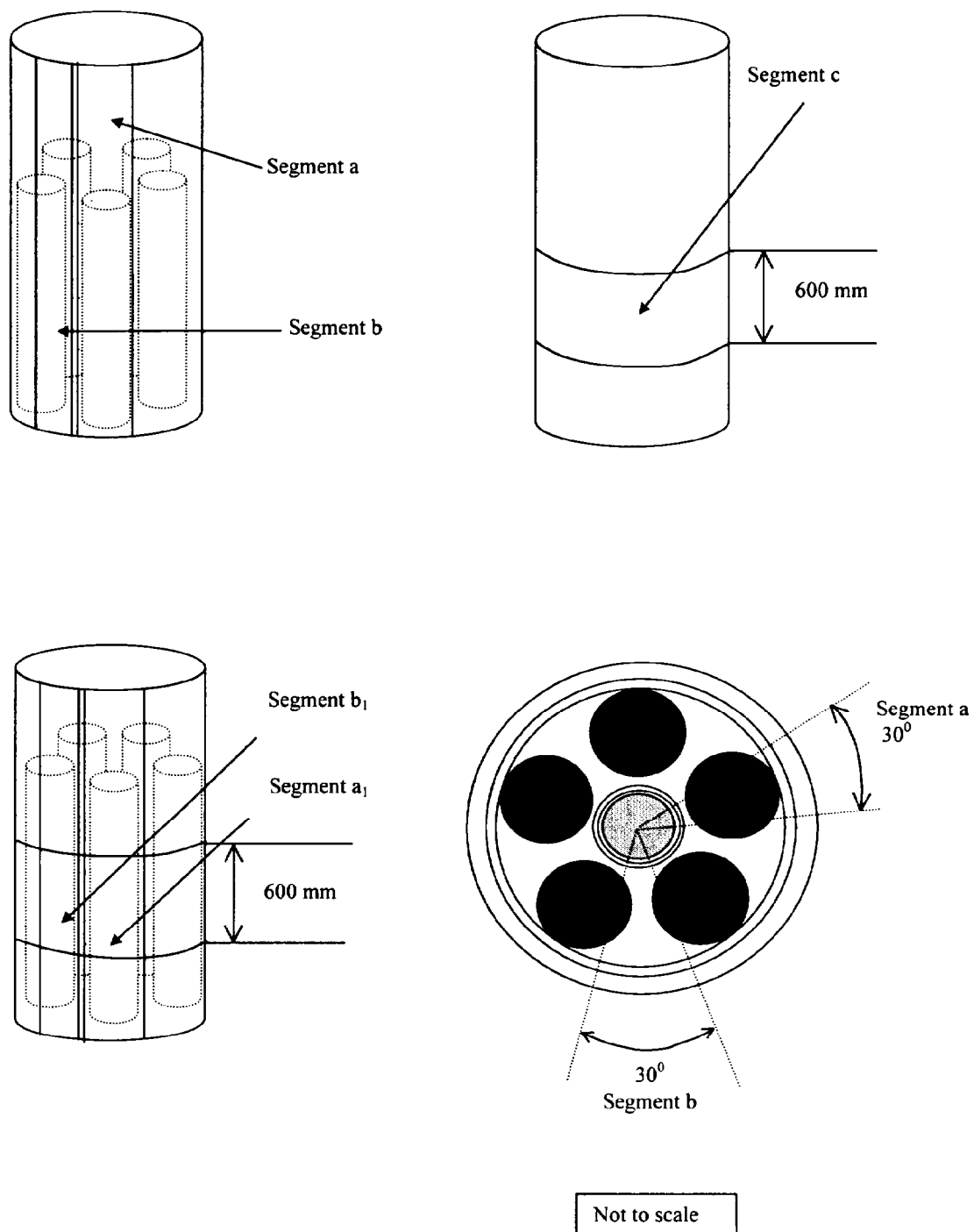


Figure 5-2. Radial Segments Used for Dose-Rate Calculations

### 5.3.1 Waste Package Containing Hanford HLW and FFTF Fuel

Tables 5-1 and 5-2 show the dose rates in rem/h on the surfaces of interest of the waste package containing the Hanford HLW glass and FFTF DOE SNF canister.

Table 5-1. Total Radial Dose Rates Averaged over a Height of 60 cm

Radial Position	Angular Position					
	Segment a <sub>1</sub>		Segment b <sub>1</sub>		Segment c	
	Dose Rate (rem/h)	Relative Error	Dose Rate (rem/h)	Relative Error	Dose Rate (rem/h)	Relative Error
Inner surface of inner barrier	9328.1	0.0246	9869.5	0.0238	9967.3	0.0086
Outer surface of outer barrier	15.9	0.0603	15.0	0.0716	15.0	0.0184

Table 5-2. Dose Rates in rem/h Averaged over Segment d

Axial Surface	Gamma Dose Rate (rem/h)	Relative Error	Neutron Dose Rate (rem/h)	Relative Error	Total Dose Rate (rem/h)	Relative Error
Outer surface of outer barrier bottom lid	1.52	0.1514	2.84E-02	0.0089	1.55	0.1486
Outer surface of outer barrier top lid	1.47	0.1317	1.28E-02	0.0131	1.48	0.1306

### 5.3.2 Waste Package Containing Only Hanford HLW

Tables 5-3 and 5-4 show dose rates on the surfaces of interest of the waste package containing the Hanford HLW glass only.

Table 5-3. Radial Gamma Dose Rates in rem/hr Averaged over a Height of 60 cm

Radial position	Angular Position					
	Segment a <sub>1</sub>		Segment b <sub>1</sub>		Segment c	
	Dose Rate (rem/h)	Relative Error	Dose Rate (rem/h)	Relative Error	Dose Rate (rem/h)	Relative Error
Inner surface of inner barrier	9.3928E+03	0.0219	1.0099E+04	0.0237	9.9595E+03	0.0070
Outer surface of outer barrier	15.83	0.0507	13.73	0.0679	14.45	0.0159

Table 5-4. Dose Rates in rem/h Averaged over Segment d

Axial Surface	Gamma Dose Rate (rem/h)	Relative Error
Outer surface of outer barrier bottom lid	3.11	0.1462
Outer surface of outer barrier top lid	1.57	0.2212



## 5.4 SUMMARY

The results of dose rate calculations are analyzed for the cases containing Hanford HLW and FFTF fuel, since that case has the highest dose rate among all cases investigated. Maximum dose rate on the outer surfaces of waste package is below 355 rem/h for all cases investigated. The highest dose rate of  $15.9 \pm 1.9$  rem/h (uncertainties reported correspond to two standard deviations) is calculated on the 600 mm long, 30-degree wide angular segment of radial outer surface of the waste package (Segment a<sub>1</sub>, see Figure 5-2). The primary gamma dose rate dominates the neutron dose rate by approximately three orders of magnitude.

The axial dose rates are higher on the bottom surfaces of waste packages because the HLW canisters rest on the bottom lids. The average dose rates on the outside of outer barrier of the bottom lid and the outside of the outer barrier of the top lid are  $1.52 \pm 0.46$  rem/h and  $1.47 \pm 0.39$  rem/h, respectively.

The dose on Segment a<sub>1</sub> is primarily due to the gamma rays of the adjacent HLW glass canister, while the dose on Segment b<sub>1</sub> is a contribution of gamma rays emitted from nearby HLW glass canisters. Source strength, geometry, and spectrum lead to a uniform angular dose over the radial surfaces of the waste packages for all analyzed cases.

The contribution to the total dose rate by the FFTF DOE SNF canister is approximately 10% for the waste package containing SRS HLW glass and approximately 5% for the waste package containing Hanford HLW glass. Figure 5-3 shows the MCNP estimates for dose rates over axial surfaces and segments in rem/h. The first value of each set is the surface dose rate for the waste package containing Hanford HLW glass and FFTF DOE SNF canister, while the second value is the surface dose rate for the waste package containing only Hanford HLW glass. The axial dose rate on Surface 10 (the inner surface of the inner barrier of the top lid) is about one order of magnitude lower than the axial dose rate on Surface 6 (inner surface of inner barrier bottom lid). The difference indicates that the doses on the axial surfaces are mainly due to HLW glass canisters. The upper surface of HLW glass canisters is about 1 m below the inner top lid and their bottom surfaces lay on the inner bottom lid, while the FFTF DOE SNF canister is symmetrically positioned at the center of the waste package.

The peak dose on the outside of top and bottom waste package outer lids (Figure 5-3, Segment d) is mainly produced by the gamma rays emitted in the HLW glass. The gamma rays from the HLW glass undergo multiple collisions and lose energy in the FFTF fuel and in the walls of the DOE SNF canister. The spectrum of gamma rays that enter the FFTF DOE SNF canister and then reach the Segment d of Surface 6 (see figure 5-3) is much softer than that of the gamma rays that travel through the less dense material of the HLW glass and reach the surrounding axial surface. The dose rate on Segment d is doubled when the FFTF DOE SNF canister is removed, indicating that its presence in the center of the waste package actually reduces the axial dose rates. This is mainly due to the fact that placing the FFTF DOE SNF canister in the center of the waste package provides shielding for the gamma rays from the HLW glass, which otherwise would only attenuate through air (or a fill gas) with a much smaller attenuation coefficient. The combined dose rate due to the gamma rays from the HLW glass that are shielded by the FFTF DOE SNF canister, and the gamma rays from the FFTF DOE SNF canister itself is, therefore,

less than the dose rate due to the gamma rays from the HLW glass in the absence of the FFTF DOE SNF canister.

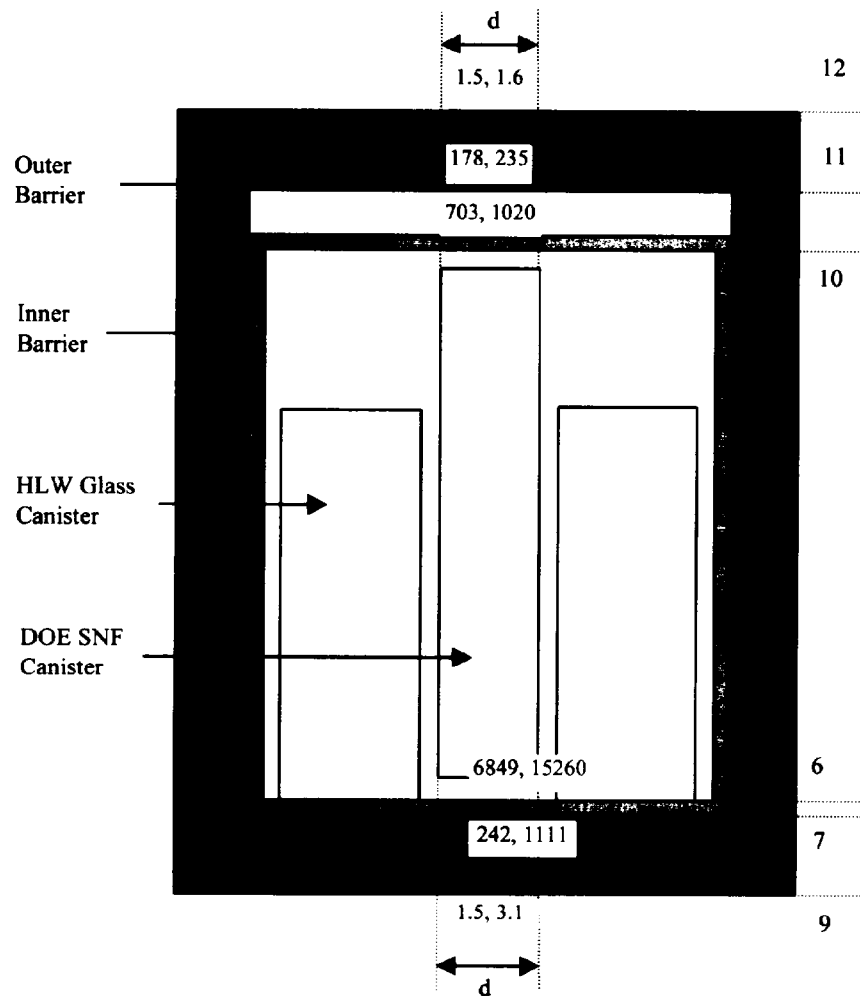


Figure 5-3. MCNP Estimates for Dose Rates in rem/h over Axial Surfaces and Segments

## 6. DEGRADATION AND GEOCHEMISTRY ANALYSIS

### 6.1 USE OF COMPUTER SOFTWARE

The EQ3/6 software package originated in the mid-1970s at Northwestern University (Wolery 1992). Since 1978, Lawrence Livermore National Laboratory (LLNL) has been responsible for maintaining of EQ3/6. The software most recently has been maintained under the sponsorship of the Civilian Radioactive Waste Management Program of the DOE. This code identified as CSCI UCRL-MA-110662 V 7.2b, SCR: LSCR198 was obtained from the SCM in accordance with appropriate procedures. The major components of the EQ3/6 package include the following: EQ3NR, a speciation-solubility code; EQ6, a reaction path code that calculates water/rock interaction or fluid mixing in either a pure reaction progress mode or a time mode; EQPT, a data-file preprocessor; EQLIB, a supporting software library; and several supporting thermodynamic data files. The software implements algorithms describing thermodynamic equilibrium, thermodynamic disequilibrium and reaction kinetics. The supporting data files contain both standard-state and activity-coefficient-related data.

EQ6 calculates the irreversible reactions that occur between an aqueous solution and a set of solid, liquid, or gaseous reactants. The code can calculate fluid mixing and the consequences of changes in temperature. This code operates both in a pure reaction progress frame as well as in a time frame.

In this study, EQ3/6 is used to provide:

- A general overview of the nature of chemical reactions to be expected
- The degradation products likely to result from corrosion of the waste forms and canisters
- An indication of the minerals, and their amounts, likely to precipitate within the waste package.

The EQ3/6 calculations reported in this document used the qualified version 7.2b of the code as documented in *EQ3/6 Software Installation and Testing Report for Pentium Based Personal Computers (PCs)* (CRWMS M&O 1998k), and is executed on personal computers (PCs) running Windows 95.

### 6.2 DESIGN ANALYSIS

#### 6.2.1 Systematic Investigation of Degradation Scenarios and Configurations

Degradation scenarios comprise a combination of features, events, and processes that result in degraded configurations to be evaluated for criticality. A configuration is defined by a set of parameters characterizing the amount, and physical arrangement, at a specific location, of the materials that can significantly affect criticality (e.g., fissile materials, neutron-absorbing materials, reflecting materials, and moderators). The variety of possible configurations is best understood by grouping them into classes. A configuration class is a set of similar configurations whose composition and geometry is defined by specific parameters that

distinguish one class from another. Within a configuration class the values of configuration parameters may vary over a given range.

A master scenario list and set of configuration classes relating to internal criticality is given in the *Disposal Criticality Analysis Methodology Topical Report* (CRWMS M&O 1998a, pp. 3-2 through 3-12) and also shown in Figures 6-1 and 6-2. This list was developed by a process that involved workshops and peer review. The comprehensive evaluation of disposal criticality for any waste form must include variations of the standard scenarios and configurations to ensure that no credible degradation scenario is neglected. All of the scenarios that can lead to criticality begin with the breaching of the waste package, followed by entry of the water, which eventually leads to degradation of the SNF and/or other internal components of the waste package. This degradation may permit neutron absorber material to be mobilized (made soluble) and either be flushed from the waste package or displaced from the fissile material, thereby increasing the probability of criticality.

The standard scenarios for internal criticality divide into two groups:

1. When the waste package is breached only on the top, water flowing into the waste package builds up a pond. This pond provides water for moderation to support a criticality. Further, after a few hundred years of steady dripping, the water can overflow through the hole in the top of the waste package, and flush out any dissolved degradation products.
2. When the waste package breach occurs on the bottom as well as the top, the water flows through the waste package. This group of scenarios allows the soluble degradation products to be removed more quickly, but does not directly provide water for moderation. Criticality is possible, however, if the waste package fills with corrosion products that can add water of hydration and/or plug any holes in the bottom of the waste package. The waste package supports this latter behavior because the silica released by the degrading HLW glass may form clay with enough water of hydration to support criticality.

The standard scenarios for the first group are designated IP-1, -2, -3 (IP stands for internal to the package) according to whether the waste form degrades before the other waste package internal components, at approximately the same time (but not necessarily at the same rate), or later than the waste package internal components. The standard scenarios for the second group are designated IP-4, -5, or -6 based on the same criteria. The internal criticality configurations resulting from these scenarios fall into six configuration classes described below (CRWMS M&O 1998a, pp. 3-10 through 3-12):

1. Basket is degraded but waste form relatively intact and sitting on the bottom of the waste package (or the DOE canister), surrounded by, and/or beneath, the basket corrosion products (see Figure 6-3). This configuration class is reached from scenario IP-3.
2. Both basket and waste form are degraded (see Figure 6-4). The composition of the corrosion product is a mixture of fissile material and iron oxides, and may contain clay. It is more complex than for configuration class 1, and is determined by geochemical calculations as described in Section 6.3.2. This configuration class is most directly reached from standard

scenario IP-2, in which all the waste package components degrade at the same time. However, after many tens of thousands of years the scenarios IP-1 and IP-3, in which the waste form degrades before or after the other components, also lead to this configuration.

3. Fissile material is moved some distance from the neutron absorber, but both remain in the waste package (see Figure 6-5). This configuration class can be reached from IP-1.
4. Fissile material accumulates at the bottom of the waste package, together with moderator provided by water trapped in clay (see Figure 6-6). The clay composition is determined by geochemical calculation, as described in Section 6.3.2. This configuration class can be reached by any of the scenarios, although IP-2 and IP-5 lead by the most direct path; the only requirement is that there be a large amount of glass in the waste package (as in the codisposal waste package) to form the clay.
5. Fissile material is incorporated into the clay, similar to configuration class 4, but with the fissile material not at the bottom of the waste package (see Figure 6-7). Generally the mixture is spread throughout most of the waste package volume, but could vary in composition so that the fissile material is confined to one or more layers within the clay. Generally, the variations of this configuration are less reactive than for configuration class 4, therefore, they are grouped together, rather than separated according to where the fissile layer occurs or whether the mixture is entirely homogeneous. This configuration class can be reached by either standard scenario IP-1 or -4.
6. Fissile material is degraded and spread into a more reactive configuration but not necessarily moved away from the neutron absorber, as in configuration class 3 (see Figure 6-8). This configuration class can be reached by scenario IP-1.

It should be noted that the configuration classes 1, 2, 4, and 5 require that most of the neutron absorber be removed from the waste package; however in configuration classes 3 and 6, the fissile material is simply moved away from the absorber or into a more reactive geometry.

In Sections 6.2.1.1 through 6.2.1.5 the scenarios and the resulting configuration classes that are applicable to the FFTF DOE SNF codisposal waste package are discussed.

Note that most of these configuration pairs (Figures 6-3 through 6-8) look quite different even though both pair members belong to the same configuration class. This apparent dissimilarity arises from the configuration class definition strategy, which classifies critical configurations according to the geometry and composition of the materials, irrespective of the container (either the DOE SNF canister, or the entire waste package).

Note: W.P. = waste package  
W.F. = waste form  
F.M. = fissile material

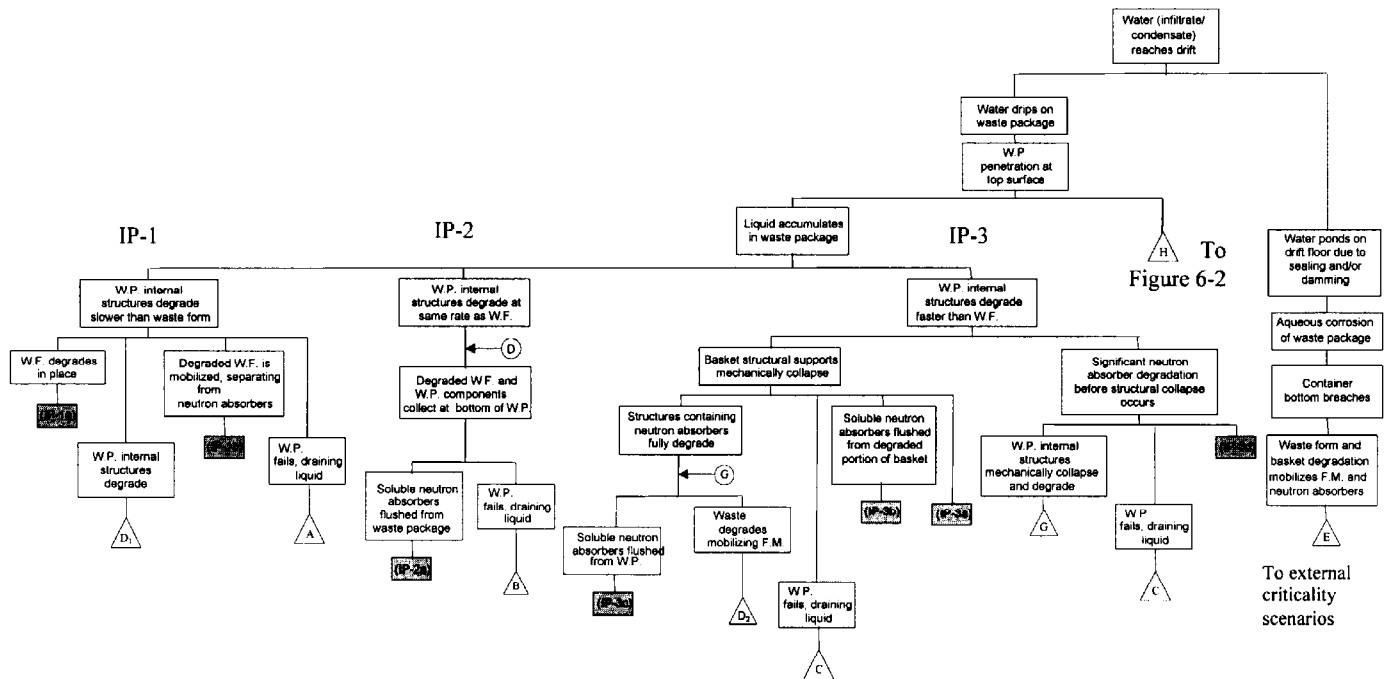


Figure 6-1. Internal Criticality Master Scenarios, Part 1

From Figure 6-1

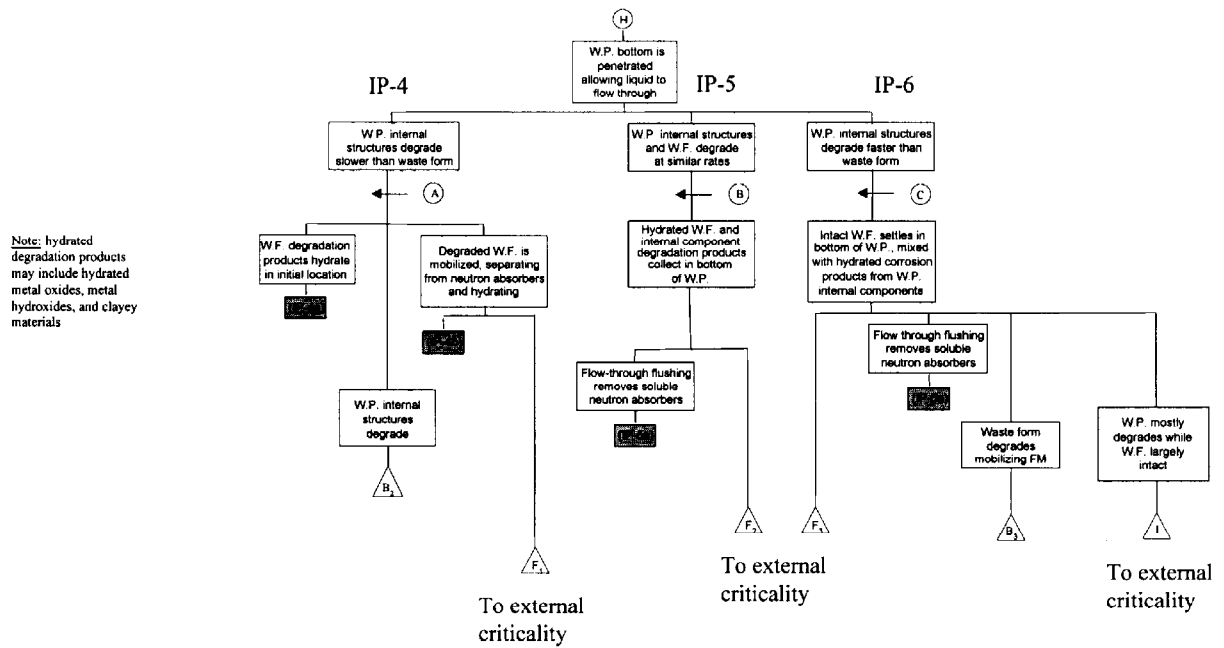


Figure 6-2. Internal Criticality Master Scenarios, Part 2

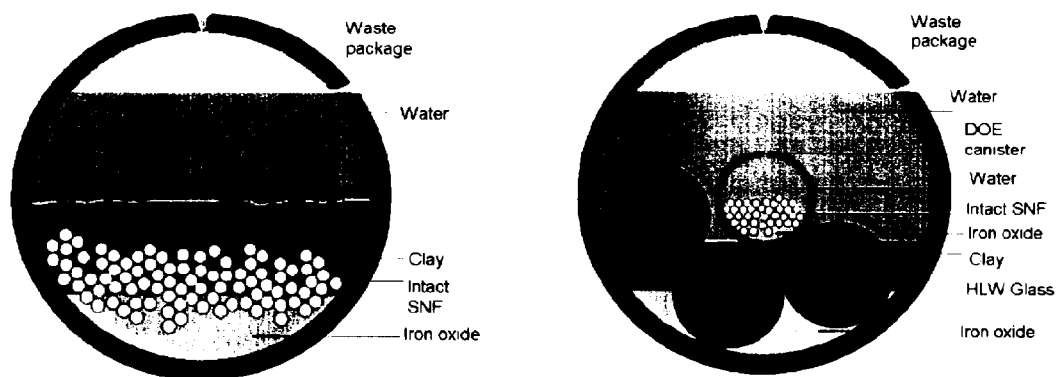


Figure 6-3. Examples of Degraded Configurations from Class 1

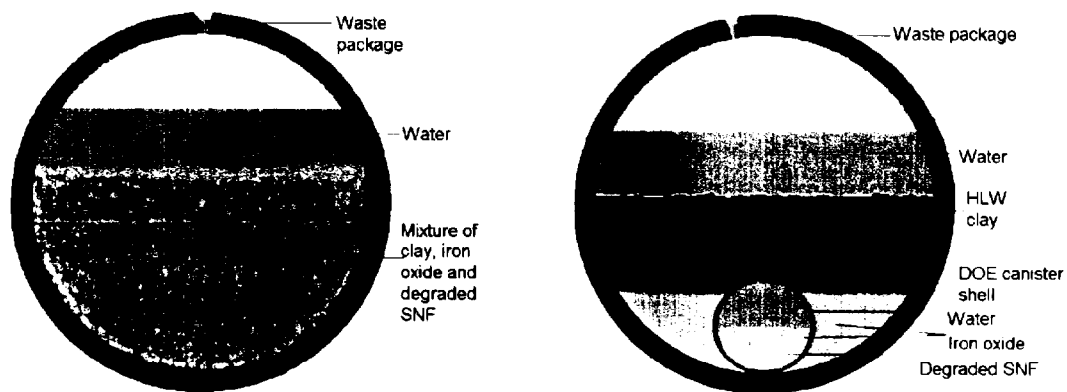


Figure 6-4. Examples of Degraded Configurations from Class 2

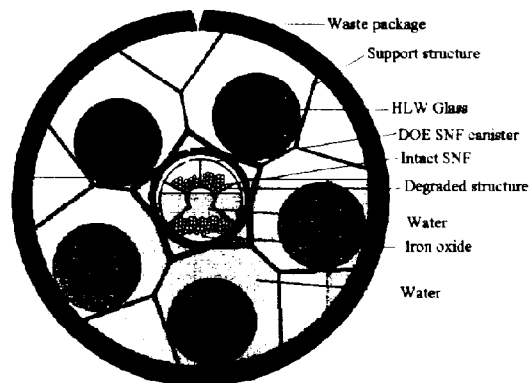


Figure 6-5. Example of Degraded Configurations from Class 3



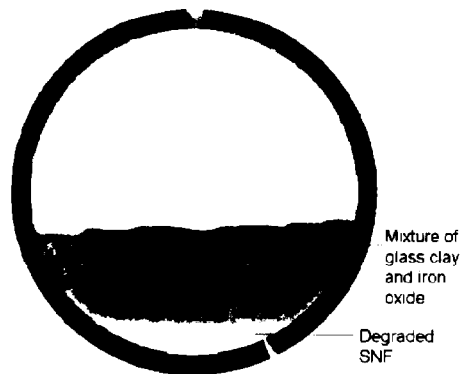


Figure 6-6. Example of Degraded Configurations from Class 4

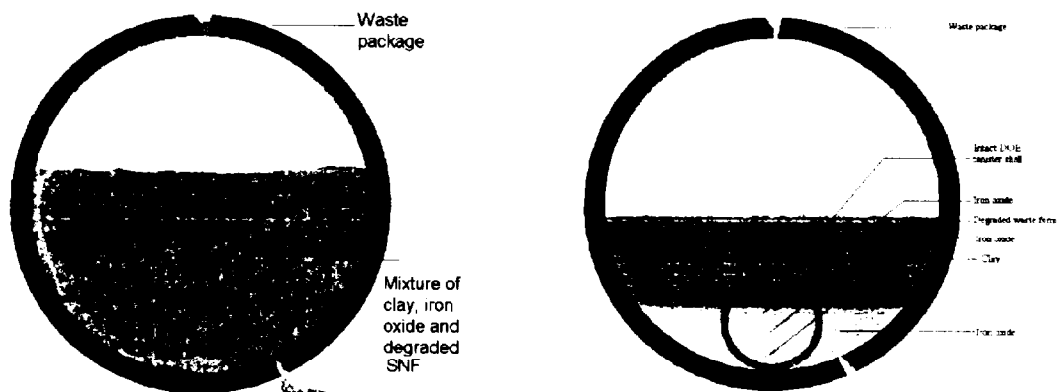


Figure 6-7. Examples of Degraded Configurations from Class 5

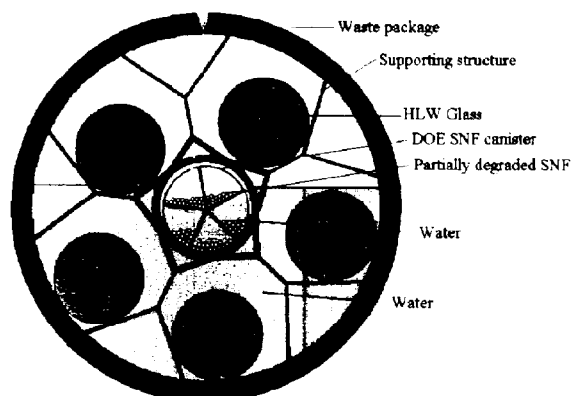


Figure 6-8. Example of Degraded Configurations from Class 6

#### **6.2.1.1 Degraded Assembly (Intact Basket)**

For these cases of degraded fuel assemblies within intact basket, the scenarios and configuration classes are applied to the DOE SNF canister and its contents. Since the SNF degrades before the basket in these configurations, this is an example of standard scenario 1. The resultant configurations correspond to refinements of configuration class 3. The varying levels of degradation of DFAs are given by the following sequence, with the section of this report containing the results of the criticality calculations for that configuration shown in parentheses:

1. Degradation of fuel pin clips and spacers (Section 7.4.1)
2. Partial and complete degradation of fuel cladding (Section 7.4.1)
3. Degradation of assembly duct along with fuel pin clips and spacers (Section 7.4.2)
4. Complete degradation of the assembly resulting in pellets stacked randomly in each basket location (Section 7.4.2).

#### **6.2.1.2 Degraded Basket and Intact SNF**

Since the basket is more than three times as thick as the FFTF assembly duct, it is virtually impossible for it to completely degrade before the FFTF assembly duct. This configuration is a variation of configuration class 1 and can be reached from standard scenario IP-3 in Figure 6-2. The refinements of this configuration are characterized by the varying levels of degradation of the DFAs and are given in the following sequence, together with the section of this report containing the results of the criticality calculations for that configuration.

1. All DFAs and Ident-69 pin container (if present) are intact (Section 7.4.3).
2. All DFAs are degraded resulting in intact fuel pins stacked inside the DOE SNF canister around an intact Ident-69 pin container (Section 7.4.4).
3. Intact Ident-69 surrounded by a homogeneous mixture resulting from complete degradation of all DFAs and the basket (Section 7.4.5).
4. Degraded Ident-69 mixed with homogeneous mixture resulting from complete degradation of all DFAs and the basket (Section 7.4.6).
5. A homogeneous mixture resulting from complete degradation of six DFAs (the nominal five, plus one replacing the Ident-69 (Section 7.4.6).

Although these configurations are all very unlikely, they are considered for reasons of completeness and conservatism. A more likely set of configurations with some basket degradation would contain some partly degraded basket plates between the remaining assemblies or rods that fall to the bottom of the DOE SNF canister. Such a configuration could arise because of the collapse of the basket structure.

#### **6.2.1.3 Degraded DOE SNF canister Contents and Degraded HLW and other Waste Package Components**

In this case, the concepts of scenario and configuration are applied to the entire waste package. These configurations have an intact DOE SNF canister shell surrounded by clay formed by degraded HLW and waste package basket. All DOE SNF canister internals, such as the basket, DFAs, and the Ident-69, if present, are degraded to form a homogeneous mixture. These configurations are from configuration class 5 discussed in Section 6.2.1 and can be reached from any of the standard scenarios shown in Figure 6-2. The calculation of the clay composition is described in Section 6.3.2, and the criticality calculations are described in Section 7.4.8.

#### **6.2.1.4 Completely Degraded DOE SNF canister above Clay from HLW and Waste Package Internals**

In this case, the concepts of scenario and configuration are also applied to the entire waste package. These configurations represent the DOE SNF canister as completely degraded and forming a layer above the clay that results from complete degradation of waste package basket and HLW glass canisters. Various combinations of the fuel and clay layers are also investigated. This configuration is a variation of configuration class 5 discussed in Section 6.2.1 and can be reached from standard scenarios IP-4 and -5 shown in Figure 6-2. The calculation of the clay composition is described in Section 6.3.2 and the criticality calculations are described in Section 7.5.1.

#### **6.2.1.5 Clay from HLW and Waste Package Internals above Completely Degraded DOE SNF canister**

This case also applies the concepts of scenario and configuration to the entire waste package. These configurations have the clay from the degradation of the waste package basket and HLW glass canisters above the completely degraded DOE SNF canister. This configuration is configuration class 4 discussed in Section 6.2.1 and can be reached from scenarios IP-1 and -4 shown in Figure 6-2. The calculation of the clay composition is described in Section 6.3.2 and the criticality calculations are described in Section 7.5.2.

### **6.2.2 Basic Design Approach for Geochemical Analysis**

The method used for this analysis involves the steps described below.

1. Use the basic EQ3/6 capability to trace the progress of reactions as the chemistry evolves, including estimating the concentrations of material remaining in solution as well as the composition of precipitated solids. (EQ3 is used to determine a starting fluid composition for a series of EQ6 calculations; it does not simulate reaction progress.)
2. Evaluate available data on the range of dissolution rates for the materials involved, to be used as material/species input for each time step.

3. Use the "solid-centered flow-through" mode (SCFT) in EQ6. In this mode, an increment of aqueous "feed" solution is added continuously to the waste package system, and a like volume of the existing solution is removed. This mode simulates a continuously stirred tank reactor.
4. Determine the concentrations of fissile materials in solution as a function of time (from the output of EQ6-simulated reaction times up to  $6 \cdot 10^5$  years).
5. Calculate the amount of fissile material released from the waste package as a function of time (which thereby reduces the chance of criticality within the waste package).
6. Determine the concentrations of neutron absorbers, such as Gd, in solution as a function of time (from the output of EQ6 over times up to  $6 \cdot 10^5$  years).
7. Calculate the amount of neutron absorbers retained within the waste package as a function of time.
8. Calculate the composition and amounts of solids (precipitated minerals or corrosion products and unreacted package materials).

### **6.3 CALCULATIONS AND RESULTS**

The calculations begin by selecting representative values from known ranges for composition, amounts, and reaction rates of the various components of the FFTF waste package. Surface areas are calculated based on the known package geometry. The input to EQ6 consists of the composition of J-13 well water, together with a rate of influx to the waste package (Section 2.1.8.3). Sometimes the degradation of the waste package is divided into stages (e.g., degradation of HLW glass before breach and exposure of the fuel assemblies and basket materials to the water). The EQ6 outputs include the compositions and amounts of solid products and the solution composition. Details of the results are presented below. The calculation process is described in more detail in CRWMS M&O (1998e).

#### **6.3.1 Gadolinium Solubility Scoping Calculations**

If the fissile material were to remain behind in the waste package while the Gd and other neutron absorbers are flushed from the system, an internal criticality could be possible. Uranium and plutonium are quite soluble in alkaline, carbonate-rich solutions produced when the HLW glass degrades (solubility up to  $\sim 10^{-1}$  molal [CRWMS M&O 1998e, p. 38]). The proposed criticality control material,  $\text{GdPO}_4$ , will likely hydrate slightly when exposed to water to form  $\text{GdPO}_4 \cdot \text{H}_2\text{O}$ . The latter is very slightly soluble in neutral solutions (Firsching, F.H. and Brune, S.N. 1991), though its solubility increases at low and high pHs; complexation at high pH is particularly enhanced by dissolved carbonate (Lee, J.H. and Byrne, R.H. 1992, Figure 8). Conditions of a low pH might be produced as stainless steel degrades separately from the HLW glass. One general scenario that maximizes the potential for internal criticality involves the early breach of the stainless steel Type 304L HLW canisters, followed by the rapid degradation of the HLW glass followed by removal of the alkaline components during a period of relatively high drip rate.

Then the stainless steel Type 316L DOE SNF canister breaches, exposing some of the MOX fuel. In this second stage, the pH of the ambient solutions remains low (~5 to ~6), due in part to the degradation of the stainless steel.

The scenarios chosen for this study build on three previous analyses of the loss of U, Pu, and Gd from waste packages containing fissile waste forms codisposed with HLW glass (CRWMS M&O 1998f; CRWMS M&O 1996b, Table C-1; and CRWMS M&O 1997f, p. 5-17). These prior studies suggested that the greatest removal of Gd would occur at slow drip rates in the second stage described in the previous paragraph. However, the previous work assumed that  $\text{GdOHCO}_3$  would be the solubility-limiting phase. When  $\text{GdPO}_4 \cdot \text{H}_2\text{O}$  is allowed to form, the overall solubility and loss of Gd will be lower. However, as the solubility product of  $\text{GdOHCO}_3$  includes both hydroxyl and carbonate ions, the solubility of  $\text{GdPO}_4 \cdot \text{H}_2\text{O}$  will increase with increasing pH and  $\text{CO}_2$  pressure (CRWMS M&O 1998e, p. 26).

Two simplified systems can be used to bound the maximum Gd solubility. For the first system, (called system A) the only source of aqueous Gd and phosphorous (P) would be the dissolution of solid  $\text{GdPO}_4 \cdot \text{H}_2\text{O}$ , that is, no P is supplied by steel or glass. Such assumptions would be reasonable if the system had been flushed for some time, thus removing the dissolved phosphate contributions from faster-reacting components. Since it could be speculated that such a system would underestimate Gd solubility via aqueous Gd-phosphate complexes, a second system is considered in which aqueous Gd concentration is still controlled by  $\text{GdPO}_4 \cdot \text{H}_2\text{O}$ , but aqueous phosphate concentration is varied independently. The second system (called system B) is used to estimate the maximum contribution of aqueous phosphate complexes, when other phosphate sources (such as glass and steel) exist. Figure 6-9 shows the Gd species concentrations as a function of pH.

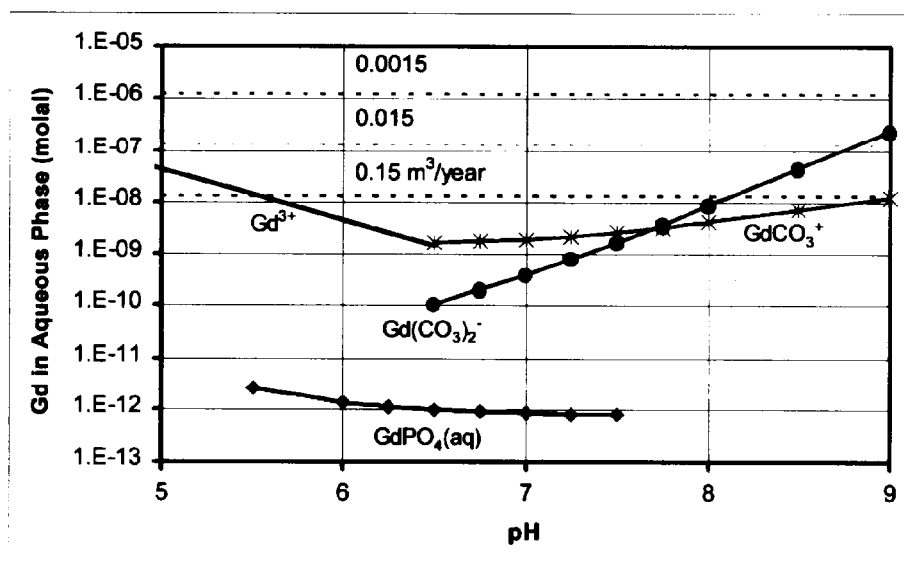


Figure 6-9. Gd Species Concentration as a Function of pH

For system A, at a drip rate of  $0.0015 \text{ m}^3/\text{year}$  (Figure 6-9, top dashed line), the concentrations of all the plotted Gd species are too low to allow significant loss. A "significant" loss is defined as: loss of 10% or more of the total Gd in the waste package over a period of one million years (the National Academy of Sciences recommended evaluation period for the repository). At  $0.015 \text{ m}^3/\text{year}$  (middle dashed line), only  $\text{Gd}(\text{CO}_3)_2^-$  achieves a concentration high enough to cause significant loss, and only with a  $\text{pH} > 8.7$  for one million years. However, with the chosen high  $\text{CO}_2$  fugacity, the long-term pH will be approximately 7.6 (CRWMS M&O 1998f, Figures 5.3.4-4 through 5.3.4-6). Therefore, it is extremely unlikely that significant loss will occur. (At lower  $\text{CO}_2$  fugacities, a higher pH is possible, but the stability of  $\text{Gd}(\text{CO}_3)_2^-$  decreases at lower  $\text{CO}_2$  fugacities). At the drip rate of  $0.15 \text{ m}^3/\text{year}$ ,  $\text{Gd}^{3+}$  reaches sufficient concentrations at a  $\text{pH} < 5.5$ , and  $\text{Gd}(\text{CO}_3)_2^-$  achieves adequate concentrations for loss at a  $\text{pH} > 8$ . As noted before, the long-term pH is likely to be approximately 7.6, so the latter species is probably not that significant. Previous studies (CRWMS M&O 1998f; and CRWMS M&O 1998e, Figures 5-11 and 5-27) suggest high pH can be achieved when glass degrades rapidly, but at such high drip rates, the period of high pH is limited to thousands, not millions, of years. Similarly, previous studies (CRWMS M&O 1998f, Figure 5.3.2-2; CRWMS M&O 1998e, Figure 5-4) showed that acid conditions ( $\text{pH} < 6$ ) could be produced in the codisposal packages, but generally only for "short" periods ranging over hundreds to tens of thousands of years. Thus, unusual conditions will be required to achieve significant loss of Gd, when the element is present in the package as solid  $\text{GdPO}_4$ .

Figure 6-10 plots the calculated total concentration of dissolved Gd phosphate complexes, as functions of pH and total dissolved phosphate ( $\text{HPO}_4^{2-}$  and  $\text{H}_2\text{PO}_4^-$ ), for system B. Even at high total dissolved phosphate ( $10^{-2}$  molal), these Gd complexes never exceed concentrations much greater than  $10^{-9}$  molal for  $4 \leq \text{pH} \leq 9$ , and thus would not result in significant Gd loss from the system.

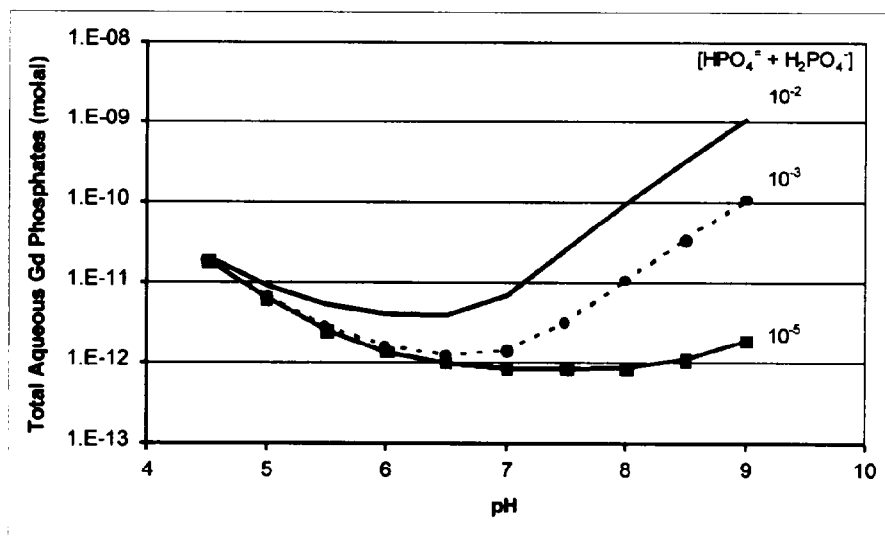


Figure 6-10. Concentrations of Phosphate Species in Equilibrium with  $\text{GdPO}_4 \cdot 2\text{H}_2\text{O}$ , for Total Phosphate Concentrations of  $10^{-5}$ ,  $10^{-3}$ , and  $10^{-2}$  molal

### 6.3.2 Results of EQ6 Runs

Table 6-1 summarizes the conditions used for the EQ6 runs and the total percentage of Gd, Pu, and U remaining at the end of the runs. Cases 1 through 8 in Table 6-1 all involve simultaneous exposure of the fuel and all package materials to J-13 water; these cases are designed to maximize exposure of the Gd-doped basket to high pH, to stress the enhanced solubility of  $\text{GdPO}_4$  under alkaline conditions (the right side of Table 6-1). In contrast, cases 9 through 12 all involve two fundamentally different stages. In the first stage, J-13 water interacts with the outside surface of the DOE SNF canister and with all package materials outside the canister (including the glass, stainless steel Type 304L HLW glass pour canister, and the A 516 outer basket). The second stage begins after the HLW glass is completely degraded; the DOE SNF canister is "breached" at the beginning of the second stage, allowing the J-13 water to interact with the fuel assemblies, fuel pin cladding, Gd-doped basket materials, the Ident-69, and the fuel components themselves (the  $[\text{U}, \text{Pu}]\text{O}_2$  MOX and  $\text{UO}_2$  insulator pellets). Cases 9 through 12 are designed to produce the lowest pH at long times, by removing the alkaline glass before the fuel and Gd-doped basket are exposed. Thus, cases 9 through 12 are intended to test the increased Gd solubility on the left side of Figure 6-9.

Table 6-1. Summary of Geochemistry Results

Case	% Left at End of Run			Rates*				Fe Oxide
	Gd	Pu	U	Steel	Glass	Fuel	J-13	
1	99.9	99.6	56.4	1	1	1	1	hematite
2	99.3	99.0	91.1	1	1	1	2	hematite
3	99.3	97.6	99.7	1	1	1	3	hematite
4	99.8	11.7	11.9	1	2	1	1	hematite
5	99.8	41.4	0.00	2	2	1	1	hematite
6	99.8	41.4	0.00	2	2	2	1	hematite
7	99.7	6.20	1.20	2	2	2	2	hematite
8	99.3	74.5	78.0	2	1	2	2	hematite
9	100	99.5	99.9	2 / 2	2 / 0	0 / 2	4 / 2	hematite
9s**	100	99.7	99.9	2 / 2	2 / 0	0 / 2	4 / 2	hematite
10	100	98.3	99.8	2 / 2	2 / 0	0 / 2	4 / 2	goethite
10s**	100	99.3	99.7	2 / 2	2 / 0	0 / 2	4 / 2	goethite
11	100	98.3	99.9	2 / 2	2 / 0	0 / 2	3 / 1	goethite
12	100	97.0	99.9	1 / 1	2 / 0	0 / 2	3 / 1	goethite

\* Rates encoding:  
 Steels: 1=average rate; 2=high rate (Table 2-17).  
 Glass: 0=no glass present; 1=low rate; 2=high rate (Table 2-18).  
 Fuel: 0=no fuel present; 1=average rate; 2=high rate (Table 2-19).  
 J-13: 1=0.0015 m<sup>3</sup>/year; 2=0.015 m<sup>3</sup>/year; 3=0.15 m<sup>3</sup>/year; 4=0.5 m<sup>3</sup>/year (Section 2.1.8.3).  
 Cases 9 through 12 are multi-stage; rates are given in format: first stage / second stage.  
 \*\* Glass composition is varied

Both hematite and goethite are observed to form in rust, though the EQ6 thermodynamic database indicates hematite is thermodynamically more stable with increasing temperature. In general, the first stage of a multi-stage run is comparatively short ( $\sim 10^3$  to  $\sim 10^4$  years) and the second stage of the run is carried out to at least 100,000 years. While the first stage is important in setting up the chemical conditions, the second stage is generally of greater interest for

neutronics calculations, since the corrosion-product compositions can vary greatly in the first stage, but achieve a quasi-steady state composition at long times.

The greatest Gd losses occur in the runs that maximize exposure of Gd to the glass. Nonetheless, the maximum Gd loss is never greater than 0.7% over 100,000 years for any of the scenarios. Furthermore, some of the cases that show some Gd loss also show large losses of Pu and U, which would decrease the potential for an internal criticality.

## 6.4 SUMMARY

Twelve EQ6 reaction-path cases are constructed to span the range of possible Gd and fuel corrosion (Table 6-1). Two additional cases test the effect of varying glass composition. Cases 1 through 8 test the alkaline regime, achieving high a pH by exposing the fuel to degrading glass. While cases 1 through 8 produce the highest Gd loss, the total loss is  $\leq 0.7\%$  in  $\geq 100,000$  years. Furthermore, when the glass degrades rapidly, the alkaline conditions produce high U and Pu loss (up to 100%), reducing the chances of internal criticality. Some of these "alkaline" cases actually produce a short-lived, very low pH ( $\sim 3$ ) when glass corrosion rates are set to low values, but steel corrosion rates are set to high values (CRWMS M&O 1998f). These low pH values may not be realistic, since the simple, glass corrosion-rate law does not allow a feedback between pH and corrosion rate (which would tend to increase pH). Cases 9 through 12 test the effect of exposing the Gd, Pu, and U to long-lived acidic conditions (pH  $\sim 5$  to 6). The highest acidity is obtained by breaking the calculations into two stages. In the first stage, the DOE SNF canister is represented as being intact, and only the outside of the DOE SNF canister, the HLW glass pour canisters (and contained glass), and the A 516 outer basket structure are allowed to interact with the water dripping into the waste package. With a sufficiently high drip rate, the alkaline components of the glass are removed during this stage. In the second stage, the Gd-doped basket, fuel, and other components within the DOE SNF canister are exposed to J-13 water at a much lower drip rate, allowing the pH to drop. When the formation of hematite is suppressed (in favor of goethite), a somewhat lower pH is achieved. None of cases 9 through 12 causes a significant loss of Gd, and none produces more than a few percent loss of either Pu or U.

For two-stage cases, small variations in the Mg content of the glass cause shifts in the times of peak pH and aqueous Gd, Pu, and U concentrations. The cause of these shifts is the production of solid, alkaline-earth carbonates, which consume some of the acid produced by steel degradation and delay the onset of the low-pH plateau. Clays that formed with the Mg-rich glass have higher Mg contents; however, the clay  $(\text{Mg}+\text{Ca}+(\text{Na}+\text{K})/2)/\text{Si}$  varies by only a fraction of a percent among the cases (as would be expected, since the one-clay phase dominates, and this ratio is fixed by structural and charge balance). The fractions of O, Si, Al, Ti, Fe, Mn, Gd, Pu, and U in the corrosion products are nearly constant (except for the early stages of runs with very low glass corrosion rates), and that overall the variation in glass composition has little effect on the amount of Gd, U, and Pu retained in the waste package. While these results are encouraging, it would be useful to perform a more systematic investigation on the effects of varying glass composition.

The predicted major corrosion products are: an iron-rich smectite clay (nontronite); hematite or goethite; pyrolusite ( $\text{MnO}_2$ ); rutile ( $\text{TiO}_2$ ); and  $\text{Ni}_2\text{SiO}_4$  or  $\text{NiFe}_2\text{O}_4$ . The smectite and hematite



typically comprise more than 90% of the corrosion-product volume. If interaction with J-13 water continues for > 10,000 years, corrosion products may fill approximately 50% of the volume within the CRM. Given the poor packing and high porosity of clay aggregates, the volume fraction occupied by corrosion products plus occluded water may be much greater than 50%. The Gd enters into rhabdophane (hydrated  $\text{GdPO}_4$ ) as the basket corrodes, the Pu enters  $\text{PuO}_2$ , and the dominant U solid is soddyite ( $(\text{UO}_2)_2(\text{SiO}_4) \cdot 2\text{H}_2\text{O}$ ).

As the basket corrodes, high aqueous orthophosphate ( $\text{HPO}_4^{2-}$ ) concentrations may be achieved. A somewhat surprising result of this study is the prediction that  $\text{HPO}_4^{2-}$  complexes may dominate Pu solubility during periods of low pH. However, high levels of dissolved phosphate are not entirely due to the basket; the HLW glass contains about three times the phosphate of the Gd-doped basket, and the abundant carbon steel also contains trace phosphate. Thermodynamic data for Pu orthophosphate are estimated and added to the calculations, but the hypothetical solid does not precipitate, and therefore does not affect solubility. Nonetheless, it would be useful to investigate the sensitivity of the calculations to the quality of the thermodynamic data for the Pu phosphate complexes.

For purposes of the calculations, it is assumed that the most insoluble oxide of Pu could form. This assumption is conservative for internal criticality, but may underestimate the release of Pu from the waste package. As summarized in Stockman 1998, page 625, experiments suggest that the solubility of Pu may be controlled by an amorphous  $\text{PuO}_2 \cdot \text{H}_2\text{O}$ , which is substantially more soluble than  $\text{PuO}_2$ . Such higher solubility conditions will need to be included in additional EQ6 calculations to develop the source term for external criticality.

The assumption of complete Cr oxidation also bears investigation. The EQ3/6 databases contain very few solids that could precipitate under oxidizing conditions. If such solids exist (e.g., Cr-goethites, Cr-clays, and  $\text{CaCrO}_4$ ), the amount of acid production and amount of Cr release from the package may be overestimated. For internal criticality, the assumption of high Cr loss is generally conservative, but these assumptions may be inappropriate when carried through as a source term for external criticality.

## **7. INTACT AND DEGRADED CRITICALITY ANALYSES**

### **7.1 USE OF COMPUTER SOFTWARE**

The Monte Carlo code, MCNP, Version 4B2, is used to calculate the effective multiplication factor of the waste package. This code identified as CSCI 30033 V4B2LV was obtained from SCM in accordance with appropriate procedures, and is qualified as documented in the SQR for the MCNP, Version 4B2 (CRWMS M&O 1998i).

### **7.2 DESIGN ANALYSIS**

The calculation method used to perform the criticality calculations consisted of using the MCNP Version 4B2 code (LANL 1997) to calculate the  $k_{\text{eff}}$  for various geometrical configurations of FFTF fuel in the 5-HLW/DOE SNF Long waste package. The  $k_{\text{eff}}$  results represent the average combined collision, absorption, and track-length estimator from the MCNP calculations. The standard deviation represents the standard deviation of  $k_{\text{eff}}$  about the average combined collision, absorption, and track-length estimate due to the Monte-Carlo-calculation statistics. The calculations are performed using continuous energy cross-section libraries that are part of the qualified MCNP code system (CSCI 30033 V4B2LV). All calculations are performed with fresh-fuel isotopics (Assumption 2.3.5.1).

The issue of minor actinides, which are fast-fissionable and non-fissile, is investigated. The critical mass of Np-237 moderated and reflected by granite is 45,000 g, and that for Am at 10,000 years is 78,900 g (ORNL 1978). The DOE SNF canister with either six assemblies or five assemblies and an Ident-69 pin container has a total of approximately 720 g Np-237 and 804 g Am-241, as a result of 150 MWd/kg exposure and decay of all Pu-241 into Np-237 (Bergsman 1994). Due to these very low quantities (less than 2% of required minimum critical mass), these minor actinides do not present a potential for criticality, and therefore, have not been included in the criticality calculations.

### **7.3 CALCULATIONS AND RESULTS – PART I: INTACT CRITICALITY ANALYSIS**

A detailed description of the Monte Carlo representations, the method of solution, and the results are provided in CRWMS M&O (1999e). Results for the intact criticality analysis are derived from two cases: one with an Ident-69 pin container in the center position of the basket inside the DOE SNF canister (see Figures ES-1 and 2-4), and the other, with a DFA in the center position (see Figure 7-1). In all cases, the other five positions in the basket contain DFAs. When the DOE SNF canister basket is doped with Gd, the amount of Gd is given in terms of the weight percent of the DOE SNF canister basket with 1% corresponding to 3.852 kg of Gd in the basket.

In this section, the criticality analyses for intact configurations are discussed. Although the components (pins, cladding, assembly, and DOE SNF canister) are considered structurally intact, water intrusion into the components is allowed to determine the highest  $k_{\text{eff}}$  resulting from optimum moderation.

First, the most reactive assemblies based on the fuel type and optimum moderation are determined. Optimal spacing and optimum number of fuel pins in an Ident-69 pin container are also determined for configurations that involve an Ident-69 pin container. Then, the DOE SNF canister configurations containing either six DFAs or five DFAs and an Ident-69 pin container are analyzed with respect to optimum moderation by assuming complete or differential flooding. Optimum positions are also determined by changing the positions of the assemblies, the Ident-69 pin container, and the DOE SNF canister. Due to the long time periods considered in degraded calculations, the decay of plutonium isotopes must be considered. Pu-239 decays to U-235 with a half-life of 24,100 years (Parrington et al. 1996, pp. 48, 49). Pu-240 decays to U-236 with a half-life of 6,560 years. Pu-241 decays to Np-237 with an effective half-life of 447.1 years. The  $k_{eff}$  of the system changes because of Pu-240 absorber decay and Pu-239 fissile decay. Therefore, the nuclide contents are modified to account for the plutonium decay effects in order to identify the most reactive isotopic composition. After scoping calculations, 0 years; 24,100 years; 48,200 years; and 241,000 years are selected as the time steps at which the plutonium decay effects are investigated. At 24,100 years, approximately 92% of the Pu-240 has decayed to U-236, practically all Pu-241 has decayed to Np-237, and only 50% of the Pu-239 has decayed to U-235. At 48,200 years, more than 99% of the Pu-240 has decayed to U-236, practically all Pu-241 has decayed to Np-237, and 75% of the Pu-239 has decayed to U-235. At 241,000 years, more than 99.9% of the Pu-239 has decayed to U-235 and all other plutonium isotopes are essentially zero. The final configurations that result in  $k_{eff}$  greater than the established interim critical limit of 0.93 are further analyzed to determine the minimum amount of absorber required to reduce the  $k_{eff}$  below the interim critical limit.

### **7.3.1 Determination of Most Reactive Assemblies**

Several comparison calculations are performed to determine the type of fuel elements that results in the highest  $k_{eff}$ . Types 3.2 and 4.1 DFAs (see Table 2-4) are compared because they contain the lowest and the highest fissile loading of the four DFA types, respectively. The results show that the Type 4.1 DFAs are more reactive and result in approximately 4% higher  $k_{eff}$  than the Type 3.2 DFAs (CRWMS M&O 1999e, p. 19). Therefore, Type 4.1 DFAs are used for the remainder of the analyses.

Water intrusion into the fuel pins was also investigated. Based on the calculation results, it was concluded that water intrusion into the fuel pins causes a 2% increase in  $k_{eff}$  (CRWMS M&O 1999e, Table 6-13). Therefore, all fuel pins are modeled with water occupying all void spaces inside the fuel pins.

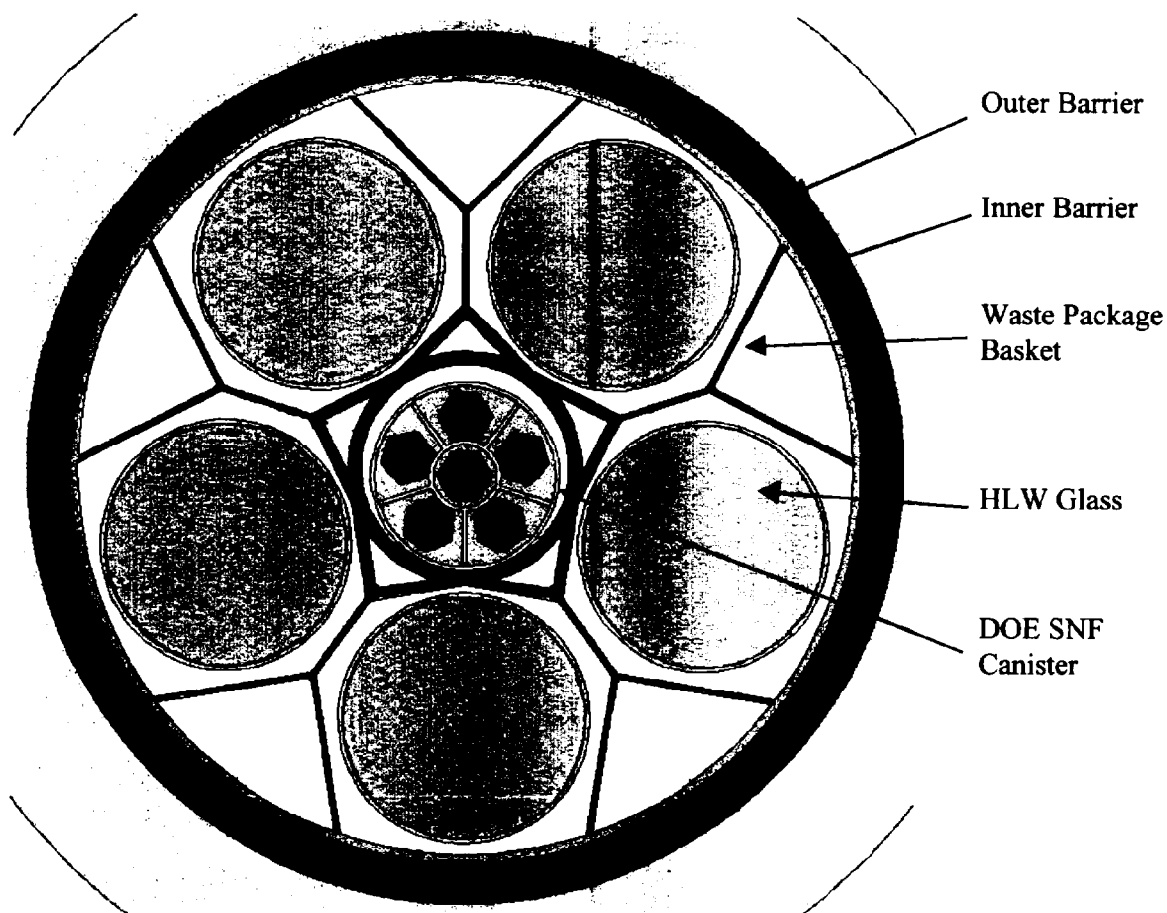


Figure 7-1. Cross Section of 5-HLW/DOE SNF Long Waste Package with Six DFAs

### 7.3.2 Optimal Spacing and Optimum Number of Fuel Pins in an Ident-69 Pin Container

Due to the variety of loading possibilities and varying number of pins in the Ident-69 pin containers, a bounding Ident-69 pin container configuration has to be determined. The Ident-69 pin container is analyzed with respect to the optimal number of fuel pins and the optimal spacing between fuel pins. The array shape is also varied between hexagonal and square.

The pins are placed in the array with uniform spacing filling the entire Ident-69 container, neglecting the inner duct (center tube) of the Ident-69 container. The container is analyzed as fully flooded. The highest  $k_{eff} + 2\sigma$  of 0.7222 is obtained with a pitch of 1.25 cm with equivalent total number of fuel pins of approximately 109 (including partial pins) in a hexagonal array (CRWMS M&O 1999e, Table 6-8). This uniform array is used to demonstrate that the interim critical limit of 0.93 is met and is shown in Figure 7-2a.

An extremely conservative alternate configuration involves a nonuniform distribution of pins in the Ident-69 pin container. In this configuration, the Ident-69 pin container with the uniform

array of pins is modified to include a ring of fuel pins around the inside perimeter of the Ident-69 pin container as shown in Figure 7-2b. This most reactive case has 60 pins around the outer edge of the container plus six pins placed just outside the inside duct with a total of 145 fuel pins and a  $k_{\text{eff}} + 2\sigma$  of 0.7321 (CRWMS M&O 1999e, Table 6-9). This Ident-69 pin container with optimum number of pins in a uniform array with a ring of fuel pins around the inside perimeter of the container is referred to as the reflected array Ident-69 pin container in this document. This configuration is used for comparison and sensitivity analysis, but not in demonstration that the interim critical limit of 0.93 is met.

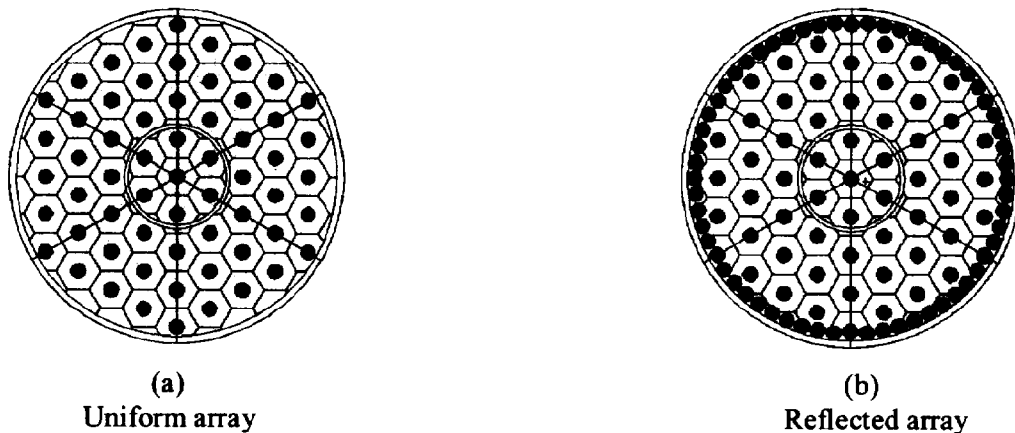


Figure 7-2. Fuel Pin Configuration for Ident-69 Pin container Representations

The reflected array Ident-69 container with a  $k_{\text{eff}} + 2\sigma$  of 0.7321, is then modeled in the basket of the DOE SNF canister surrounded by five DFAs. Since the basket and additional fuel is being placed around the Ident-69 container, the spacing of the fuel pins inside the Ident-69 container must be varied to determine if a significantly more reactive configuration can be found. The results show that  $k_{\text{eff}}$  is essentially constant for values of the pitch ranging from 1.40 to 1.60 cm (recall that the original pitch is 0.72644 cm), and decreases as the pitch decreases with a maximum  $k_{\text{eff}} + 2\sigma$  of 0.9343 for a pitch of 1.4 cm (CRWMS M&O 1999e, Table 6-11). This configuration did not include any Gd.

### 7.3.3 Optimum Moderation in the Waste Package and DOE SNF canister

If the waste package internal space (excluding all components such as HLW canisters and DOE SNF canister) is void instead of being flooded with water, the  $k_{\text{eff}}$  is approximately 1% higher (CRWMS M&O 1999e, Table 6-13). This is due to the fact that the carbon steel support tube acts as a reflector when the waste package internal space is void. When this space is flooded, the water slows the neutrons down, thereby increasing the absorption of neutrons in other waste package components such as the basket.

The effect of differential flooding in the Ident-69 pin container, the DOE SNF canister, and the waste package (CRWMS M&O 1999e, Table 6-16) (i.e., only the Ident-69 pin container, only

the DOE SNF canister, or only the waste package is flooded) is also investigated by changing the density of the water from 0 g/cm<sup>3</sup> (void) to 1 g/cm<sup>3</sup> (flooded) gradually in these components. The results indicated that flooding (water at 1 g/cm<sup>3</sup> density) the Ident-69 pin container increases  $k_{\text{eff}}$  by approximately 16% (CRWMS M&O 1999e, Table 6-17) and flooding the DOE SNF canister increases  $k_{\text{eff}}$  by approximately 18% (CRWMS M&O 1999e, Table 6-18). Therefore, in all configurations in the following sections the Ident-69 pin container, the assemblies, and the DOE SNF canister are modeled as being flooded whereas the waste package internal cavity space is modeled as void.

#### 7.3.4 DOE SNF Canister in the Waste Package

The center position of the basket contains either a DFA or an Ident-69 pin container. The DOE SNF canister is placed in the center position in the waste package and is surrounded by five HLW glass canisters as shown in Figure 7-1. Cases are investigated where the canister is either centered in the waste package or offset from the center to account for settling due to gravity. This change in canister position has no effect on the  $k_{\text{eff}}$  of the system (results are within 1 $\sigma$ ). Also varying levels of flooding and different spacings (between assemblies in outer basket positions and either an Ident-69 or another assembly occupying the inner basket position) are investigated. In all cases, even though the environment outside the waste package, whether tuff, water, or a mixture, has no significant impact on the configuration  $k_{\text{eff}}$ , the waste package is water reflected. The amount of outgoing neutrons penetrating the waste package barriers is less than 1% of the total number of neutrons in the system; and typically less than 0.2% based on the evaluation of the neutron activity reported in the outputs. When the factor of four attenuation through the waste package barriers is factored in, even mirror reflection of these neutrons would have no statistically significant effect. Hence, having a different reflector (e.g., tuff, rock, clay, etc.) on the outside of the waste package would have negligible or no effect on the results.

The maximum  $k_{\text{eff}} + 2\sigma$  for six DFAs is 0.908 (CRWMS M&O 1999f, Table 6-21). This  $k_{\text{eff}}$  is obtained when fuel pins, fuel assemblies, and the DOE SNF canister are flooded and the plutonium isotopes are decayed for 48,200 years, which corresponds to two half-lives of Pu-239 isotope. The analysis of the results indicates that for the intact criticality configurations the  $k_{\text{eff}}$  increases by as much as 5% after approximately 48,200 years of plutonium decay. No Gd was required for this configuration.

The maximum  $k_{\text{eff}} + 2\sigma$  for five DFAs and a reflected array Ident-69 pin container is 1.001 with the plutonium isotopes decayed for 48,200 years, and no Gd in the DOE SNF canister basket (CRWMS M&O 1999f, Table 6-21). The maximum  $k_{\text{eff}} + 2\sigma$  for five DFAs and a uniform array Ident-69 pin container is 0.894 (CRWMS M&O 1999f, Table 6-21). This  $k_{\text{eff}}$  is obtained when the fuel pins, the fuel assemblies, the uniform array Ident-69 pin container, and the DOE SNF canister are flooded, the plutonium isotopes are decayed for 48,200 years, and 0.5 wt% (1.93 kg) Gd uniformly distributed in the DOE SNF canister basket.

#### 7.3.5 Summary

In this section the worst-case configurations are determined for intact criticality. The worst-case configurations are obtained when the entire contents of the DOE SNF canister including fuel

pins, assemblies, and the Ident-69 pin container, if present, are flooded and the waste package internal cavity is dry. The plutonium isotopes are also decayed to their daughter isotopes, which result in the highest  $k_{\text{eff}}$  after approximately 48,200 years. The results show that the configuration of six DFAs in the DOE SNF canister does not need any absorber in the basket or elsewhere in the waste package to achieve a  $k_{\text{eff}} + 2\sigma$  of  $\leq 0.93$ . For the cases that include an Ident-69 container and five DFAs, 0.5 wt% (1.93 kg) Gd must be uniformly distributed on (e.g., flame deposit), or in, the entire DOE SNF canister basket to achieve a  $k_{\text{eff}} + 2\sigma$  of  $\leq 0.93$ .

#### **7.4 CALCULATIONS AND RESULTS – PART II: SCENARIOS WITH FISSILE MATERIAL RETAINED IN DOE SNF CANISTER**

A detailed description of the Monte Carlo representations, the method of solution, and the results are provided in CRWMS M&O (1999f). From the intact configuration results discussed in Section 7.3, the presence of an Ident-69 pin container in the center position is shown to result in higher  $k_{\text{eff}}$  than the presence of a DFA. Therefore, the focus of degraded calculations is on the configurations including an Ident-69 pin container in the center position. Results from the calculations for the partial degradation in the DOE SNF canister can be divided into three general categories depending upon the level of degradation of the fuel components. The categories are defined as follows: partially degraded DFAs and an intact Ident-69 pin container; completely degraded DFAs and an intact Ident-69 container; and DFAs and an Ident-69 container, both completely degraded. In the first two categories, the basket may or may not be intact. However, in the third category, the entire contents of the (intact) DOE SNF canister are degraded, including the basket. Additional calculations are performed with the center position of the basket of the DOE SNF canister containing a DFA rather than an Ident-69 container.

In the configurations investigated in this section, the waste package carbon steel basket and the HLW glass canisters are considered intact. Degradation inside the DOE SNF canister, which is stainless steel Type 316L, is extremely unlikely while the waste package carbon steel basket remains intact. However, the calculations indicate that the position of the DOE SNF canister in the waste package (centered in the clay that would form from the degradation of the waste package basket and HLW glass, or at the bottom against the inner barrier) has no effect on  $k_{\text{eff}}$  since the results are within statistical uncertainty (CRWMS M&O 1999f, Table 6-18 and CRWMS M&O 1999g, Table 6.1-1).

In analyzing the configurations described above, parametric studies have been performed to determine the optimum moderation and configuration. These parametrics include optimizing the moderation in the DOE SNF canister by varying the amount of water in the degradation products, and by varying the density of water in the degradation products; varying the amount of absorbers (both Gd and  $\text{Fe}_2\text{O}_3$ ); and varying the position of remaining intact elements (e.g., the fuel pins, the Ident-69 pin container, etc.). The plutonium decay effects due to long times considered in performing the criticality calculations are also determined. As explained in Section 7.3, all configurations are analyzed with respect to the plutonium decay effects at 0 years, 24,100 years, 48,200 years, and 241,000 years.

Some of the configurations in the following sections include an intact Ident-69 pin container while all other DOE SNF canister components and all DFAs are degraded. The configurations

with an intact Ident-69 pin container are the most reactive configurations. Although the water intrusion into the DOE SNF canister will cause some degradation in the Ident-69 pin container shell, due to its position in the canister it is possible that the Ident-69 pin container will stay intact longer than all other components inside the DOE SNF canister. The Ident-69 pin container resides in a 10 mm thick stainless steel Type 316L tube, which is the central section of the DOE SNF canister basket. The maximum clearance between the DOE SNF canister basket and this tube is 11.7 mm when the waste package is horizontally emplaced. The average clearance is 5.85 mm. After water intrusion into the DOE SNF canister and therefore into this clearance space, the outside of the Ident-69 pin container and the inside wall of this center tube will corrode. The corrosion products ( $\text{FeOOH}$  and/or  $\text{Fe}_2\text{O}_3$ ) will take more space, since they have a lower density, by expanding into the clearance space between the DOE SNF canister basket center tube and the Ident-69 pin container. This may exclude water from the clearance space and stop the corrosion in between the center tube and the Ident-69 pin container. This may create an approximately 19 mm thick shell that is composed of the center tube, corrosion layer, and the Ident-69 pin container. This thick shell may take longer to degrade, thereby allowing the fuel pins inside the Ident-69 pin container to stay in their most reactive configuration longer than all other DOE SNF canister components and DFAs.

In the description of the configurations, the term “degraded fuel” is used generically to represent the degradation products of the fuel.

#### **7.4.1 Degradation Inside the DFAs**

The effect of degraded fuel pin clips/spacers in the DFAs is calculated by varying the fuel pin pitch. Only reduction of fuel pin pitch is considered in the analyses, as there are no known physical mechanisms for expanding the pitch. This configuration has five DFAs and a reflected array Ident-69 pin container as shown in Figure 7-3a. The pitch is held uniform within the DFAs in all cases and the pins inside the Ident-69 pin container remain intact. This configuration is described in Section 6.2.1.1 and corresponds to the configuration class 3. As the spacing between the fuel pins decreases, the  $k_{\text{eff}}$  decreases – with the original pitch of the DFA being the most reactive. Reducing the pitch decreases the  $k_{\text{eff}}$  by as much as 10%. The maximum  $k_{\text{eff}} + 2\sigma$  of the system is 0.8950 with the original pitch and 0.1% Gd (0.381 kg) in the DOE SNF canister basket (CRWMS M&O 1999f, Table 6-1).



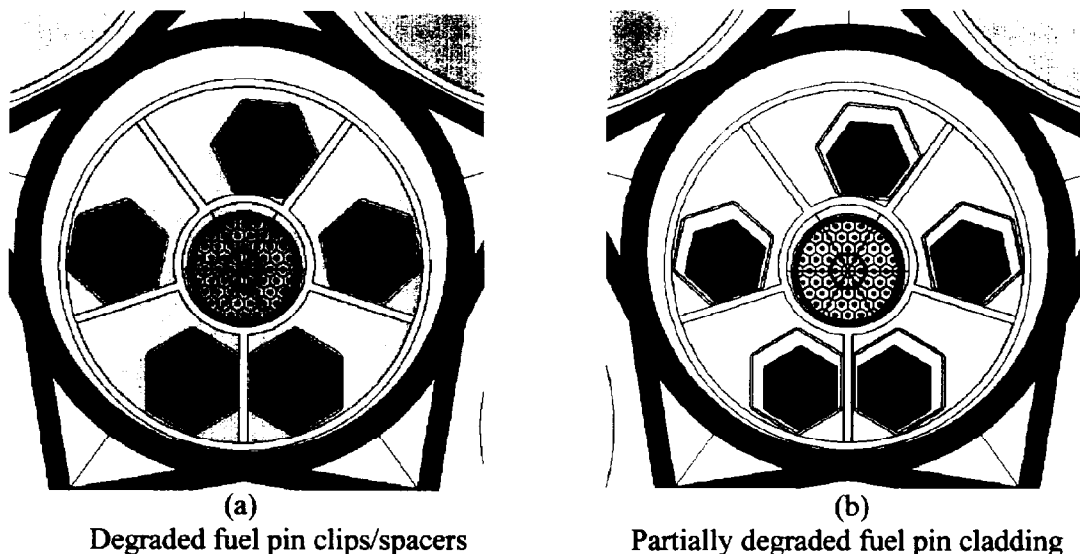


Figure 7-3. Degradation Inside the DFAs

The effect of partially degraded fuel pin cladding in the DFAs is analyzed with a parametric on the fuel pin pitch. This configuration involves five DFAs and a reflected array Ident-69 pin container as shown in Figure 7-3b. The fuel pins remain radially separated while the cladding thickness is reduced since goethite sludge surrounds the pins and takes the place of the cladding. The volume fraction of water in the sludge determines the separation between the fuel pins. The maximum volume fractions of water considered for each fraction of remaining cladding correspond to the original pin pitch for the DFAs. The plutonium decay effects are investigated at four decay times described in Section 7.3. Cladding degradation increases  $k_{\text{eff}}$  by as much as 3%. The maximum  $k_{\text{eff}} + 2\sigma$  with 0.1% (0.381 kg) Gd in the DOE SNF canister basket is 0.9592 after approximately 48,200 years of plutonium radioactive decay (CRWMS M&O 1999f, Tables 6-2 and 6-20). (Note that the difference in  $k_{\text{eff}} + 2\sigma$  between this configuration and the configuration described in previous paragraph appears to be more than 3%. This is due to the plutonium decay effects, which are taken into account for this configuration only). The minimum required Gd content for this configuration was identified as 2% (7.62 kg) to reduce the maximum  $k_{\text{eff}} + 2\sigma$  to 0.9222.

A parametric study on pellet axial spacing is performed by analyzing the fuel pellets dispersed in the goethite sludge, which is formed from the complete degradation of the fuel pin cladding. The maximum radial separation for the pellets is assumed to be the same as for the fuel pin spacing of an intact DFA. The water volume fraction in the sludge is varied to give differing pellet separations. This configuration involves five DFAs and a uniform array Ident-69 pin container as shown in Figure 7-4. The results show that an axial separation of 1 cm and a radial separation of 0.72644 cm (original pitch) give the highest  $k_{\text{eff}}$ . The configurations with 2% (7.62 kg) Gd in the entire basket, and five DFAs and a uniform array Ident-69 pin container (intact) result in a maximum  $k_{\text{eff}} + 2\sigma$  of 0.8977 after 48,200 years of plutonium decay (CRWMS M&O 1999f, Section 6.1.3 and Table 6-20). The configurations with 2% (7.62 kg) Gd in the entire basket and six DFAs result in a maximum  $k_{\text{eff}} + 2\sigma$  of 0.8810 after 48,200 years of plutonium decay

(CRWMS M&O 1999f, Table 6-20). The results corresponding to different times for six DFAs, and five DFAs and a uniform array Ident-69 pin container are shown in Figure 7-5.

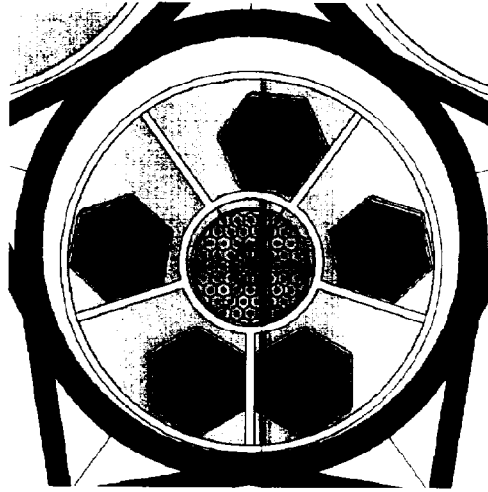


Figure 7-4. Axially Separated Fuel Pellets Inside the DFAs with Reflected Array Ident-69 Pin Container

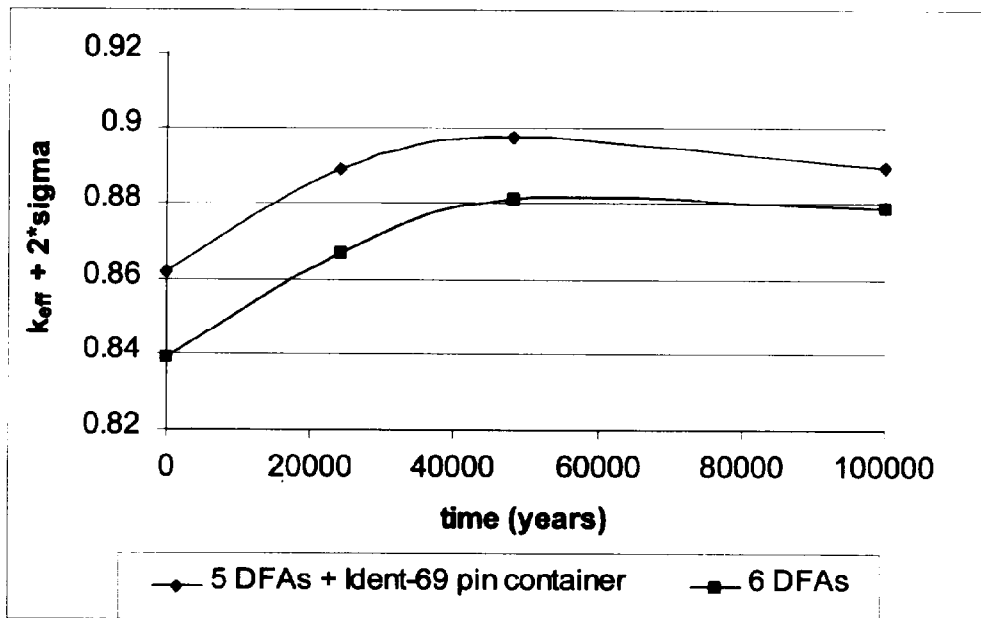


Figure 7-5. Plutonium Decay Effects for Six DFAs and Five DFAs and a Uniform Array Ident-69 Pin Container

### 7.4.2 Degraded DFA Ducts

These analyses consider loose pins settling in each position of the basket as a result of the degradation of the assembly ducts and fuel pin clips/spacers. Since the assembly duct is eight times as thick as the cladding, this is an unlikely configuration. This configuration has five DFAs and a reflected array Ident-69 pin container as shown in Figure 7-6a. The orientation of the DOE SNF canister is also varied. The placement of fuel pins in the DOE SNF canister basket is either irregular (triangular and square array) or random to account for the pins having fallen from a DFA. This configuration is described in Section 6.2.1.1, and corresponds to the configuration class 3. The results show that the maximum  $k_{\text{eff}} + 2\sigma$  is 0.9167 after 48,200 years of plutonium decay (CRWMS M&O 1999f, Tables 6-5 and 6-20). The minimum amount of Gd required is 0.1% (0.3811 kg) of the DOE SNF canister basket.

The effects of degradation of fuel pin cladding and axial separation of fuel pellets with degraded fuel pin clips/spacers, and degraded assembly ducts are also analyzed. This configuration has five DFAs and a uniform array Ident-69 pin container as shown in Figure 7-6b. Individual fuel pellets are placed in each of the positions of the intact basket. The corrosion products from the ducts would be expected to surround the fuel pellets but are neglected for these cases. The degradation products from the cladding surround the fuel pellets, which are assumed to be axially aligned, and separate the pellets in the radial direction depending on the volume fraction of water in the sludge. In no case is this separation greater than that of the fuel pins in the intact DFA. The plutonium decay effects are investigated at four decay times. The results show that an axial separation of 0.6 cm and completely degraded fuel pin cladding with the original pitch produces the largest value of  $k_{\text{eff}}$  after 48,200 years of plutonium decay. The minimum amount of Gd required is 3% (11.43 kg) in the entire DOE SNF canister basket, and the maximum  $k_{\text{eff}} + 2\sigma$  is 0.9295 with 3% (11.43 kg) Gd. If one of the DFAs is removed, the maximum  $k_{\text{eff}} + 2\sigma$  is 0.8843 with 2% (7.62 kg) Gd (CRWMS M&O 1999f, Tables 6-6 and 6-20).

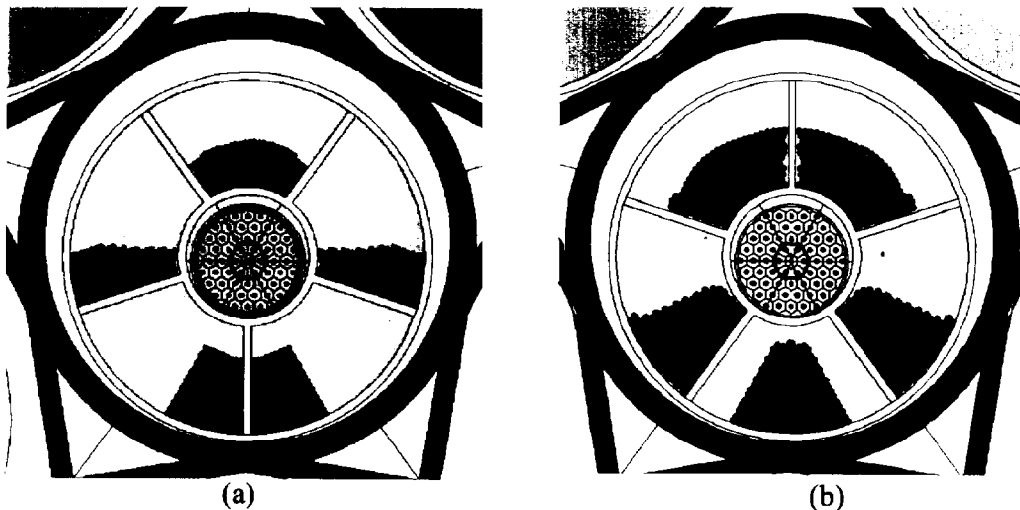


Figure 7-6. Degraded Assembly Ducts Inside Intact DOE SNF Canister Basket

### **7.4.3 Degraded Basket and Intact SNF**

The cases where the basket is fully degraded with all other fuel components intact are analyzed. This configuration is not considered credible, as the basket structure is approximately three times thicker than the assembly ducts and the Ident-69 container. The DFA ducts and the Ident-69 container will naturally degrade before the basket structure. These cases are presented to provide insight into the role of the Ident-69 container and the measures that can be taken to mitigate the contribution of the Ident-69 container to the overall reactivity of the system. In these cases, the DFAs and the Ident-69 container or the center DFA are at the bottom of the DOE SNF canister and the degradation products, with varying water volume fractions, are settled around the fuel components. The cases with six DFAs in the DOE SNF canister as well as the cases with an Ident-69 container with a uniform array of pins surrounded by five DFAs are analyzed. This configuration is described in Section 6.2.1.2 and corresponds to the configuration class 1.

The results support the conclusion that the Ident-69 pin container is driving the system neutronically, and that the Gd placed in the DOE SNF canister is not very efficient when all DFAs and the Ident-69 pin container are close enough to touch each other, since the interaction between the DFAs and the Ident-69 pin container is mostly through fast neutrons (CRWMS M&O 1999f, Tables 6-7 and 6-20). The  $k_{\text{eff}} + 2\sigma$  for the system with a uniform array Ident-69 pin container surrounded by five DFAs is 0.9272. The minimum amount of Gd required for this configuration is 4% (15.24 kg).

### **7.4.4 Intact Fuel Pins in DOE SNF Canister with Degraded Basket and Assembly Ducts**

The results for intact fuel pins with a degraded basket, degraded assembly ducts, and degraded fuel pin clips/spacers are analyzed. Fuel pins surround the uniform array Ident-69 container, if present, and the minimum distance between the outer edge of the Ident-69 container and the DOE SNF canister is varied. This configuration is described in Section 6.2.1.2 and corresponds to the configuration class 1. This configuration is shown in Figure 7-7. The results show that 2% (7.62 kg) Gd is sufficient to reduce the  $k_{\text{eff}} + 2\sigma$  below 0.93 (CRWMS M&O 1999f, Section 6.1.7).

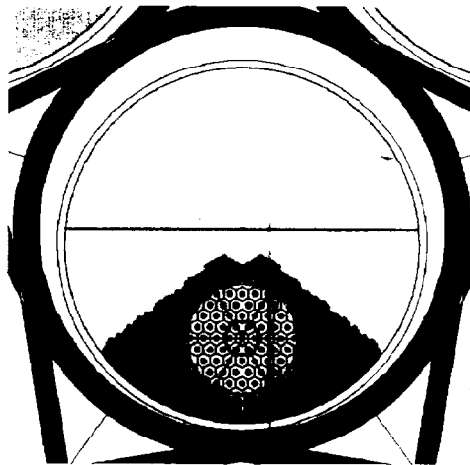


Figure 7-7. Intact Fuel Pins in DOE SNF Canister with Degraded Basket and Assembly Ducts

#### 7.4.5 DOE SNF Canister Containing an Intact Ident-69 Container and Five Degraded DFAs

As described in Section 7.4, the Ident-69 pin container may stay intact long after all DFAs and the DOE SNF canister basket are degraded. The effect of intact versus degraded Ident-69 pin container is analyzed. The results show that the waste package with completely degraded DFAs is the most reactive when the Ident-69 pin container is intact (CRWMS M&O 1999f, Tables 6-11 and 6-12).

The effect of components outside the DOE SNF canister is investigated by neglecting the waste package (thereby neglecting the waste package basket and HLW canisters). The results indicate that the intact waste package configurations result in approximately 2% higher  $k_{eff}$  (CRWMS M&O 1999f, Tables 6-11 and 6-14). As indicated in Section 7.4, the degradation of the stainless steel DOE SNF canister internal components before the carbon steel waste package basket structure is extremely unlikely.

The effect of degraded fuel slurry length, which is along the length of the DOE SNF canister, on the  $k_{eff}$  is investigated for the configurations with and without Gd at four plutonium radioactive decay times. The results indicate that if the basket contains Gd then the shorter fuel slurries are more reactive, whereas if the basket contains no Gd the longer slurries are more reactive (CRWMS M&O 1999f, Section 6.1.9). The maximum  $k_{eff} + 2\sigma$  is 0.9209 with 2.5% (8.45 kg) Gd in the DOE SNF canister basket after 48,200 years of plutonium decay (CRWMS M&O 1999f, Tables 6-11 and 6-20). The  $k_{eff} + 2\sigma$  is 0.9333 with 2.0% (6.76 kg) Gd.

The configurations for a DOE SNF canister containing an intact uniform array Ident-69 container and degraded fuel from the DFAs are further analyzed. The DOE SNF canister is placed in the intact waste package. The configuration is shown in Figure 7-8. These configurations are described in Section 6.2.1.2 and correspond to the configuration class 1. The fuel in the Ident-69

container is centered in the fuel slurry, which is 0.9144 m (3 ft) long and exactly aligns with the fuel slurry from the DFAs. The Ident-69 pin container centered in the fuel slurry (densities are similar) results in the highest  $k_{\text{eff}}$  (CRWMS M&O 1999f, Table 6-14). A range of values of goethite volume fractions from 0.746 to 0.472 is investigated. The larger values of volume fraction are greater than the represented maximum of 0.6 and show the sensitivity of the results to this value, whereas the smallest value corresponds to a sludge volume that radially fills the DOE SNF canister for the length of the fuel slurry. The results indicated that larger goethite volume fractions result in higher  $k_{\text{eff}}$  (CRWMS M&O 1999f, Table 6-14).

A search on optimum moderation in the sludge was also performed. The worst-case identified in the previous paragraph was used as the starting point. The effect of water content in the degraded fuel sludge and in the goethite adjacent to the fuel is determined by again considering the case with the Ident-69 container centered in the fuel sludge and varying the amount of water in the degraded fuel mixture and in the adjacent goethite mixture. The remaining volume fraction within the fuel is treated as void. The results show that water content in the fuel sludge and in the goethite adjacent to the fuel affects the  $k_{\text{eff}}$  by as much as 2%, and the optimum moderation is achieved with water at 1 g/cm<sup>3</sup> density in the sludge to fill the entire DOE SNF canister (CRWMS M&O 1999f, Table 6-16). The worst-case in this set is, therefore, the same as the worst-case that was used as the starting point.

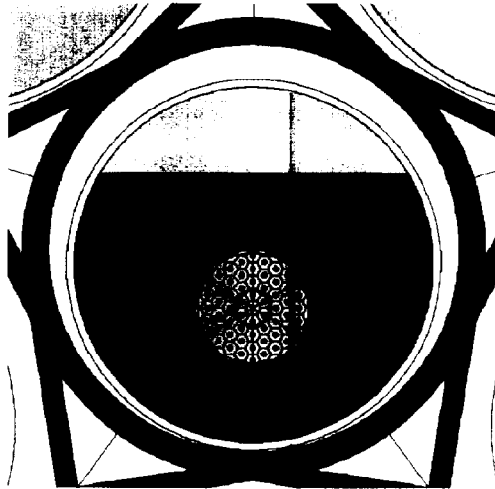


Figure 7-8. Intact Ident-69 Container and Five Fully Degraded DFAs

#### **7.4.6 DOE SNF Canister Containing a Degraded Ident-69 Container and Five Degraded DFAs in the Waste Package**

Results for a fully degraded Ident-69 container that holds various numbers of fuel pins (maximum 217 fuel pins) and five degraded DFAs are analyzed. The degraded Ident-69 pin container with 217 fuel pins is equivalent to a degraded DFA; therefore, this configuration also covers the DOE SNF canister with six completely degraded DFAs. These results are for a 0.9144 m (3 ft) fuel slurry and a basket that contains 2% Gd (7.62 kg). The space not occupied by fuel slurry or goethite in the DOE SNF canister is filled with water at 1 g/cm<sup>3</sup> density. The

goethite volume in the fuel sludge is varied from 60% to a low of 45.71% corresponding to a volume that radially fills the DOE SNF canister for a 0.9144 m (3 ft) length. Vacant space in the waste package is treated as a void. The waste package is fully reflected by water. This configuration is described in Section 6.2.1.2 and corresponds to the configuration class 1. The configuration is shown in Figure 7-9. The results show that the highest  $k_{\text{eff}} + 2\sigma$  is 0.920 with 217 fuel pins in the Ident-69 pin container, 45.71% goethite volume fractions, and 2% (7.62 kg) Gd in the DOE SNF canister basket (CRWMS M&O 1999f, Section 6.1.10.2).

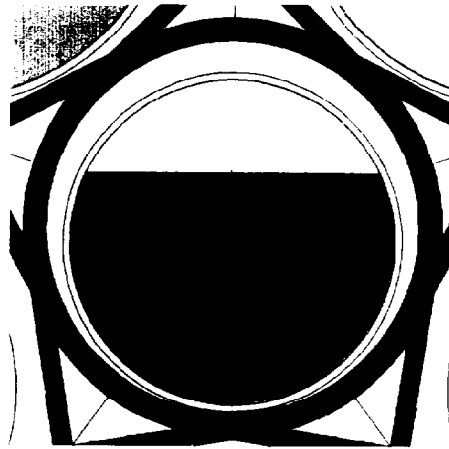


Figure 7-9. DOE SNF Canister Containing a Degraded Ident-69 Container and Five Fully Degraded DFAs

#### 7.4.7 DOE SNF Canister Containing Degraded Fuel or Fuel Components with the Waste Package Contents Degraded

The contents of the waste package external to the DOE SNF canister are now analyzed as completely degraded. The contents of the DOE SNF canister are taken to be same as the most reactive case in Section 7.4.5. Recall that the most reactive case in Section 7.4.5 required 2.5% (8.45 kg) Gd in the DOE SNF canister basket and resulted in  $k_{\text{eff}} + 2\sigma$  of 0.9209. The position of the DOE SNF canister in the clay formed from the HLW glass (HLW glass degrades to a clay like material, “clayey”, that will be referred to simply as clay throughout this document) and the water content of that clay are the parameters that are varied. The plutonium decay effects are also investigated at four decay times described in Section 7.3. The position of the canister (center of the waste package versus bottom of the waste package) effects  $k_{\text{eff}}$  by less than 1% with the highest being the bottom position. The water volume in the clay does not affect the results since all results are within statistical uncertainty indicating that the clay is a good reflector with or without water (CRWMS M&O 1999f, Table 6-18).

The results indicate that even with 6% (20.28 kg) Gd in the DOE SNF canister basket, the  $k_{\text{eff}} + 2\sigma$  is 0.9510 after 24,100 years of plutonium decay. Therefore, the number of DFAs needs to be reduced from five to four and 2.75% (9.29 kg) Gd needs to be added to reduce  $k_{\text{eff}} + 2\sigma$  below the interim critical limit of 0.93. This configuration results in the highest  $k_{\text{eff}} + 2\sigma$  of 0.9269 after 24,100 years of plutonium decay (CRWMS M&O 1999f, Tables 6-18 and 6-20). The results for different times are shown in Figure 7-10. These results also support the conclusion

that the Ident-69 pin container is driving the system neutronically. This configuration is the limiting case driving the design/loading solution.

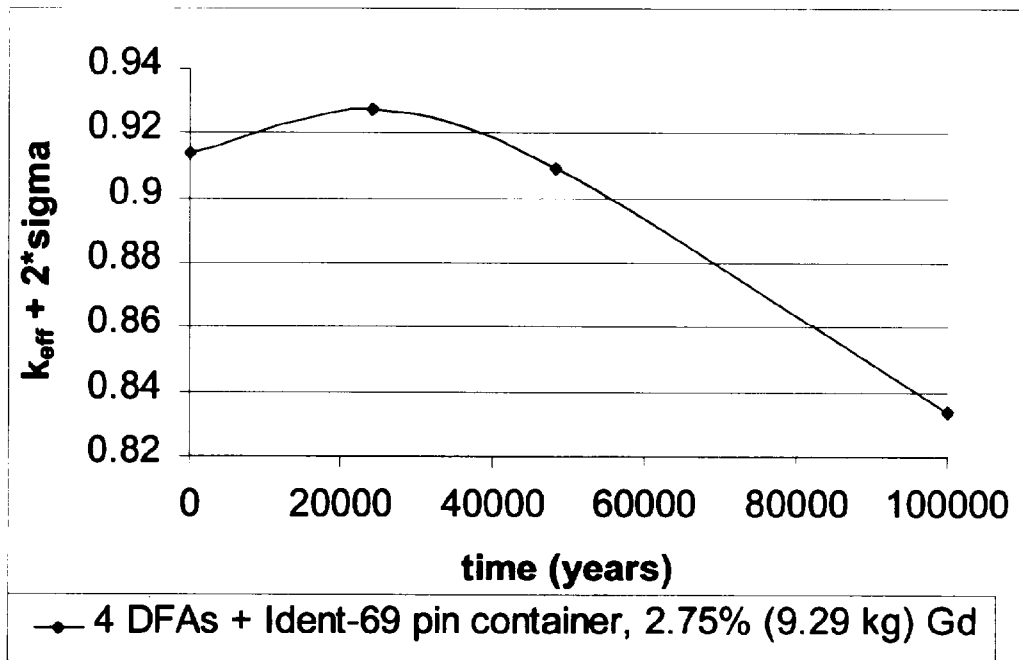


Figure 7-10. Plutonium Decay Effects for Four DFAs and a Uniform Array Ident-69 Pin Container

#### 7.4.8 DOE SNF Canister with Degraded FFTF Fuel and Surrounded by Degraded HLW

In this section, the waste package with degraded HLW canisters and degraded SNF is analyzed. This configuration is described in Section 6.2.1.3 and corresponds to the configuration class 5. The DOE SNF canister shell is represented as being intact, and confines the SNF. The DOE SNF canister contents are completely homogenized and distributed inside the DOE SNF canister. This is different from the previous configurations in that the fuel length is not preserved during homogenization. Instead, the degraded FFTF fuel (equivalent fissile amount of six DFAs, which is the maximum amount in an FFTF DOE SNF canister) is distributed into the homogenized mixture axially and radially.

The effect of the position of the DOE SNF canister is investigated by placing the DOE SNF canister either in the middle or on the bottom of the waste package as shown in Figure 7-11. The amount of water in the clay, the amount of water in the fuel, the minimum amount of absorber required, and flooding in the DOE SNF canister are among the parameters that are varied.



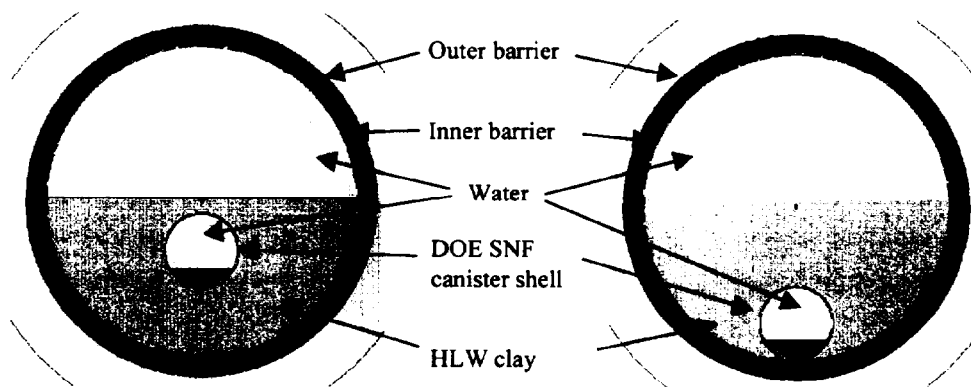


Figure 7-11. Cross-sectional View of the DOE SNF Canister Settled in the Middle and on the Bottom of the WP

#### 7.4.8.1 Degraded FFTF Mixture in a Flooded DOE SNF Canister

In investigating the intact DOE SNF canister shell with the degraded FFTF fuel settled at the bottom of the flooded canister, the percentage of water in the clay (along with the volume of clay) is increased. The position of the DOE SNF canister in the waste package is also varied (Figure 7-11). The results show that the  $k_{\text{eff}} + 2\sigma$  is less than 0.3 for all cases (CRWMS M&O 1999g, Section 6.1), and the position of the DOE SNF canister in the waste package has no effect on criticality (CRWMS M&O 1999g, Table 6.1-1 and CRWMS M&O 1999f, Table 6-18).

The next configuration investigated is an intact DOE SNF canister shell having degraded FFTF fuel located in the center of the waste package, with the FFTF fuel mixed with different amounts of water. The  $k_{\text{eff}}$  of a degraded waste package as a function of the amount of water in the hematite is investigated. In all of these cases, the clay is not diluted. Results of the variations show that the  $k_{\text{eff}} + 2\sigma$  is less than 0.6 for all cases (CRWMS M&O 1999g, Section 6.1). In this configuration, the optimal moderation of the waste package is achieved when the fuel contains 50-65% by volume water.

#### 7.4.8.2 Minimum Mass of Gd Required

If some of the main absorbers (Gd and  $\text{Fe}_2\text{O}_3$ ) are lost, the  $k_{\text{eff}}$  of the waste package will increase. In the configurations investigated, some of the principal absorbers have been removed. Also the DOE SNF canister shell is intact in the middle of the waste package.

With all of the  $\text{Fe}_2\text{O}_3$  remaining in the waste package, the minimal mass of Gd needed in the DOE SNF canister to meet the interim critical limit in such a configuration is 0.1% Gd (0.387 kg) (CRWMS M&O 1999g, Section 6.1). This configuration results in a  $k_{\text{eff}} + 2\sigma$  of 0.9217. In the absence of  $\text{Fe}_2\text{O}_3$ , 2% (7.7 kg) Gd is required to be distributed in the DOE SNF canister. This configuration results in a  $k_{\text{eff}} + 2\sigma$  of 0.6288 at time zero, which corresponds to the time of disposal (CRWMS M&O 1999g, Tables 6.1-3 and 6.4-1). If all the Gd is driven from the waste package and all the fuel are to remain in the DOE SNF canister, the interim critical limit may be

exceeded. However, geochemistry results indicate that maximum Gd loss is less than 0.7% in 100,000 years (see Section 6.4). Therefore, this configuration is not a concern for criticality.

## **7.5 CALCULATIONS AND RESULTS – PART III: SCENARIOS WITH FISSILE MATERIAL DISTRIBUTED IN WASTE PACKAGE**

A detailed description of the Monte Carlo representations, the method of solution, and the results are provided in CRWMS M&O (1999g). This section documents the criticality analyses that are performed for a degraded 5-HLW/DOE SNF Long waste package containing FFTF fuel in the DOE SNF canister. Sections 7.5.1 and 7.5.2 present the  $k_{eff}$  results for different scenarios in which the degradation external to the DOE SNF canister is investigated. These scenarios include the following: (1) the degraded DOE SNF canister on top of the degraded HLW; and (2) degraded HLW on top of degraded DOE SNF canister. Since all configurations consider completely degraded fuel, the worst-case is achieved with the maximum amount of fissile elements in the DOE SNF canister. This is obtained by assuming that all basket locations are filled with a DFA (a total of six DFAs).

In analyzing the configurations from the two scenarios described above, parametric studies have been performed to determine the optimum moderation and configuration. These parametrics include varying the amount of water in the clay and fuel layers, varying the density of water in the clay and fuel layers, varying the amount of absorbers (both Gd and  $Fe_2O_3$ ), and varying the amount of clay mixed with the fuel layer. The bounding results are not dependent on the retention of the clay in the waste package, since the  $Fe_2O_3$ -fuel mixture with no clay is included. The plutonium decay effects due to long times considered in performing the criticality calculations are also determined.

### **7.5.1 Degraded DOE SNF Canister above Settled HLW Clay**

This section describes the calculations that assume the HLW degrades and settles before the DOE SNF canister. The degraded HLW forms a clay material that is collected at the bottom of the waste package, and the degraded FFTF SNF deposits in a layer at the top of the clay material, as shown in Figure 7-12. This section also investigates the  $k_{eff}$  of the waste package for different degrees of hydration of both the FFTF SNF and the HLW clay layers (CRWMS M&O 1999g, Section 6.2). These configurations are described in Section 6.2.1.4 and correspond to the configuration class 5.

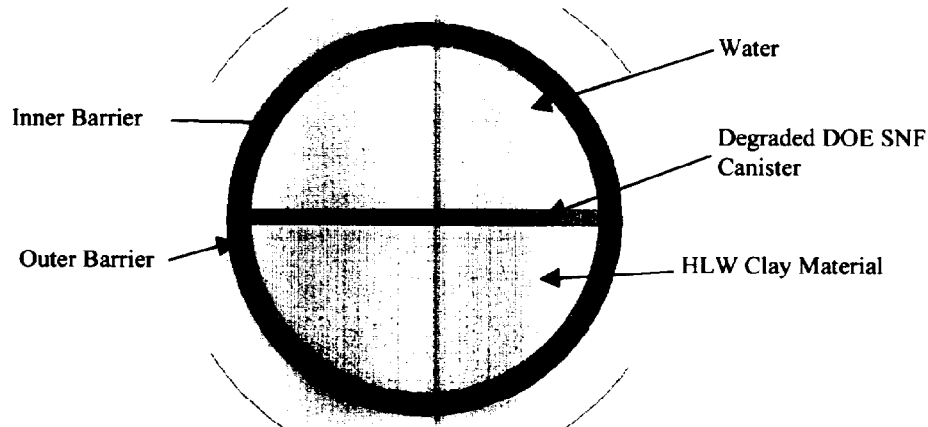


Figure 7-12. Degraded DOE SNF on Top of the Degraded HLW Glass Clay

The following configurations are investigated: the amount of water in the clay layer varies and the fuel is modeled with no free-water fraction; the amount of water in the FFTF SNF layer varies, the HLW clay material is modeled with no free-water (however, it does contain some hydrogen in the form of hydrates) to maximize the potential volume of the degraded FFTF fuel in the layer above the HLW clay; the HLW clay and the fuel layer fill the entire waste package so there is no void space (Figure 7-13) and the density of the water is varied within the clay and/or the fuel; the layer of fuel and the layer of HLW glass are mixed partially or totally as shown in Figure 7-14, any available void space in the waste package is flooded with water; the waste package contains a mixture of FFTF SNF, HLW, and water so that the inner volume of the waste package is filled. All these configurations are also investigated with respect to the plutonium decay effects at four decay times described in Section 7.3.

The results show that the  $k_{\text{eff}} + 2\sigma$  of the configurations investigated are all below 0.5 with 2% (7.62 kg) Gd. When Gd is present, the  $k_{\text{eff}}$  of the system decreases as plutonium isotopes decay. In these configurations, even if all the Gd is driven out of the waste package, the  $k_{\text{eff}} + 2\sigma$  of the system is still below the interim critical limit of 0.93 with a maximum of 0.9025 after 24,100 years of plutonium radioactive decay.

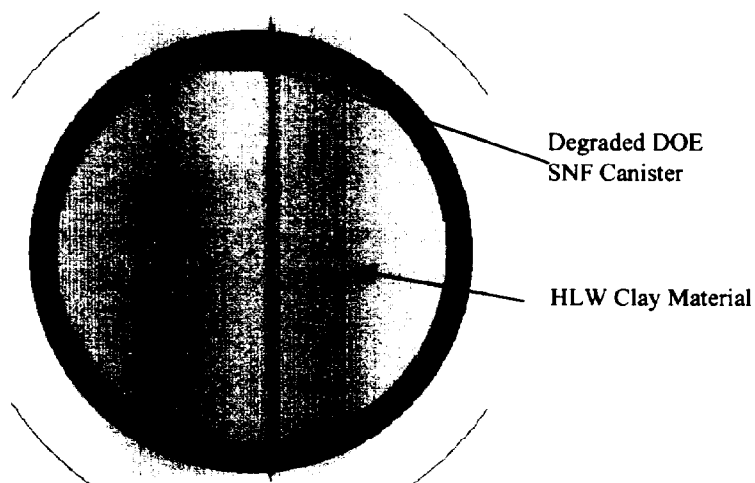


Figure 7-13. WP Filled with HLW Clay Material Layer and FFTF SNF Layer

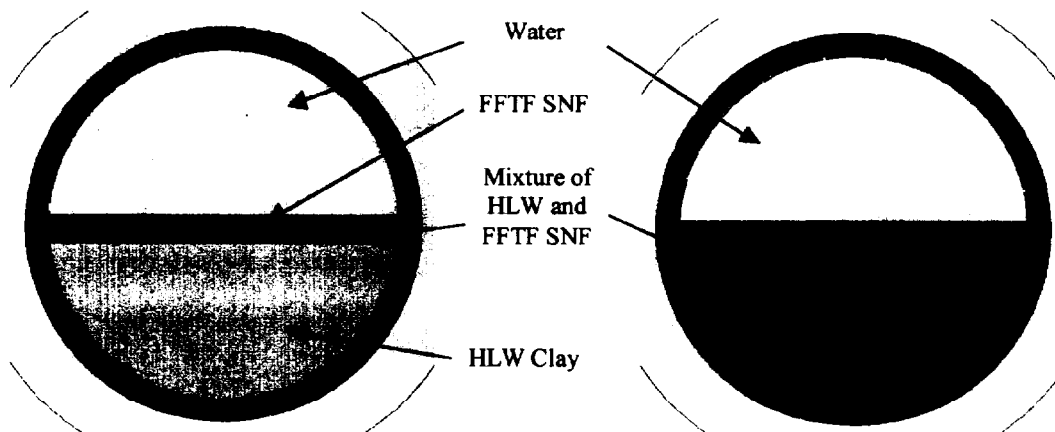


Figure 7-14. Layer of Fuel Mixed with the Layer of HLW Clay

### 7.5.2 Degraded DOE SNF Canister Settled at the Bottom

This section describes the calculations performed assuming the DOE SNF canister sinks to the bottom of the degraded HLW clay during the degradation process. As the DOE SNF canister degrades, some of the HLW clay and the FFTF SNF will mix as shown in Figure 7-15. The water fractions in the bottom layer and in the clay material are represented as being the same (CRWMS M&O 1999g, Section 6.3). These configurations are described in Section 6.2.1.5 and correspond to the configuration class 4. The results indicate that the highest  $k_{\text{eff}}$  is achieved if the fuel and clay layers do not mix. Even without any credit for Gd or iron oxide, the maximum  $k_{\text{eff}} + 2\sigma$  of the system is 0.9145 after 24,100 years of plutonium decay.

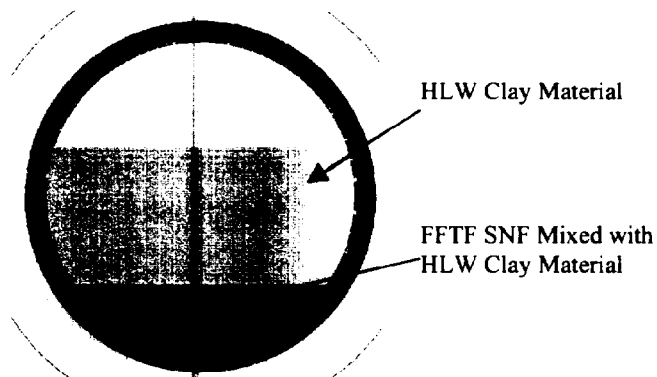


Figure 7-15. Degraded DOE SNF Mixed with HLW Glass Clay at the Bottom of the WP

The Pu-239 neutron fission cross section is somewhat higher than the U-235 neutron fission cross section in the thermal energy range. Pu-239 has a fission resonance at 0.3 eV, which is an order of magnitude higher than the corresponding U-235 resonance at approximately 0.18 eV. The total number of neutrons emitted by Pu-239 fission ( $\nu$ ) is approximately 15% higher than the total number of neutrons emitted by U-235. Total capture of neutrons that are in the thermal range by Pu-240 is approximately three orders of magnitude higher than total capture of neutrons by U-236, which is the isotope Pu-240 decays to.

The results from considering the effect of Pu decay indicate that for homogenous layers of fuel and clay, if Gd is present in the waste package, the  $k_{eff}$  is maximum at time zero and decreases in time. When Gd is present, the thermal neutrons are absorbed by Gd rather than by Pu-240. Therefore, Pu-240 decay has no significant effect on  $k_{eff}$ . However, as Pu-239 decays to U-235, the  $k_{eff}$  decreases. If the Gd is not present, the decay of Pu-240 reduces the overall neutron absorption (Pu-240 is a much stronger absorber than U-236). As a consequence, the  $k_{eff}$  peaks at approximately 24,100 years. At that time, approximately 92% of the Pu-240 has decayed to U-236 and only 50% of the Pu-239 has decayed to U-235. As more Pu-239 decays to U-235,  $k_{eff}$  decreases.

## 7.6 SUMMARY

Six DFAs with 2% (7.62 kg) Gd in the DOE SNF canister basket can be disposed of in the waste package without any criticality concerns. However, the waste packages with an Ident-69 pin container must have one of the basket locations blocked so that only four DFAs can be disposed of with the Ident-69 container, and at least 9.29 kg of Gd must be distributed on (e.g., flame deposit), or in the DOE SNF canister basket.

## 8. CONCLUSIONS

### 8.1 STRUCTURAL ANALYSIS

The results from the 2-D FEA calculations given in Section 3.3 show that there is sufficient clearance between the inner diameter of the support tube and the outer diameter of the DOE SNF canister for the DOE SNF canister to be removed from the waste package after a tipover DBE, which results in the bounding dynamic load.

The maximum deformations in each component of the waste package are acceptable. The outer barrier is directly exposed to a dynamic impact with an essentially unyielding surface. Therefore, local plastic deformations are unavoidable on the outer surface. Similarly, the basket support structure receives the direct impacts of pour canisters, which result in limited permanent deformations of the basket plates. The pour canisters remain intact after the impact.

The results given in Section 3.3.3 show that there would be no interference between any of the fuel assemblies and the basket structure inside the DOE SNF canister. Thus, the waste package will be able to be unloaded after a tipover DBE.

In the light of the above discussions, it is concluded that the performance of the 5-HLW/DOE SNF Long waste package design is structurally acceptable when exposed to a tipover event, which is the bounding DBE within the criteria specified in the SDD, as long as the 3400 kg DOE SNF canister loaded mass limit is not exceeded.

### 8.2 THERMAL ANALYSIS

Based on the 2-D FEA calculations given in Section 4, the FFTF waste package satisfies all relevant governing criteria, as listed in Table 8-1. The maximum temperatures are shown in Table 8-1. The HLW glass dominates the thermal heat output of the waste package. The HLW glass and FFTF fuel temperatures are below the limits.

Table 8-1. FFTF Codisposal WP Thermal Results and Governing Criteria

WP Metric	SDD Criterion	FFTF Codisposal WP Value
Maximum waste package heat output	< 18,000 W	13,533 W
Maximum HLW temperature	< 400 °C	247.6 °C
Maximum DOE SNF temperature in codisposal waste package	< (TBD-179)	280.3 °C

### 8.3 SHIELDING ANALYSIS

The results of 3-D Monte Carlo dose rate calculations show that maximum dose rate on the outer surfaces of waste package is below the 355 rem/h design limit by a factor of approximately 23. The highest dose rate is only  $15.9 \pm 1.9$  rem/h. The primary gamma dose rate dominates the neutron dose rate by approximately three orders of magnitude. The presence of the FFTF DOE SNF canister in the center of the waste package reduces the axial dose rate by as much as 50%.

## 8.4 GEOCHEMISTRY ANALYSIS

The degradation analyses followed the general methodology developed for application to all waste forms containing fissile material that evaluates potential critical configurations from intact through degraded. Sequences of events and/or processes of component degradation were developed. Standard scenarios from the master scenario list in the topical report were refined using unique fuel characteristics. Potentially critical configurations were identified and analyzed.

The cases that evaluate the alkaline regime produce the highest Gd loss which is  $\leq 0.7\%$  in  $\geq 100,000$  years. When the glass is allowed to degrade rapidly, the alkaline conditions produce high uranium and plutonium loss (up to 100%), reducing the chances of internal criticality.

The cases that evaluate the effect of exposing the Gd, Pu, and U to long-lived acidic conditions (pH  $\sim 5$  to 6) show no loss of Gd (due primarily to the use of  $\text{GdPO}_4$  instead of  $\text{Gd}_2\text{O}_3$ ), and the highest fissile loss is less than 3% of either Pu or U.

## 8.5 INTACT AND DEGRADED CRITICALITY ANALYSES

All aspects of intact configurations, including optimum moderation conditions, absorber distribution, water intrusion into the fuel pins, and positioning of the DFAs and the Ident-69 pin container were investigated. The results of 3-D Monte Carlo calculations from the intact criticality analysis show that the requirement of  $k_{\text{eff}} + 2\sigma$  less than or equal to 0.93 is satisfied for six DFAs in the DOE SNF canister. This configuration does not need any Gd in the basket or elsewhere in the waste package to meet this requirement. For the cases that include an Ident-69 container (uniform array) and five DFAs, the DOE SNF canister basket must contain 0.5% (1.93 kg) Gd uniformly distributed over the entire basket.

A number of parametric analyses were run to address or bound the configuration classes discussed in Section 6.2.1. These parametric analyses addressed identification of optimum moderation, optimum spacing, optimum fissile concentration, decay of Pu isotopes, and absorber concentration/ distribution requirements.

The results from the criticality analysis for the intact DOE SNF canister show that the criteria of  $k_{\text{eff}} + 2\sigma$  less than or equal to 0.93 is satisfied with the following restrictions. For the cases that include an Ident-69 container, all degradation configurations result in  $k_{\text{eff}} + 2\sigma$  of less than or equal to 0.93 with 2.75 wt% Gd on or in the DOE SNF canister basket as long as only four DFAs are included in the package. All degradation configurations for six DFAs in the DOE SNF canister result in  $k_{\text{eff}} + 2\sigma$  of less than or equal to 0.93 if the Gd content is at least 2 wt%.

The results from the criticality analysis for the degraded DOE SNF canister (fissile material distributed in the waste package) indicate that the highest  $k_{\text{eff}}$  is achieved if the fuel and clay layers do not mix. Therefore, the amount of clay in the waste package has no effect on the bounding case, which is a layer of optimally moderated fuel not mixed with any clay. Although

varying the amount of water mixed with the fuel changes the  $k_{\text{eff}}$ , the peak  $k_{\text{eff}} + 2\sigma$  of the system is less than 0.5, which is well below the interim critical limit. Even without any credit for Gd or iron oxide, the maximum  $k_{\text{eff}} + 2\sigma$  of the system is below the interim critical limit.

In summary, the DOE SNF canister can contain six DFAs, which corresponds to the maximum number of basket locations, with at least 7.62 kg of Gd distributed on (e.g., flame deposit), or in the DOE SNF canister basket. However, the DOE SNF canister with the Ident-69 pin container must have one of the basket locations blocked so that only four DFAs can be disposed of with the Ident-69 container with at least 9.29 kg of Gd on, or in the DOE SNF canister basket. With this design, there will be approximately 64 DOE SNF canisters with FFTF SNF, which corresponds to 64 waste packages. Alternatively, the Ident-69 pin container could be filled with iron shot, thereby allowing five DFAs to be disposed of with the Ident-69 pin container. With this design, there will be approximately 58 DOE SNF canisters with FFTF SNF, which corresponds to 58 waste packages.

## 8.6 ITEMS IMPORTANT TO SAFETY

As part of the criticality licensing strategy, items that are important to safety will be identified during evaluation of the representative fuel type designated by the NSNFP. As a result of the analyses performed for the evaluation of the codisposal viability of MOX (FFTF) DOE-owned fuel, several items are identified as important to safety. DOE SNF canister shell is naturally an item that is important to safety since it confines the fissile elements to a specific geometry and location within the waste package. The basket that was designed for the DOE SNF canister containing the FFTF fuel is also an important safety item since it confines the fissile elements to a specific geometry and location within the DOE SNF canister. The DOE SNF canister basket also provides thermal neutron absorption due to its high iron content. The DOE SNF canister loaded weight, which must be less than 3400 kg, is also an important safety item. Based on the conclusions derived in Section 8.5, some small amount of neutron absorber will have to be distributed on or in the DOE SNF canister basket. Therefore, the absorber material that will be placed on or in the basket is also an item important to safety. All calculations are based on assemblies with 217 fuel pins. It was shown, in Section 7.3 (intact criticality analysis), that having a fewer number of fuel pins, which in turn results in increased fuel pin pitch, results in higher  $k_{\text{eff}}$ . On the other hand, it was shown in Sections 7.4 and 7.5 (degraded criticality) that having more fuel pins increases the  $k_{\text{eff}}$ . It was also shown in Section 7 that degraded configurations with fuel pellets spread out axially and radially bound the intact configurations. The degraded configurations include varying degrees of degradation resulting in many different geometric configurations and fissile distributions. Therefore, these degraded configurations also bound the other types of MOX fuels as long as the limits on mass and enrichment are not exceeded. The total mass of fissile elements (U-235 and Pu-239) in an assembly should not exceed the one used in deriving the conclusions in this report, which is 8.6 kg per assembly, with total fissile to U-238 ratio of 0.34 or less. All analyses are based on the fuel pin type that has the highest plutonium enrichment (enriched in Pu-239) and the highest plutonium loading per pin. In Section 7, it was shown that as the total amount of Pu-240 decreases with radioactive decay, the  $k_{\text{eff}}$  increases. Since Pu-240 was decayed, the fraction of Pu-239 in plutonium is not a factor that is important to safety.



The shielding source terms and thermal heat output of the fuel assemblies must not exceed the ones used in the analyses. Specifically, the total gamma sources from the HLW glass and the fuel assembly must not exceed  $4.94\text{E}+15$  gammas/sec/canister and  $1.84\text{E}+15$  gammas/sec/assembly, respectively. HLW glass thermal power should not exceed 2,540 W. Alternatively, it must be demonstrated that HLW glass canisters and/or fuel assemblies with higher shielding source terms or thermal heat outputs will not result in violation of the required criteria.

## 9. REFERENCES

### 9.1 DOCUMENTS CITED

Bergsman, K.H. 1994. *Hanford Spent Fuel Inventory Baseline*. WHC-SD-SNF-TI-001. Richland, Washington: Westinghouse Hanford Company. ACC: MOL.19980625.0163.

Bierman, S.R.; Durst, B.M.; Clayton, E.D.; Scherpelz, R.I.; and Kerr, H.T. 1979. "Critical Experiments with Fast Test Reactor Fuel Pins in Water." *Nuclear Technology*, vol. 44, pp. 141-151. La Grange Park, Illinois: American Nuclear Society. TIC: 239579.

CRWMS M&O 1995a (Civilian Radioactive Waste Management System Management and Operating Contractor). *Thermal Evaluation of the Conceptual DHLW Disposal Container*. BBAC000000-01717-0200-00002 REV 00. Las Vegas, Nevada: CRWMS M&O. ACC: MOL.19960626.0161.

CRWMS M&O 1995b. *Total System Performance Assessment - 1995: An Evaluation of the Potential Yucca Mountain Repository*. B000000000-01717-2200-00136 REV 01. Las Vegas, Nevada: CRWMS M&O. ACC: MOL.19960724.0188.

CRWMS M&O 1996a. *Second Waste Package Probabilistic Criticality Analysis: Generation and Evaluation of Internal Criticality Configurations*. BBA000000-01717-2200-00005 REV 00. Las Vegas, Nevada: CRWMS M&O. ACC: MOL.19960924.0193.

CRWMS M&O 1996b. *Status Report on Degraded Mode Criticality Analysis of Immobilized Plutonium Waste Forms in a Geologic Repository*. A000000000-01717-5705-00013 REV 00. Vienna, Virginia: CRWMS M&O. ACC: MOL.19970324.0023.

CRWMS M&O 1997a. *Waste Package Materials Selection Analysis*. BBA000000-01717-0200-00020 REV 01. Las Vegas, Nevada: CRWMS M&O. ACC: MOL.19980324.0242.

CRWMS M&O 1997b. *DHLW Canister Source Terms for Waste Package Design*. BBA000000-01717-0200-00025 REV 00. Las Vegas, Nevada: CRWMS M&O. ACC: MOL.19970711.0019.

CRWMS M&O 1997c. *Criticality Evaluation of Degraded Internal Configurations for the PWR AUCF WP Designs*. BBA000000-01717-0200-00056 REV 00. Las Vegas, Nevada: CRWMS M&O. ACC: MOL.19971231.0251.

CRWMS M&O 1997d. *Preliminary Design Basis for WP Thermal Analysis*. BBAA000000-01717-0200-00019 REV 00. Las Vegas, Nevada: CRWMS M&O. ACC: MOL.19980203.0529.

CRWMS M&O 1997e. *MCNP Evaluation of Laboratory Critical Experiments: Homogeneous Mixture Criticals*. BBA000000-01717-0200-00045 REV 00. Las Vegas, Nevada: CRWMS M&O. ACC: MOL.19971230.0134.

CRWMS M&O 1997f. *Degraded Mode Criticality Analysis of Immobilized Plutonium Waste Forms in a Geologic Repository*. A00000000-01717-5705-00014 REV 01. Las Vegas, Nevada: CRWMS M&O. ACC: MOL.19980422.0911.

CRWMS M&O 1998a. *Disposal Criticality Analysis Methodology Topical Report*. B00000000-01717-5705-00095 REV 00. Las Vegas, Nevada: CRWMS M&O. ACC: MOL.19980918.0005.

CRWMS M&O 1998b. *5-High Level Waste DOE Spent Fuel Waste Package Structural Calculations*. BBA000000-01717-0210-00021 REV 00. Las Vegas, Nevada: CRWMS M&O. ACC: MOL.19981006.0187.

CRWMS M&O 1998c. *Dose Calculations for the Co-Disposal WP of HLW Canisters and the Fast Flux Test Facility (FFTF) Fuel*. BBA000000-01717-0210-00019 REV 00. Las Vegas, Nevada: CRWMS M&O. ACC: MOL.19980911.0001.

CRWMS M&O 1998d. *Controlled Design Assumptions Document*. B00000000-01717-4600-00032 REV 05. Las Vegas, Nevada: CRWMS M&O. ACC: MOL.19980804.0481.

CRWMS M&O 1998e. *EQ6 Calculations for Chemical Degradation of Fast Flux Test Facility (FFTF) Waste Packages*. BBA000000-01717-0210-00028 REV 00. Las Vegas, Nevada: CRWMS M&O. ACC: MOL.19981229.0081.

CRWMS M&O 1998f. *EQ6 Calculations for Chemical Degradation of Pu-Ceramic Waste Packages*. BBA000000-01717-0210-00018 REV 00. Las Vegas, Nevada: CRWMS M&O. ACC: MOL.19980918.0004.

CRWMS M&O 1998g. *Complete Draft VA UZ Abstraction/Test Document*. B00000000-01717-2200-00201. Las Vegas, Nevada: CRWMS M&O. ACC: MOL.19980428.0202.

CRWMS M&O 1998h. *DOE Spent Nuclear Fuel Disposal Container System Description Document*. BBA000000-01717-1705-00003 REV 00. Las Vegas, Nevada: CRWMS M&O. ACC: MOL.19981214.0036.

CRWMS M&O 1998i. *Software Qualification Report for MCNP Version 4B2, A General Monte Carlo N-Particle Transport Code*. CSCI: 30033 V4B2LV. DI: 30033-2003 REV 01. Las Vegas, Nevada: CRWMS M&O. ACC: MOL.19980622.0637.

CRWMS M&O 1998j. *Software Qualification Report for ANSYS V5.4, A Finite Element Code*. CSCI: 30040 V5.4. DI: 30040-2003 REV 00. Las Vegas, Nevada: CRWMS M&O. ACC: MOL.19980609.0847.

CRWMS M&O 1998k. *EQ3/6 Software Installation and Testing Report for Pentium Based Personal Computers (PCs)*. CSCI: LLYMP9602100. Las Vegas, Nevada: CRWMS M&O. ACC: MOL.19980813.0191.

CRWMS M&O 1999a. *FY99 Criticality DOE SNF, 2101 9076 M3*. Activity Evaluation. Las Vegas, Nevada: CRWMS M&O. ACC: MOL.19990330.0477.

CRWMS M&O 1999b. *Thermal Evaluation of the FFTF Codisposal Waste Package*. BBAA00000-01717-0210-00012 REV 01. Las Vegas, Nevada: CRWMS M&O. ACC: MOL.1999.0610.0180.

CRWMS M&O 1999c. *LCE for Research Reactor Benchmark Calculations*. B00000000-01717-0210-00034 REV 00. Las Vegas, Nevada: CRWMS M&O. ACC: MOL.19990329.0394.

CRWMS M&O 1999d. *Laboratory Critical Experiment Reactivity Calculations*. B00000000-01717-0210-00018 REV 01. Las Vegas, Nevada: CRWMS M&O. ACC: MOL.19990526.0294.

CRWMS M&O 1999e. *Fast Flux Test Facility (FFTF) Reactor Fuel Criticality Calculations*. BBA000000-01717-0210-00016 REV 00. Las Vegas, Nevada: CRWMS M&O. ACC: MOL.19990426.0142.

CRWMS M&O 1999f. *Fast Flux Test Facility (FFTF) Reactor Fuel Degraded Criticality Calculations: Intact SNF Canister*. BBA000000-01717-0210-00051 REV 00. Las Vegas, Nevada: CRWMS M&O. ACC: MOL.19990607.0075.

CRWMS M&O 1999g. *Fast Flux Test Facility (FFTF) Reactor Fuel Degraded Criticality Calculation: Degraded SNF Canister*. BBA000000-01717-0210-00033 REV 01. Las Vegas, Nevada: CRWMS M&O. ACC: MOL. 19990607.0239.

DOE (U.S. Department of Energy) 1998a. *Preliminary Design Concept for the Repository and Waste Package*. Volume 2 of *Viability Assessment of a Repository at Yucca Mountain*. DOE/RW-0508. Washington, D.C.: U.S. Department of Energy, Office of Civilian Radioactive Waste Management. ACC: MOL.19981007.0029.

DOE 1998b. Design Specification, Volume I of II. *Preliminary Design Specification for Department of Energy Standardized Spent Nuclear Fuel Canisters*. DOE/SNF/REP-011, Rev. 0. Idaho Falls, Idaho: DOE. TIC: 239252.

DOE 1998c. Design Specification, Volume I of II. *Preliminary Design Specification for Department of Energy Standardized Spent Nuclear Fuel Canisters*. DOE/SNF/REP-011, Rev. 1. Idaho Falls, Idaho: DOE. TIC: 241528.

Firsching, F.H. and Brune, S.N. 1991. "Solubility Products of the Trivalent Rare-Earth Phosphates." *Journal Chemical and Engineering Data*, 36, 93-95. Washington, D.C.: American Chemical Society. TIC: 240863.

Harrar, J.E.; Carley, J.F.; Isherwood, W.F.; and Raber, E. 1990. *Report of the Committee to Review the Use of J-13 Well Water in Nevada Nuclear Waste Storage Investigations*. UCID-21867. Livermore, California: Lawrence Livermore National Laboratory. ACC: NNA.19910131.0274.

INEEL (Idaho National Engineering and Environmental Laboratory) 1998. *FFTF (MOX) Fuel Characteristics for Disposal Criticality Analysis*. DOE/SNF/REP-032, Rev 0. Idaho Falls, Idaho: Idaho National Engineering and Environmental Laboratory. TIC: 241492.

LANL (Los Alamos National Laboratory) 1997. *MCNP – A General Monte Carlo N-Particle Transport Code, Version 4B – UC 705 and UC 700*. LA-12625-M, Version 4B. Los Alamos, New Mexico: Los Alamos National Laboratory. ACC: MOL.19980624.0328.

Lee, J.H. and Byrne, R.H. 1992. "Examination of Comparative Rare Earth Element Complexation Behavior Using Linear Free-Energy Relationships." *Geochimica et Cosmochimica Acta*, 56, 1127-1137. Oxford, Great Britain: Pergamon Press Ltd. TIC: 240861.

OECD-NEA (Organization for Economic Cooperation and Development-Nuclear Energy Agency) 1997. *International Handbook of Evaluated Criticality Safety Benchmark Experiments*. NEA/NSC/DOC(95)03, September 1997 Edition. Paris, France: Organization for Economic Cooperation and Development-Nuclear Energy Agency. TIC: 243013.

ORNL (Oak Ridge National Laboratory) 1978. *Criticality Analysis of Aggregations of Actinides from Commercial Nuclear Waste in Geological Storage*. ORNL/TM-6458. Oak Ridge, Tennessee: Oak Ridge National Laboratory. TIC: 229251.

Parks, C.V.; Broadhead, B.L.; Hermann, O.W.; Tang, J.S.; Cramer, S.N.; Gauthery, J.C.; Kirk, B.L.; and Roussin, R.W. 1988. *Assessment of Shielding Analysis Methods, Codes, and Data for Spent Fuel Transport/Storage Applications*. ORNL/CSD/TM-246. Oak Ridge, Tennessee: Oak Ridge National Laboratory. ACC: NN1.19880928.0023.

Parrington, J.R.; Knox, H.D.; Breneman, S.L.; Baum, E.M.; and Feiner, F. 1996. *Nuclides and Isotopes 15th Edition*. San Jose, California: General Electric Co. TIC: 233705.

PNL (Pacific Northwest Laboratory) 1987. *The TN-24P PWR Spent Fuel Storage Cask: Testing and Analysis*. PNL-6054. Richland, Washington: Pacific Northwest Laboratory. ACC: NNA.19870903.0089.

Radulescu, G. and Abdurrahman, N.M. 1997. "MCNP Criticality Benchmark Calculations of the Saxton Plutonium Program Experiments." *Transactions of the American Nuclear Society*. ISSN: 0003-018X, Volume 76. La Grange Park, Illinois: American Nuclear Society. TIC: 242666.

Stockman, H.W. 1998. "Long-Term Modeling of Plutonium Solubility at a Desert Disposal Site, Including CO<sub>2</sub> Diffusion, Cellulose Decay, and Chelation." *Jour. Soil Contamination*, 7, 615-647. Boca Raton, Florida: Lewis Publishers. TIC: 240836.

Stout, R.B. and Leider, H.R. 1991. *Preliminary Waste Form Characteristics Report*. Livermore, California: Lawrence Livermore National Laboratory. ACC: MOL.19940726.0118.

Taylor, E.G. 1965. *Saxton Plutonium Program Critical Experiments for the Saxton Partial Plutonium Core*. WCAP-3385-54 (EURAE-1493). Pittsburgh, Pennsylvania: Westinghouse Electric Corporation, Atomic Power Division. TIC: 223286.

Taylor, W.J. 1997. *Incorporating Hanford 15 Foot (4.5 meter) Canister into Civilian Radioactive Waste Management System (CRWMS) Baseline*. Memorandum from William J. Taylor (DOE, Richland Operations Office) to Jeffrey Williams (Office of Waste Acceptance and Storage and Transportation), April 10, 1997. 97-WDD-053. ACC: HQP.19970609.0014.

Wolery, T.J. 1992. *EQ3/6, A Software Package for Geochemical Modeling of Aqueous Systems: Package Overview and Installation Guide (Version 7.0)*. UCRL-MA-110662 PT I. Livermore, California: Lawrence Livermore National Laboratory. ACC: MOV.19980504.0006.

## **9.2 CODES, STANDARDS, REGULATIONS, AND PROCEDURES**

ASM 1990. *Metals Handbook Tenth Edition, Volume 1, Properties and Selection: Irons, Steels, and High Performance Alloys*. Materials Park, Ohio: American Society for Metals International. TIC: 241248.

ASME (American Society of Mechanical Engineers) 1995. *1995 ASME Boiler and Pressure Vessel Code*. New York, New York: American Society of Mechanical Engineers. TIC: 238901.

ASTM A 240/A 240M-97a. 1997. *Standard Specification for Heat-Resisting Chromium and Chromium-Nickel Stainless Steel Plate, Sheet, and Strip for Pressure Vessels*. West Conshohocken, Pennsylvania: American Society for Testing and Materials. TIC: 241744.

ASTM A 276-91a. 1991. *Standard Specification for Stainless and Heat-Resisting Steel Bars and Shapes*. Philadelphia, Pennsylvania: American Society for Testing and Materials. TIC: 240022.

ASTM A 516/A 516M-90. 1991. *Standard Specification for Pressure Vessel Plates, Carbon Steel, for Moderate- and Lower-Temperature Service*. Philadelphia, Pennsylvania: American Society for Testing and Materials. TIC: 237681.

ASTM B 575-94. 1994. *Standard Specification for Low-Carbon Nickel-Molybdenum-Chromium, Low-Carbon Nickel-Chromium-Molybdenum, and Low-Carbon Nickel-Chromium-Molybdenum-Tungsten Alloy Plate, Sheet, and Strip*. Philadelphia, Pennsylvania: American Society for Testing and Materials. TIC: 237683.

ASTM G 1-90. 1994. *Standard Practice for Preparing, Cleaning, and Evaluating Corrosion Test Specimens*. Philadelphia, Pennsylvania: American Society for Testing and Materials. TIC: 238771.

Inco Alloys International, Inc. 1985. *Inconel Alloy 625*. Hereford, England: Inco Alloys International, Inc. TIC: 241920.

Inco Alloys International, Inc. 1988. *Product Handbook*. IAI-38. Huntington, West Virginia: Inco Alloys International, Inc. TIC: 239397.